Investigation of Layer-specific Responses to Colon Anastomosis and Disturbed Healing Pathways in Non-steroidal Anti-inflammatory Drug (NSAID)-induced Colon Anastomotic Leakage

Doctoral thesis

to obtain a doctorate (PhD)

from the Faculty of Medicine

of the University of Bonn

Hilal Şengül

Yenimahalle, Turkey

2025

Written with authorization of

the Faculty of Medicine of the University of Bonn

First reviewer: Prof. Dr. Sven Wehner

Second reviewer: Prof. Dr. Irmgard Förster

Day of oral examination: 16/12/2024

For the institute of Klinik für Allgemein-, Viszeral-, Thorax- und Gefäßchirurgie

To my beloved family

Table of Contents

List of Abbreviations

AA	Arachidonic Acid
ANOVA	Analysis of Variance
B.i.d	Bidaily
BSA	Bovine serum albumin
CAH	Colon Anastomotic Healing
CAL	Colon Anastomotic Leakage
CM	Complete medium
COX	Cyclooxygenase
COX1	Cyclooxygenase 1
COX2	Cyclooxygenase 2
CRP	C-reactive protein
Cytof	Cytometry by Time of Flight
DEGs	Differentially Expressed Genes
Diclofenac Sodium	DCF
dmPGE2	16,16-dimethyl Prostaglandin E2
DTT	Dithiothreitol
ECM	Extracellular Metrix
ERAS	Enhanced Recovery After Surgery
FC	Flow Cytometry
FCS	Fetal Calf Serum
g	Gram
GI	Gastrointestinal
GO	Gene Ontology
GSEA	Gene Set Enrichment Analysis
h	Hours
i.p.	Intraperitoneal
IBD	Inflammatory Bowel Disease
IFN	Interferon

KCl	Potassium chloride
kg	Kilogram
M/SM	Mucosa and Submucosa
ME	Muscularis Externa
mg	Milligram
MMPs	Matrix Metalloproteinases
NaCl	Sodium chloride
Nano-DESI MSI	Nanospray Desorption Electrospray Ionization Mass Spectrometry Imaging
NK-T	Natural Killer T cells
NSAID	Non-steroidal Anti-inflammatory Drugs
PBS	Phosphate Buffered Saline
PCA	Principal Component Analysis
PG	Prostaglandin
PGDS	Prostaglandin D Synthase
PGES	Prostaglandin E Synthase
PGFS	Prostaglandin F Synthase
PGIS	Prostacyclin Synthase
PLA2	Phospholipase A2
POD	Postoperative day
qPCR	Quantitative Polymerase Chain Reaction
RNA	Ribonucleic Acid
ROI	Region of Interest
s.c.	Subcutanous
TBXAS1	Thromboxane A synthase 1
TH2	T Helper 2
TIMPs	Tissue inhibitors of MMPs
TNF	Tumor necrosis factor
TXA2	Thromboxane A2
µ	Micro

1 Introduction

1.1 Colon Anastomotic Healing and Leakage

Surgical resection of malignant tissue is a common treatment for numerous intestinal disorders such as inflammatory bowel disease (IBD), colorectal cancer, and diverticular disease (Matsuda et al. 2018; Sawayama et al. 2022). After the removal of a pathogenic entity during colorectal surgery, continuity of the bowel is restored by suturing the parts of the tissue, and this surgical side is called anastomosis (Nandakumar et al. 2009). Upon construction of an anastomosis, the tissue enters a complex healing program, however, in 1-20 % of patients, colonic anastomotic healing (CAH) is disturbed leading to leakage of the luminal content to the abdominal cavity resulting in abscess formation, peritonitis, and even sepsis (Zarnescu et al. 2021; Lee et al. 2018; Chadi et al. 2016). This serious complication is known as colon anastomotic leakage (CAL) and remains one of the most feared postoperative complications as it is associated with increased mortality rate, decreased quality of life and increased recurrence in local and distant cancer (Chiarello et al. 2022; Weber et al. 2023, Snijders et al. 2012; Ramphal et al. 2018). Thus, further research is necessary to develop new technologies to prevent CAL and effectively manage its consequences.

1.1.1 Phases of Colon Anastomotic Healing

Similar to the other wound healing processes in the body, CAH is categorized into three stages: inflammation, proliferation, and tissue remodelling (Morgan and Shogan 2022)

1.1.1.1 Inflammation

Upon injury, inflammation begins with the recruitment of the platelets to form a fibrin clot, which ceases any bleeding and creates a scaffold for immune cell migration and deposition of matrix proteins (Bosmans et al. 2015). Alongside platelets, granulocytes are the first inflammatory cells that migrate to the anastomotic side which is followed by macrophages (van Helsdingen et al. 2023; Lam et al. 2020; Morgan and Shogan 2022). Neutrophils remove the debris in the early phases of the healing, while protecting the wound from invasion of the pathogens by releasing antimicrobial proteins (Zhang et

al. 2020). Macrophages, which can be resident or derived from infiltrating monocytes, also represent a key part of the immune response due to their diverse and versatile nature (Shi et al. 2018). Their activation can result in two distinct polarization states with different functions, which are named M1 and M2 macrophages (Schepper et al. 2018). Whilst pro-inflammatory M1 macrophages are the dominant type in the initial response to the wounding, anti-inflammatory M2 macrophages contribute to the formation of new tissue in the later stages of the healing (Shi et al. 2018). Though the innate immune responses are the main component of the inflammatory phase, transcriptional signatures of the adaptive immune responses (i.e. T-cell response) have also been detected in a rat anastomosis model (van Helsdingen et al. 2023). One of the prominent cytokines produced by T cells is interferon-gamma (IFNγ), which is known to polarize macrophages into the M1 subtype (Martinez and Gordon 2014). Interestingly, elevated IFNγ levels have been detected in patients with CAL (Qi et al. 2023), however, molecular mechanisms behind its regulation and its roles in CAH and CAL remain unknown. Although immune responses upon anastomotic injury are considered indispensable for proper healing, preoperative inflammation detected in circulation and bowel wall of patients has been associated with CAL indicating that the level and components of the immune response need fine-tuning (Hajjar et al. 2023; Binnebösel et al. 2014; Haghi et al. 2024). Therefore, factors regulating inflammation need detailed investigation.

1.1.1.2 Proliferation

The inflammation phase is followed by a proliferation phase, which is marked by fibroblast activity (Morgan and Shogan 2022). Fibroblasts deposit collagens, which are structural components of extracellular matrix (ECM), and replace the fibrin clot with granulation tissue (Thompson et al. 2006). Angiogenesis and epithelialization have also been reported as important features of the proliferation phase (Zhang et al. 2020). Especially vascular endothelial growth factor (VEGF) and fibroblast growth factor (FGF) have been recognized as key growth factors that play a role in this stage of healing (Morgan and Shogan 2022). While VEGF stimulates angiogenesis by promoting endothelial cell migration and proliferation, FGF stimulates fibroblast proliferation (Rijcken et al. 2014). Adas et al. showed that increasing the expression level of VEGF and FGF has improved CAH (Adas et al. 2011)

indicating that the activity of these growth factors in the proliferation stage is crucial.

1.1.1.3 Tissue Remodelling

The last stage of CAH is tissue remodelling during which ECM undergoes a series of changes to restore the tissue integrity (Morgan and Shogan 2022; Singh et al. 2023). In this stage, type III collagen is replaced with type I collagen, which restores the tensile strength and provides mechanical stability (Lam et al. 2020; Lundy 2014). Stumpf et al reported a lower Type I/III ratio in patients with CAL indicating the critical importance of this conversion (Stumpf et al. 2005). The main regulator of the collagen content and levels within the wound is matrix-metalloproteinases (MMPs). There are 28 different types of MMPs in humans, which can selectively degrade collagens (Laronha and Caldeira 2020; Singh et al. 2023). While their activity is crucial for ECM remodelling, over-expression or -activity of Mmp2, Mmp7, Mmp9, and Mmp13 have been associated with CAL development due to excessive degradation of collagens (Neumann et al. 2018; Shogan et al. 2016; Stumpf et al. 2005; Stumpf et al. 2002). There are several factors involved in the regulation of MMP activity. One of these is tissue inhibitors of MMPs (TIMPs) (Singh et al. 2023). There are four types of TIMPs whose dysregulation has been associated with intestinal wound healing deficiencies (Biel et al. 2024; Marônek et al. 2021). Even though altered levels of TIMP1 and TIMP2 were not observed in patients with CAL (Pasternak et al. 2010), a detailed investigation of their roles on the tissue level has not been conducted before. Another important regulator of MMPs is the microbiome. Mice studies have shown that specific bacteria strains within the microbiome can lead to over degradation of collagens by either inducing MMP expression or by cleaving it into its active form (Shi et al. 2022; Shogan et al. 2016). Recently, these bacteria strains have been also detected in patients with CAL (Jørgensen et al. 2023) further highlighting the possible roles of the microbiome in CAL development. Overall, tissue remodelling is a critical stage of wound healing where the balance between collagen deposition and degradation needs to be tightly regulated by numerous factors. Therefore, the identification and detailed investigation of these factors is crucial.

1.1.1.4 Knowledge Gaps in CAH Processes

Although these wound healing phases are usually described as distinct and temporally confined events, it has been recognized that they overlap and transition gradually (Guo and DiPietro 2010). However, the duration of these phases and their specific signatures have not been studied in detail in the case of CAH. Moreover, the majority of our knowledge on CAH processes has been extrapolated from skin studies (Bosmans et al. 2015; Chadi et al. 2016; Lam et al. 2020; Lee et al. 2018; Lundy 2014), however, significant differences between skin and gut wound healing have been recognized (Bosmans et al. 2015; Chadi et al. 2016; Morgan and Shogan 2022). For example, whilst skin fibroblasts only produce collagen type I and III, in the gastrointestinal (GI) tract, collagen I, III, and V are produced (Thompson et al. 2006; Lundy 2014). Inflammatory response to injury and the function of immune cells also differ between the colon and skin (Alzoghaibi and Zubaidi 2014; Torkvist et al., 2001, Karger). Additionally, in the GI tract, wound healing happens more rapidly than skin most probably due to higher microbial load, and the microbial composition of colon and skin, which has been shown to impact wound healing, is vastly different (Thompson et al. 2006; Lundy 2014). Therefore, factors regulating CAH stages might be colon-specific and can only be identified by analyzing the colonic anastomotic tissues. In line with this, van Helsdinger et al. recently characterized transcriptional signatures of CAH using a rat anastomosis model (van Helsdingen et al. 2023), however, this study analyzed the transcriptional profile of only the first 24 h of CAH. Therefore, more research is needed to fully characterize the CAH processes in detail.

1.1.2 The Role of Intestinal Layers in CAH

Another important factor to consider in CAH is the architecture of the intestinal wall consisting of four main layers: mucosa, submucosa, muscularis propria, and serosa (Rao and Wang 2010). As anastomotic surgery induces an injury in all layers, all of them undergo a healing process for a successful CAH, but only a few studies focused on the individual local roles of the different layers in the healing process. The mucosa layer for example contains the mucus-producing epithelium, the lamina propria, and the muscularis, and mice lacking a functional mucus layer develop CAL (Bosmans et al. 2017). Moreover, recent

studies showed that mucosa-microbiome interaction is one of the factors in CAL development, which further highlights its importance for successful healing (Lee et al. 2018; Shogan et al. 2016; Hajjar et al. 2023; Bachmann et al. 2022; Shi et al. 2022). The underlying submucosa contains collagens and has the greatest tensile strength of the four layers (Thompson et al. 2006; Lundy 2014; Rosendorf et al. 2022) and is thought to be the source of strength in anastomotic tissue (Thompson et al. 2006; Lam et al. 2020; Rosendorf et al. 2022). The muscularis propria consists of mainly smooth muscle cells within a network of collagens (Thompson et al. 2006) but also contains immune and neuronal cell types (Schepper et al. 2018; Mogor et al. 2021), while the serosa contains a thin layer of mesothelial cells covering the muscularis externa (Daams et al. 2013; Thompson et al. 2006). Overall, previous research indicates that these layers have individual cellular compositions, fulfill different roles, and might be differentially regulated during CAH. However, a comprehensive analysis of the different layers during CAH and in CAL has not been conducted.

1.2 Clinical Aspects of CAL

1.2.1 Diagnosis and Treatment

While the majority of CAL is diagnosed within the first two weeks of surgery, about 12 % is diagnosed after the 30th postoperative day (Hyman et al. 2007; Chadi et al. 2016). Early diagnosis of CAL remains challenging since its clinical presentation such as fever, pain, and elevated serum levels of inflammatory markers such as C-reactive protein (CRP) is not CAL-specific, and patients are expected to display these symptoms to a certain extent due to immune responses to surgical injury (Su'a et al. 2017; Komen et al. 2008). Because of this, CAL diagnosis is still delayed, which has been associated with poor outcomes (McDermott et al. 2015). Imaging technologies such as computed tomography scan, contrast enema of the abdomen, and endoscopic examination are some of the standard methods for CAL diagnosis (Chiarello et al. 2022; Vardhan et al. 2023). Recently there has been a significant effort to develop a predictive scoring system that could allow early diagnosis (Tsalikidis et al. 2023). Moreover, search of the last decade identified several potential serum, intraperitoneal fluid, tissue, and microbiome CAL markers using

patient material (Su'a et al. 2017; Wright et al. 2017; Jørgensen et al. 2023). However, further evidence is needed for their implementation as predictive and/or diagnostic tools. Once diagnosed, treatment of CAL is based on the site of the anastomosis and the severity of the leak. Whilst, the small leaks and abscesses can be treated with percutaneous drainage, endoluminal vacuum therapy, or antibiotic treatment, the severe leaks usually require reoperation (Chadi et al. 2016; Chiarello et al. 2022).

1.2.2 Socio-economic Burden

Despite all the advances in the surgical field, the prevalence of CAL has remained unchanged in the last decade, and up to 16 % mortality rate has been reported (Chiarello et al. 2022; Weber et al. 2023). CAL has been associated with decreased quality of life and increased recurrence in local and distant cancer (Snijders et al. 2012; Ramphal et al. 2018). Additionally, CAL-related readmissions to the hospital, longer hospital and intensive care unit stays, and additional interventions increase the medico-economic burden (Flor-Lorente et al. 2023; Hammond et al. 2014). Therefore, more research is needed to develop novel technologies to prevent CAL and to manage its consequences efficiently.

1.2.3 Risk Factors

There are multiple risk factors associated with CAL which can be categorized as preoperative, intraoperative, and perioperative (McDermott et al. 2015). Preoperative risk factors include male gender, old age, smoking, alcohol consumption, preoperative chemotherapy, and other comorbidities such as diabetes mellitus, renal failure, and immunosuppression (Zarnescu et al. 2021). In addition to these, there are several intraoperative risk factors. For example, low colorectal anastomoses, lack of proper blood supply to the surgical side, and longer duration of the operation are known to increase the risk of CAL (Tsalikidis et al. 2023). Lastly, there are numerous perioperative risk factors such as perioperative blood loss, the presence of collagen-degrading bacteria, and the use of non-steroidal anti-inflammatory drugs (NSAIDs) (Zarnescu et al. 2021; Tsalikidis et al. 2023).

1.2.3.1 Non-Steroidal Anti-inflammatory Drugs and CAL

Early Recovery After Surgery (ERAS) protocols have been designed to ensure fast recovery of surgical patients by supporting preoperative organ function and controlling postoperative stress (Gelman et al. 2018). For postoperative pain control, ERAS protocols recommend the replacement of opioids with NSAIDs due to short-term and long-term side effects of opioids such as nausea and vomiting, urinary retention, and intestinal obstruction (Gelman et al. 2018). NSAIDs are a large group of drugs that exert anti-inflammatory, antipyretic, and analgesic effects by blocking cyclooxygenase-1 (COX1) and/or cyclooxygenase-2 (COX2) and thereby preventing prostaglandin (PG) production (Hakkarainen et al. 2015; Vane and Botting 1998). Long-term use of NSAIDs has been associated with GI tract damage (Bjarnason et al. 1993; Lengeling et al. 2003; Maiden et al. 2007). Morever, numerous meta-analyses showed that the use of non-selective NSAIDs, which block both COX1 and COX2, in the immediate post-operative period significantly increases the CAL incidence (Modasi et al. 2019; Huang et al. 2018; Jamjittrong et al. 2020; Smith et al. 2016; Chen et al. 2022). However, reports that did not find any significant effect of postoperative NSAID use on CAL development have been also published (EuroSurg Collaborative 2020; Arron et al. 2020). There are several confounding factors such as the disease category of patients, type of the drug, dosage, and duration of the treatment that might explain these contradictory results (Sun and Feng 2020). Currently, a consensus on NSAID use after surgery has not been reached and postoperative NSAID use is not avoided worldwide most probably due to conflicting clinical results and unexplained pathophysiology. Therefore, understanding the mechanism of NSAIDs-related leakage has clinical importance and implications.

In line with this, recent studies have analyzed the effects of NSAIDs on CAL development using animal models. Reisinger et al. showed that diclofenac sodium (DCF), which is a non-selective NSAID, leads to CAL in the proximal colon in mice (Reisinger et al. 2017). Interestingly, Yauw et al. showed that DCF treatment causes CAL in the proximal colon but not in the distal colon and a delay in its administration by 2 days prevents CAL in the proximal colon (Yauw et al. 2015). Albeit non-selective, DCF is known to have a strong COX2 inhibiting activity (Kozlowska et al. 2017), therefore, researchers speculated that COX2

rather than COX1 inhibition could be the reason behind higher CAL rates. Confirming this a selective COX2 inhibitor was associated with CAL development in a rat anastomosis model and *COX2*$^{-/-}$ mice showed higher rates of CAL (Cahill et al. 2004; Reisinger et al. 2017). Moreover, the prevalence of CAL was found to be higher in patients with low COX2 expression due to genetic polymorphism (Reisinger et al. 2017). However, according to clinical studies, while COX2 inhibitors increase the risk of CAL development, this effect is not statistically significant (Arron et al. 2020; Jamjittrong et al. 2020; Smith et al. 2016). Currently, studies regarding the mechanisms behind NSAID-induced CAL remain limited. A reduction in anastomotic bursting pressure and collagen content was reported in a DCF-induced CAL rat model suggesting that DCF treatment might intervene with collagen regulation (Inan et al. 2006). Yauw et al. provided an alternative explanation by showing that the bile toxicity caused by DCF metabolites leads to leakage development, which could be prevented by inhibiting the reactivation of the DCF metabolites in the gut (Yauw et al. 2018a; Yauw et al. 2018b). Recent studies have also speculated that a reduction in PG levels due to NSAID injection might be causative for CAL development (Huang et al. 2018; Jamjittrong et al. 2020; Reisinger et al. 2017). However, cellular, and molecular changes in the anastomotic tissue upon NSAID administration and the role of PGs in CAH have not been studied in detail. Altogether, these studies indicate that the role of NSAIDs in CAL development is multi-factorial. In-depth analyses are needed to identify the conditions when NSAIDs are detrimental to CAH and to understand the underlying pathophysiology.

1.3 Prostaglandins and Intestinal Wound Healing

1.3.1 Prostaglandin Production and Signalling

Prostaglandins (PGs) are potent lipid mediators that are derived from arachidonic acid (AA), which is an essential fatty acid (Funk 2001; Gilman and Limesand 2021). AAs are present in phospholipids of the cell membrane, which are cleaved and released into the cytosol by phospholipase A2 (PLA2) (Gilman and Limesand 2021). Free AAs are then

converted into Prostaglandin H2 (PGH2) by COX1 and COX2 enzymes at the endoplasmic reticulum and nuclear membrane (Funk 2001). Importantly COX1 is constitutively active and responsible for providing basal levels of PGs, whereas COX2 is induced under inflammatory conditions (Funk 2001; Tilley et al. 2001). Upon production, PGH2 acts as an intermediate from which different PGs are derived by specific enzymes and they signal through distinct receptors (Funk 2001) **(Figure 1)**. These PGs are produced by most cells and function in an autocrine and paracrine manner (Funk 2001). They are generated when required and several signals such as injury, release of specific cytokines, and growth factors might trigger their production (Funk 2001).

1.3.2 Types and Functions of Prostaglandins

There are five different PGs with distinct functions, namely Thromboxane A2 (TXA2), PGI2, PGF2α, PGD2, and PGE2 **(Figure 1)**.

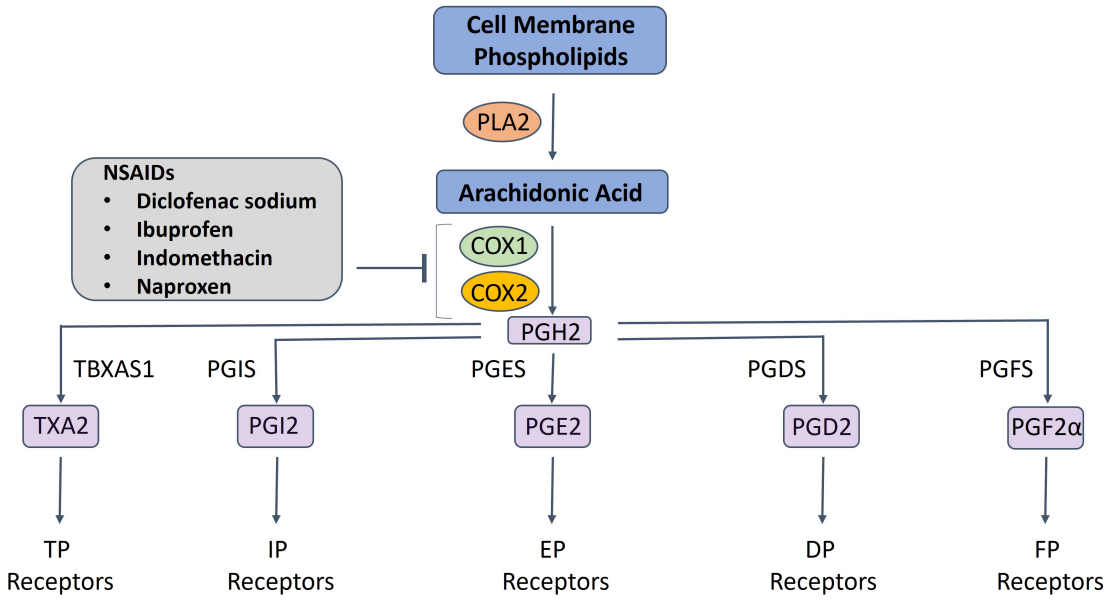

Fig 1: **Prostaglandin Synthesis Pathway** Prostaglandins (PGs) are synthesized via a multi-step process in which membrane phospholipids are first converted into arachidonic acid, which is then used to produce PGH2. TXA2, PGI2, PGF2α, PGD2, and PGE2 are then derived from PGH2 by the enzymatic activity of TBXAS1, PGIS, PGFS, PGDS and PGES, respectively. These PGs are extracellular mediators that function via their specific receptors as indicated.

1. TXA2: It is generated by Thromboxane A Synthase 1 (TBXAS1) and signals through a cell surface receptor TP, which induces platelet aggregation and constriction of blood vessels upon stimulation (Coleman et al. 1994).

2. PGI2: It is produced by the activity of Prostacyclin Synthase (PGIS) and acts on its receptor IP (Funk 2001). Signalling of its receptor leads to vasodilation and inhibition of platelet aggregation (Stitham et al. 2011). However, recently it was shown that PGI2 also increases intestinal epithelial barrier integrity *in vitro* and PGI2 supplementation can prevent epithelial damage in mouse models of IBD (Pochard et al. 2021). Moreover, the immunomodulatory effects of PGI2 have been also recognized (Dorris and Peebles 2012).

3. PGF2α: PGF2α is synthesized by Prostaglandin F Synthase (PGFS) and binds to its receptor called FP (Funk 2001). Although our knowledge of its roles in intestinal wound healing is limited, a recent study showed low levels of PGF2α in patients with IBD and its secretion restores the intestinal barrier *in vitro* (Coquenlorge et al. 2016).

4. PGD2: PGD2 is made by Prostaglandin D Synthase (PGDS) and signals via DP1 and DP2 receptors. (Markovič et al. 2017). Hayashi et al. showed that DP1 signalling enhances intestinal barrier integrity *in vivo* by stimulating mucus production from goblet cells (Hayashi et al. 2023). For DP2, Sturm et al showed that blocking DP2 signalling improved wound healing in an IBD mouse model (Sturm et al. 2014).

5. PGE2: PGE2 is synthesized by Prostaglandin E Synthases (PGES) and signals through four different receptors, namely EP1, EP2, EP3, and EP4 (Markovič et al. 2017; Funk 2001). These receptors are G-protein coupled receptors which induce distinct biological outcomes by modulating intracellular calcium or cAMP levels (Markovič et al. 2017; Cheng et al. 2021). They are expressed across different cell types and regulate various processes such as vascular pressure, cytokine release, immune response, and epithelial cell proliferation (Cheng et al. 2021; Gilman and Limesand 2021). Due to the broad influence of PGE2 on biological systems under hemostasis, and disease state, its roles in intestinal wound healing including CAH have been extensively researched (Cheng et al. 2021; Gilman and Limesand 2021).

1.3.3 PGE2 and Intestinal Wound Healing

Although the functions of PGE2 are multifaceted, their role in inflammation during wound healing has been the major focus of many studies. PGE2 can act pro-inflammatory since it can promote inflammation by inhibiting regulatory T-cells and stimulating T helper cell 17 differentiation (Yao et al. 2009; Crittenden et al. 2021; Boniface et al. 2009). On the contrary, PGE2-EP2/4 signalling can also suppress immune response including T-cell activity, and alleviate chronic inflammation in mice indicating its dual effects (Pinchuk et al. 2011; Gao et al. 2021; Kabashima et al. 2002; Mehta et al. 2023). It has also been reported that the role of PGE2 during wound healing is not limited to immune regulation and it can impact epithelial cell regeneration by promoting stem cell expansion and preventing epithelial cell death via EP4 signalling (Lee et al. 2022; Miyoshi et al. 2017; Patankar et al. 2021). Due to these findings, PGE2 is considered essential for successful wound healing, however, it is important to note that when prolonged this signalling can be detrimental to epithelial regeneration highlighting the importance of its regulation (Jain et al. 2018; Li et al. 2018). The role of PGE2 in CAH has also been reported. Reisinger et al showed that anastomotic leakage rates in *COX2*$^{-/-}$ mice can be reduced with PGE2 supplementation (Reisinger et al. 2017). However, its protective effect against CAL has not been tested in another case including NSAID-induced CAL.

1.4 Aims and Objectives of the Thesis

1.4.1 Aim 1: Identification of Layer-Specific Transcriptional Changes in CAH and CAL

Despite of improvements in the perioperative management, surgical techniques, and diagnostic tools, rates of CAL and associated morbidity have not changed suggesting that the cause of CAL might be biological rather than technical (Alverdy and Schardey 2021). Hence, in recent years, there has been an increase in studies aiming to identify CAL mechanisms to prevent/minimize CAL and/or its consequences. However, these attempts have not been successful mainly because the mechanisms of CAH are not well understood, and

molecular pathways within the intestinal layers in CAH and CAL have not been defined in detail (Bosmans et al. 2015; Lam et al. 2020). Hence, the first aim of this thesis was to fill this knowledge gap by achieving two objectives:

Objective 1: Comprehensive transcriptional description of the CAH in mucosa/submucosa (M/SM) and muscularis externa (ME) layers of the colon anastomotic tissues.

Objective 2: Analysis of transcriptional pathways within M/SM and ME layers in tissue with CAL

1.4.2 Aim 2: Investigation of Molecular Mechanisms of NSAID-induced CAL

Recent studies have identified postoperative NSAID use as a potential risk factor for CAL development (Modasi et al. 2019; Huang et al. 2018; Jamjittrong et al. 2020; Smith et al. 2016; Chen et al. 2022). Consequently, there has been an increase in studies investigating the biological reasons behind this observation, however, CAH pathways affected by the NSAID treatment have not been completely mapped (Reisinger et al. 2017; Yauw et al. 2018a; Yauw et al. 2018b; Yauw et al. 2015). As discussed above, PGs, whose levels are reduced as a result of NSAID treatments, have been associated with improved wound healing. Especially PGE2 has gained attention in the last decade owing to its multifaceted beneficial effects on intestinal wound healing (Gilman and Limesand 2021). Therefore, the lack of PGE2 as a result of NSAID treatment has been forwarded as a possible explanation for NSAID-induced CAL development (Reisinger et al. 2017). However, the roles of PGE2 in NSAID-(un)related CAL have not been explored before. Hence, the second aim of this study includes the following two objectives:

Objective 1: Analysing the cellular and transcriptional profile of the NSAID-induced CAL using a mouse model and identifying causative cellular pathways involved in NSAID-related wound healing deficiencies.

Objective 2: Testing the role of PGE2 in preventing NSAID-(un)related CAL using NSAID-induced and spontaneously occurring CAL mouse models.

2 Materials and Methods

2.1 Materials

2.1.1 Consumables

Reagent / Kit	Company	Cat Number
SPE Cartridges (C18) (6 ml)	Cayman chemical	400020-25
Miltenyi Columns	Miltenyi	130-042-201
8-0 Vicryl sutures	Ethicon	V1027G
5-0 Vicryl sutures	Ethicon	V303
5-0 Silk sutures	Assut Europe	KX503 AP
0.2 µm Syringe Filter Unit	Merck Medical Millex	10795534
Glass Microscopy Slides	VWR	631-1550
Tissue-Tek O.C.T. Compound	Sakura	4583
ECOSURF SA-9	PanReac AppliChem	A9779
ImmunoMount	Immunochemistry Technologies	AR-6516-01
Cover Glass 24 x 60 mm	Engelbrecht	K12460
Framestar 480, 96 well semiskirted qPCR Plate	Bioké	4TI-0952
Adhesive PCR plate seals for framestar plates	Bioké	4TI-0500/12
EasyStrainer 70 µM	Grenier Bio-One	542070
PCR tubes (0,2 mL strips 8 + caps	VWR	732-4809
Syringes (1 mL)	BD Plastipak	303172
25G Needles	BD Microlance	300600
Prostaglandin E2 ELISA Kit - Mono-clonal	Cayman chemical	514010-96
Miltenyi Dead Cell Removal kit	Miltenyi	130-090-101
Rneasy Minikit	Qiagen	74106

SensiFAST SYBR® No-ROX Kit	GC-Biotech	BIO-98020
Glucose-D	Merck	108337
Cremophor EL	MedChem Express	HY-Y1890
RNA later	Invitrogen	AM7020
Potassium Phosphate Anhydrous	Merck	P-5629
Ultrapure EDTA 0.5 M pH 8.0	Invitrogen	15575-020
DTT	Sigma	D9779
Pen/Strep 100x	Gibco	15140122
GlutaMAX Supplement	Invitrogen	35050-038
FCS	Bodinco	5010
RPMI1640 -L/glut	Gibco	31870-074
HEPES	Gibco	15630-056
Liberase TM	Roche	5401119001
Dnase	Roche	11284932001
NaN3	Merck	822335
BSA	Sigma	A7906
Methanol	Meck	106009
Ethanol	Orphi Farma	
Sodium acetate	Sigma	S5636
Ethyl acetate	Merck	868
Random Hexamer primers	Promega	SO142
Oligo-dT primers (oligo(dT)14VN custom made) (TTTTTTTTTTTTTTVN)	Invitrogen	
dNTPs	Fisher Scientific	28-4065-51
Revertaid transcriptase	Fermentas	EP0442
Ribolock RNAse inhibitor	Fermentas	EO0382
DMSO	Sigma	D8418

2.1.2 Antibodies

Antibody	Application	Company	Cat Number
CD45-BV510	Flow Cytometry	Biolegend	103137
Ly6G-FITC	Flow Cytometry	Biolegend	127606
Ly6C-BV605	Flow Cytometry	Biolegend	128035
CD11b-PeCy7	Flow Cytometry	Biolegend	101215
F4/80-BV421	Flow Cytometry	Biolegend	123131
EP2-AF647	Flow Cytometry	Bioss Antibodies	bs-4196R-A647
EP4-PE	Flow Cytometry	Bioss Antibodies	bs-24918R-PE
Zombie NIR	Flow Cytometry	Biolegend	423105
CD45-PB	Flow Cytometry	Biolegend	103125/103126
CD8-Pecy7	Flow Cytometry	Biolegend	100721/100722
CD4-BV785	Flow Cytometry	Biolegend	100551
CD3-FITC	Flow Cytometry	Biolegend	100203
CD19-AF700	Flow Cytometry	Biolegend	115527
70NK1.1-PE/Dazzle	Flow Cytometry	Biolegend	108747
TruStain FcX	Flow Cytometry	Biolegend	101319
Ly6G	Immunofluorescence	Biolegend	127602
Iba-1	Immunofluorescence	Synaptic Sytems	234009
Anti-Rat IgG–AF647	Immunofluorescence	Biozol	712-605-153
Anti-Rat IgG-AF488	Immunofluorescence	Invitrogen	A21208
DAPI	Immunofluorescence	Invitrogen	D1306

2.1.3 Drugs

Drugs	Company	Cat Number
Diclofenac Sodium (Salt)	Cayman chemical	70680
16,16-dimethyl Prostaglandin E2	Cayman chemical	14750
SW033291	Cayman chemical	18040
Indomethacin	Sigma	I-7378
Tralieve	Dechra	
Tramadol	Aliud Pharma	
Baytril	Bayer	
Buprenorphine	Ecuphar N.V.	

2.1.4 Software Applications

Softwares	Company
CFX Maestro 5.0	CFX Maestro 5.0 Biorad
LinReg PCR 2021.1	Amsterdam UMC
FlowJo V10	BD Bioscience
FACS Diva	Canto II BD Bioscience
Image J	Open Source
RStudio	Open Source
Partek Flow	Partek
Prism 10.1.2	Graph Pad 10.1.2
Citavi	Swiss Academic Software GmbH

2.1.5 Devices

Devices	Company
The BioRad® CFX96™	BioRad
PCR Thermocycler	MJ Research

NanoDrop 1000	ThermoScientific
Sonicator	Virtis Virsonic 100
Incubating Mini Shaker	VWR
Precellys Homogenizer	Bertin Technologies
Tapestation	Agilent

2.2 Methods

2.2.1 Mice

For the establishment of the diclofenac sodium (DCF)-induced CAL model, 3' bulk RNA-Seq analysis of the DCF-induced CAL model, nanospray desorption electrospray ionization mass spectrometry imaging (nano-DESI MSI) of the anastomotic tissues, and SW033291 supplementation (2.5 kg/mg dosing), female C57BL6/J inbred mice (8–9 weeks old) were purchased from Janvier (Saint Berthevin Cedex, France). Mice were acclimated for 1 week before performing experiments. Mice were maintained under specific pathogen-free (SPF) conditions with a 12 h dark/light illumination cycle, temperature of 20–25 °C, humidity of 45–65 %, standard rodent food and tap water ad libitum at the University Hospital Bonn, Germany. State Agency for Nature, Environment and Consumer Protection (LANUV) approved the experiments (81-02.04.2021.A055 and 81-02.04.2020.A098).

For DCF-induced CAL experiments involving *Rag1*$^{-/-}$ mice, female B6.129S7-Rag < tm1Mom>/J [RAG1-/-] mice were purchased from Jackson Laboratories (Bar Harbor, ME, USA0 and further bred in the animal facility of the Academic Medical Center, Amsterdam. As *Rag1*$^{+/+}$ (wild-type) controls, female C57Bl/6nCrl inbred mice (8-9 weeks old) were purchased from Charles River Laboratories (Maastricht, The Netherlands). For flow cytometry (FC) and ELISA analysis of colon anastomosis and naive tissues, and 16,16-dimethyl Prostaglandin E2 (dmPGE2) and SW033291 supplementation (5 mg/kg and 10 mg/kg dosing) experiments, female C57Bl/6nCrl inbred mice (8–9 weeks old) were purchased from Charles River Laboratories (Maastricht, the Netherlands). Mice were acclimated for 1 week before performing experiments. The animals were housed under SPF conditions in the animal facility at the Amsterdam University Medical Centers,

location AMC, Amsterdam, the Netherlands. Animals were maintained on a 12 h light/dark cycle with a constant temperature (20 ± 2 °C) and humidity (55 %) conditions and ad libitum drinking water and chow. Experiments were approved by the Dutch Central Animal Experiments Committee. Individual experiments were revised and approved by the Animal Research Ethics Committee of the University of Amsterdam (DMO20-11104-1).

2.2.2 Anastomotic Surgery

For the experiments approved by University Hospital Bonn, Germany, mice were injected with 10 mg/kg tramadol sub-cutaneously (s.c.) 15 minutes before operation and were anesthetized by inhalation of isoflurane (2 %, 3-5 L/min flow). After the median laparotomy, the cecum and proximal colon were located. The proximal colon (approximately 0.5 cm away from the cecum), was cut and an end-to-end anastomosis was constructed using 8-0 Vicryl sutures. The colon was placed back, and the peritoneum and abdomen were sutured with 5-0 two independent sutures. After surgery, mice were inspected, and their well-being was scored twice per day. Drinking water was supplied with 1 mg/kg tramadol until the mice were sacrificed.

For the experiments approved by Academic Medical Center, Amsterdam, mice were injected with 5 mg/kg Baytril and 0.1 mg/kg buprenorphine s.c. 15 minutes before surgery. Mice anesthetized by inhalation of isoflurane (2-4 %, 2 L/min flow) and after median laparotomy, the cecum and proximal colon were located. The rest of the surgery was performed as described above. 8 h and 24 h after the operation, the mice were s.c. injected with 0.1 mg/kg buprenorphine.

2.2.3 Colon Anastomotic Leakage Mouse Models

2.2.3.1 DCF-induced CAL Mouse Model

The DCF-induced CAL model was adapted from a previous study in which the mice underwent proximal colon surgery as described above to create an end-to-end anastomosis with 8 interrupted sutures (Reisinger et al. 2017). Mice were administered 10 mg/kg DCF bidaily (b.i.d) via intraperitoneal (i.p.) injection starting from one day before surgery until the end of the experiments.

2.2.3.2 Insufficient Suture CAL Mouse Model

The insufficient suture CAL model was adapted from a previous study, in which an anastomosis was created with 6 interrupted sutures (Hove et al. 2023).

2.2.4 Anastomotic Complication Scoring

Anastomotic complications were scored based on the scoring system established before (Bosmans et al. 2016; van Helsdingen et al. 2023): 0) No adhesions and abnormalities; 1) Adhesions to the fat pad, clean anastomosis underneath; 2) Adhesion to intestinal loop, abdominal wall or other organs; 3) Anastomotic defect found underneath adhesion, no other abnormalities; 4) Sign of possible contamination (e.g., small abscesses); 5) Clear anastomotic complication; spread of pus, obstruction at the anastomosis, a sign of peritonitis; 6) Fecal peritonitis/Death due to peritonitis (Figure 2). Anastomotic complication score (ACS) 0-2, ACS 3-4, and ACS 5-6 are accepted as colon anastomotic healing (CAH), moderate colon anastomotic leakage (CAL), and severe CAL, respectively.

2.2.5 Drug Preparations and *In Vivo* Supplementations

2.2.5.1 Diclofenac Sodium Salt

DCF was dissolved in saline at 1 mg/mL concentration and sterile filtered with a 0.2 µm filter. 200 µL of DCF solution was injected per 20 g of mouse to achieve a 10 mg/kg dosing.

2.2.5.2 16,16-dimethyl Prostaglandin E2

dmPGE2 was dissolved in absolute ethanol to achieve a 1 mg/mL concentration. To achieve dmPGE2-DCF combined treatment, dmPGE2 stock solution was diluted in 2 ug/200 µL concentration using 1 mg/kg DCF solution as solvent. 200 µL of volume was injected per 20 g of mouse to achieve 100 µg/kg dmPGE2 and 10 mg/kg DCF dosing.

Mice underwent 8 suture proximal anastomotic surgery and were treated with either 10 mg/kg DCF + 100 µg/kg dmPGE2 (n=19) or 10 mg/kg DCF + vehicle (n=17) solutions b.i.d via i.p. injection starting from one day before surgery until the end of the experiment at postoperative day (POD) 3.

2.2.5.3 SW033921

SW033291 was dissolved in DMSO in 25 mg/mL concentration. It was further diluted using a solvent of 10 % ethanol, 5 % cremophor EL, 5 % dextrose in water to achieve 1 mg/kg concentration of drug solution. 200 µL was injected to 20g of mouse to achieve 10 mg/kg dosing. Adjustments were made in drug concentrations to achieve 5 mg/kg and 2.5 mg/kg dosing.

Insufficient suture CAL mouse model was treated with SW033291 (n=8 for 2.5 mg/kg, and n=11 for 5 mg/kg and 10 mg/kg dosing) or vehicle (n=8 for 2.5 mg/kg, n=12 for 5 mg/kg, and n=11 for 10 mg/kg dosing) b.i.d via i.p. injection starting at the day of surgery until the end of the experiment at POD5.

2.2.6 Mechanical Layer Separation of Colon Anastomotic and Naive Tissues

Anastomotic tissues and additional naive proximal colon tissues from non-operated control mice (n=4-8) were collected. They were cut open longitudinally and pinned to an agar-covered plate. Pre-cooled, oxygenated Krebs-Henseleit buffer (126 mM NaCl; 2.5 mM KCl: 25 mM NaHCO3; 1.2 mM NaH2PO4; 1.2 mM MgCl2; 2.5 mM CaCl2, 100 IU/ml Pen, 100 IU/ml Strep and 2.5 µg/ml Amphotericin) was used to wash the tissues to remove feces. Then the buffer was removed and RNAlater was poured over the tissues. Using forceps, the mucosa and submucosa (M/SM) were separated from and muscularis externa including serosa (ME) **(Figure 2)**. After separation, the tissues were stored in RNAlater for 48h at 4 ^{0}C before the RNA isolation.

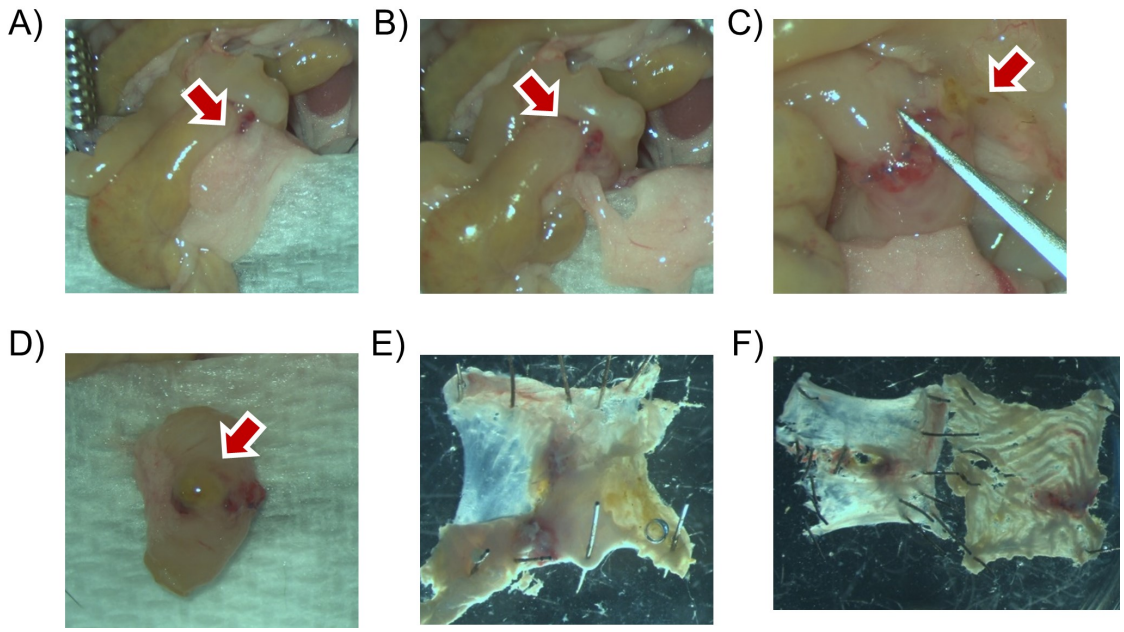

Fig 2: **Step-by-step illustration of layer separation process. A-B)** Anastomosis is identified, and adhesions are removed. The red arrows indicate the location of the anastomosis and the adhesions. **C)** CAL is detected as shown with the red arrow, and tissue is scored. **D)** 1 cm colon including the anastomosis is removed. The arrow indicates the CAL. **E)** The colon is cut open longitudinally, pinned, and immersed into ice cold RNAlater. M/SM is pulled away from the ME using forceps. **F)** M/SM and ME are separated successfully with minor defects in the tissue. ME is shown on the left and M/SM shown on the right.

2.2.7 RNA Isolation

Total RNA was isolated from the samples using the RNeasy Mini Kit based on the manufacturer's instructions. For the homogenization step, the Precellys homogenizer was used at 5000 RPM for 30 seconds. The samples were kept on ice throughout the extraction process. RNA concentrations were measured using the NanoDrop 1000 spectrophotometer and quality was assessed using the Agilent 2200 Tapestation. RNA samples with an RNA Integrity Number (RIN) score of ≥7 were analyzed with bulk mRNA sequencing.

2.2.8 Elisa for Tissue PGE2 Measurement

About 0.5 cm of anastomotic or naive proximal tissues were harvested and rinsed in ice-cold PBS, snap-frozen in liquid nitrogen, and stored at -80 ^{0}C until the measurement. PGE2 was purified and measured in 1:1000 dilution according to the manufacturer's instructions. Data was normalized to the tissue weight recorded at the time of collection.

2.2.9 Nanospray Desorption Electrospray Ionization Mass Spectrometry (nano-DESI MSI)

Anastomotic tissues were harvested at POD1 and snap-frozen with liquid propane. Water was used to mount the tissue on the cryotome specimen holder. Tissued were cryosectioned onto glass slides in 14 µm thickness and sections were stored at -80 until imaging.

MSI experiments were conducted using pneumatically assisted nanospray desorption electrospray ionization (PA nano-DESI). The PA nano-DESI probe was designed according to Duncan et al. with 50/150 µm I.D./O.D. fused silica capillaries (Polymicro Technologies, USA) (Duncan et al. 2017). The solvent used was acetonitrile: methanol 9:1 v/v with 0.1 % formic acid and 10 ppm 107Ag+ and was delivered at 0.5 µL min-1 through a syringe pump (Legato 180, KD Scientific, USA). For stable solvent flow through the capillaries, a backpressure of ~4 bar was used with nitrogen gas. The solvent contained isotopically la-

beled standards for signal normalization. Specifically, PGF2a-d9 and arachidonic acid-d8 were spiked at 0.5 and 2 µM, respectively (Cayman Chemicals, USA). Thin tissue sections (14 µm) were thaw-mounted on glass microscope slides and analyzed with PA nano-DESI MSI. The sample was moving under the PA nano-DESI probe at 0.02 mm s-1 along the x-axis and at a step size of 100 µm along the y-axis using motorized X-Y-Z stages (Zaber Technologies Inc, Canada). A QExactive mass spectrometer (Thermo Fisher Scientific, Germany) was used, and data were recorded using a full scan (m/z 189-1500) and a SIM scan (m/z 441-473) with a resolution of 140000, ion transfer capillary temperature of 300 °C, AGC target of 1e6 and maximum injection time of 300 ms. Electrospray ionization was facilitated using 3.2 kV in the positive ion mode. The final pixel size of the ion images was ~40 x 100 µm2.

Data and region of interest (ROI) analysis was done using in-house MATLAB scripts and Ion-to-Image (Lillja et al. 2023). For ion image generation and ROI analysis, the data from endogenous analytes were normalized to the signal of appropriate internal standards. Arachidonic acid, DHA, Resolving D-series, HETE (all isomers), and LTA4 were normalized to the signal of arachidonic acid-d8 while PGE2/PGD2 and PGF2α to the signal of PGF2α-d9. Annotations were based on accurate mass and searches on databases (HMDB, Metlin).

For the fold change analysis, the average of the normalized signal in the ROI within unaffected, i.e. not operated, M/SM, ME and anastomotic region was calculated. For each molecule analyzed, the average signal obtained within the anastomotic region was divided by the mean of the average signal within the M/SM and ME regions.

2.2.10 Flow Cytometry Analysis

Anastomotic tissues or naive proximal tissues were harvested and washed in an ice-cold complete medium (CM) made up of RPMI containing 10 % FCS, 5 % Pen/Strep, 5 % L-glutamine, and 0.15 % HEPES. To remove epithelial cells, tissues were incubated in 2 mL of strip medium (CM containing 1 % 0.5 M EDTA and 1 % 0.5 M DTT) for 10 min-

utes at 37 ^{0}C in a shaker. After incubation, samples were washed two times with CM and incubated in 2 mL of CM containing 4 % Liberase TM and 0.1 % DNase at 37 ^{0}C in a shaker for 20 minutes for digestion. After the incubation, 2 mL of ice-cold CM was added, and the samples were passed through 70 µm strainers. Samples were then centrifuged at 600 g for 5 minutes at 4 ^{0}C and the supernatant was discarded. Dead cells were removed using the Miltenyi Dead Cell removal kit according to the manufacturer's instructions. Samples were then centrifuged at 600 g for 5 minutes at 4 ^{0}C, and the supernatant was discarded. Cells were first blocked with Fc block (1:50) for 10 mins on ice followed by dead cell staining using Zombie NIR (1:500) at room temperature for 15 mins. After dead cell staining, surface staining was performed with CD45-BV510 (1:100), CD45-PB (1:100), CD8-Pecy7 (1:50), CD4-BV785 (1:80), CD3-FITC (1:100), CD19-AF700 (1:50), NK1.1-PE/Dazzle (1:50), Ly6G-FITC (1:50), Ly6C-BV605 (1:200), CD11b-PeCy7 (1:50), F4/80-BV421 (1:80), EP2-AF647 (1:100), and EP4-PE (1:50), and samples were incubated on ice for 30 mins. Between each step, the samples were washed using FACS buffer, which is made up of PBS containing 0.5 % BSA, 0.01 % NaN3, and 0.3 mM EDTA. After centrifuging at 600 g for 5 minutes at 4 ^{0}C, cells were resuspended with 300 µL of FACS buffer for acquisition.

Data analysis was performed using FlowJo (V10). Forward scatter area (FSC-A) versus side scatter area (SSC-A) gating was used to eliminate cell debris. After singlets were selected, dead cells were excluded based on Zombie NIR staining. The rest of the gating strategy is described in the figure legends.

2.2.11 Bulk mRNA Sequencing, Statistical Data Analysis and Visualization

RNA-Seq libraries were prepared with QuantSeq 3'-mRNA Library Prep kit (Lexogen, Greenland, NH, USA) by the Genomics Core Facility of the University Hospital Bonn. Barcoded samples were sequenced on the Illumina HiSeq 2500 Instrument (50 bp single-end, 10 M reads). Raw data from the RNA-Seq was analyzed with "Partek Flow" software (Lexogen pipeline 12,112,017). The pipeline trimmed unique molecular identifiers (UMIs) and adapter sequences, aligned the reads with star2.5.3, and counted the genes with Feature-

Counting. Ensemble transcripts release 99 for mm10 mouse alignment was used as the reference genome. Unnormalized counts were downloaded for the subsequent bioinformatics analyses. Differential gene expression (DEG) analysis of the annotated raw data was performed using Bioconductor package DESeq2 (1.40.2) using Rstudio (2023.06.0, Build 421). M/SM and ME layers were analyzed separately. Comparisons were made between different time points and between CAH and CAL samples using the contrast function, where the Wald statistic and the associated P values were calculated. Benjamini–Hochberg-adjusted P values ≤ 0.05 were considered significant. Only coding genes were included in the analysis. ClusterProfiler (4.8.2) (Wu et al. 2021; Yu et al. 2012) was used for gene set enrichment (GSE) and GeneOntology (GO) analysis. ggplot2 (3.4.3), DOSE (3.26.1) (Yu et al. 2015), tidyverse (2.0.0) (Wickham et al. 2019), AnnotationDbi (1.62.2), org.Mm.eg.db (3.17.0), forcats (1.0.0), RColorBrewer (1.1-3) and pheatmap (1.0.12) packages were used to visualize the data.

2.2.12 Statistical Analysis

The statistical analysis was performed with GraphPad Prism version 10.1.2 (324) software. The values are expressed as mean ± SEM (standard error of the mean). The significance was assessed by using either unpaired t-tests, one-way multiple comparison ANOVA, Kruskal Wallis, Chi-square, or the Mantel COX and correlation tests. A normality test was applied before choosing the type of statistical test. The significance levels were indicated as $p \leq 0.05$ (*), $p \leq 0.01$ (**), and $p \leq 0.001$ (***), $p \leq 0.0001$ (****).

3 Results

3.1 Identification of Layer-Specific Transcriptional Changes in CAH and CAL in mice

Result Section 3.1 of the thesis has been published as a preprint under the title of “Layer-specific Transcriptional Signatures of Colon Anastomotic Healing and Leakage in Mice (Sengul et al. 2024)”

3.1.1 Transcriptional description of CAH in mucosa/submucosa and muscularis externa of the colon anastomotic tissues using a mouse model

3.1.1.1 Validation of successful intestinal layer separation

To analyze the healing processes at different time points, we used a mouse model in which an end-to-end proximal colon anastomosis was constructed with 8 sutures. 6 h, 24 h, and 72 h after surgery, we sacrificed the mice and assessed the anastomotic complication score (ACS). At 6 h and 24 h, ACS was 1-2, indicating no observable anastomotic defects **(Figure 3A)**. At 72 h, 50 % of the mice (n=4) showed ACS 1 or 2, and 50 % (n=4) had ACS 3 or 4 which corresponds to anastomotic defect and/or abscess formation, hence, hereafter, the mice with ACS 3-4 will be referred to as moderate CAL **(Figure 3B)**.

Next, we separated the mucosa and submucosa (M/SM) layer of the anastomotic tissues from the muscularis externa and serosa (ME) layer **(Figure 2)**. As control samples, we obtained M/SM and ME from non-operated naive proximal colon samples. After performing 3’ bulk RNA-Seq, we first assessed whether M/SM and ME were separated successfully. The M/SM-specific genes *Muc2* and *Vil1* were significantly higher in the M/SM compared to the ME layer. In contrast, *Acta2* (smooth muscle cell marker (Chen et al. 2023)), *Tuba1a* (alpha-tubulin marker (Aiken et al. 2017)) and *Uchl1* (enteric neuron marker PGP9.5 (Blair et al. 2012)) expression were significantly higher in the ME compared to the M/SM **(Figure 3C)**. Although detectable levels of *Muc2* and *Vil1* within the ME samples might indicate minor cross-contamination, their difference between the layers was significant indicating that the layer separation was successful. Interestingly, although the granulation tissue developing at the anastomotic site spans both layers in vivo, it remained mainly attached

to the ME after mechanical separation **(Figure 2)**. In line, we detected higher levels of *Fn1* (fibronectin marker), which plays a role in granulation tissue formation (Lenselink 2015), and *Ptprc* (CD45, a pan-immune cell marker) transcripts in the ME compared to M/SM (**Figure 3C**).

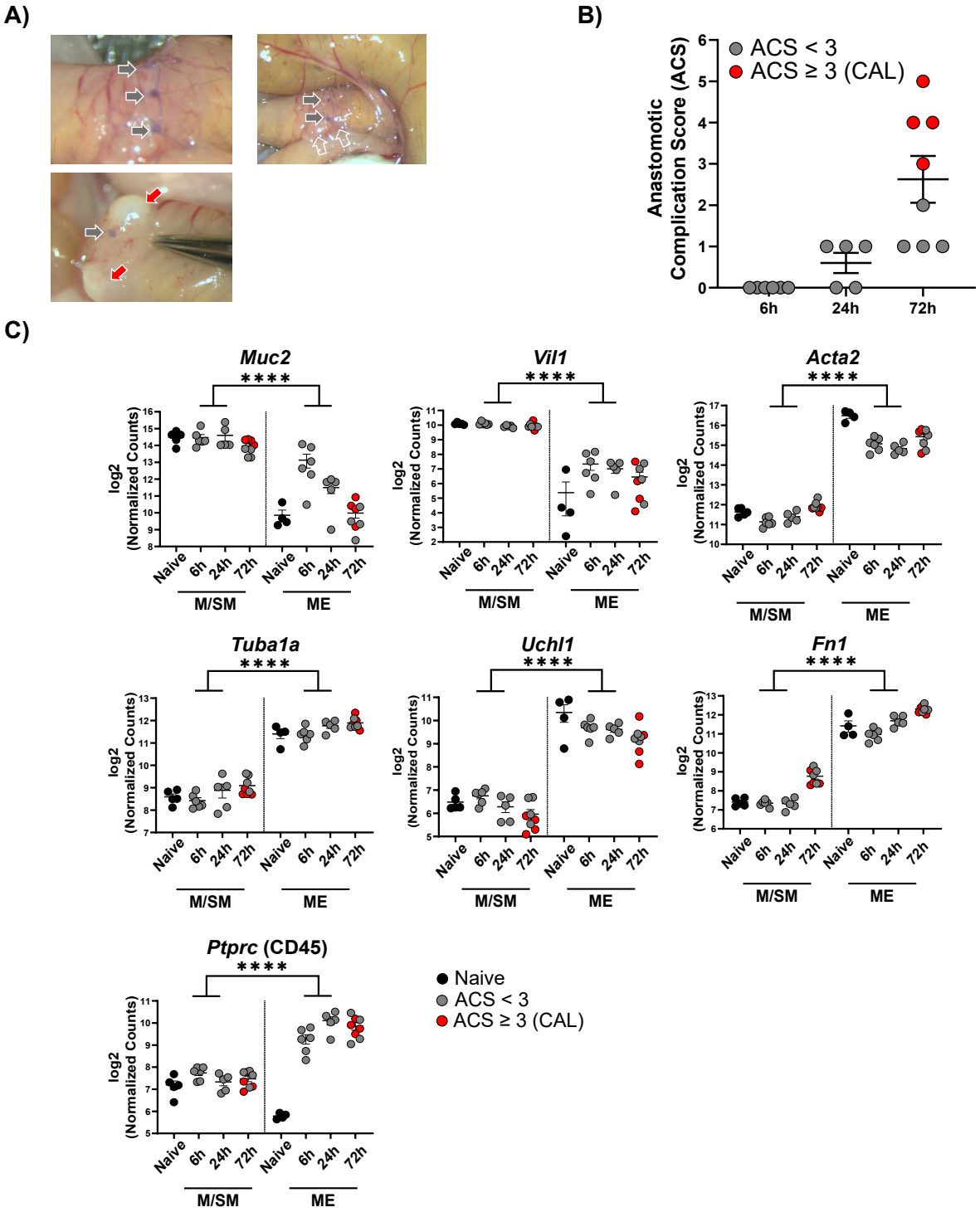

Fig 3: **ACS of the mice and analysis of layer separation efficiency.** Mice underwent anastomotic surgery and were euthanized at different postoperative time points. **A)** Representative images for anastomotic complication score (ACS) 0 (left-top), ACS 2 (right-top) and ACS 4 (bottom left). Arrows point towards single sutures (grey), abscesses (red), and adhesions (clear). **B)** ACS of the mice included in this study. **C)** Comparison of the expression level of the M/SM- and ME-specific genes to determine the quality of the layer-separation procedure. n=4-8, Wald test with Benjamin-Hochberg correction, ****padj ≤ 0.0001.

3.1.1.2 M/SM and ME initiate inflammation and angiogenesis 6 h after surgery.

To achieve a longitudinal transcriptional analysis of anastomotic healing, we performed comparisons between different time points. We started by comparing the anastomotic tissues collected at 6 h to the naive condition to identify the very first pathways activated after surgery **(Figure 4A)**. Afterward, we compared 24 h to 6 h and 72 h to 24 h time points.

A comparison of M/SM at 6 h and naive samples identified 1037 and 617 genes as significantly upregulated and downregulated at 6 h, respectively **(Figure 4B)**. Gene set enrichment analysis (GSEA) showed that the most prominently induced pathways 6 h post-surgery were related to inflammation, including neutrophil and macrophage chemotaxis, cytokine response, and positive regulation of bacterial defense **(Figure 4C)**. Interestingly, besides the expected innate immune response, our data indicate that adaptive immune responses, e.g. enrichment of the lymphocyte (T and B cell) associated gene sets, **(Figure 4C)** are also upregulated early on in CAH.

Vascularization is considered crucial for successful healing and research shows that hypoxia followed by devascularization causes CAL in mice (Shogan et al. 2015; Miltschitzky et al. 2021). Interestingly, our data show that angiogenesis pathways were enriched 6 h after surgery. Other pathways that were altered at the 6 h time point included the enrichment of epithelial cell differentiation and reduction in mesenchymal cell proliferation **(Figure 4C)**. Overall, these data show that although the most prominent defining feature of the 6 h time point is inflammation, the tissue upregulates several wound healing-related pathways simultaneously.

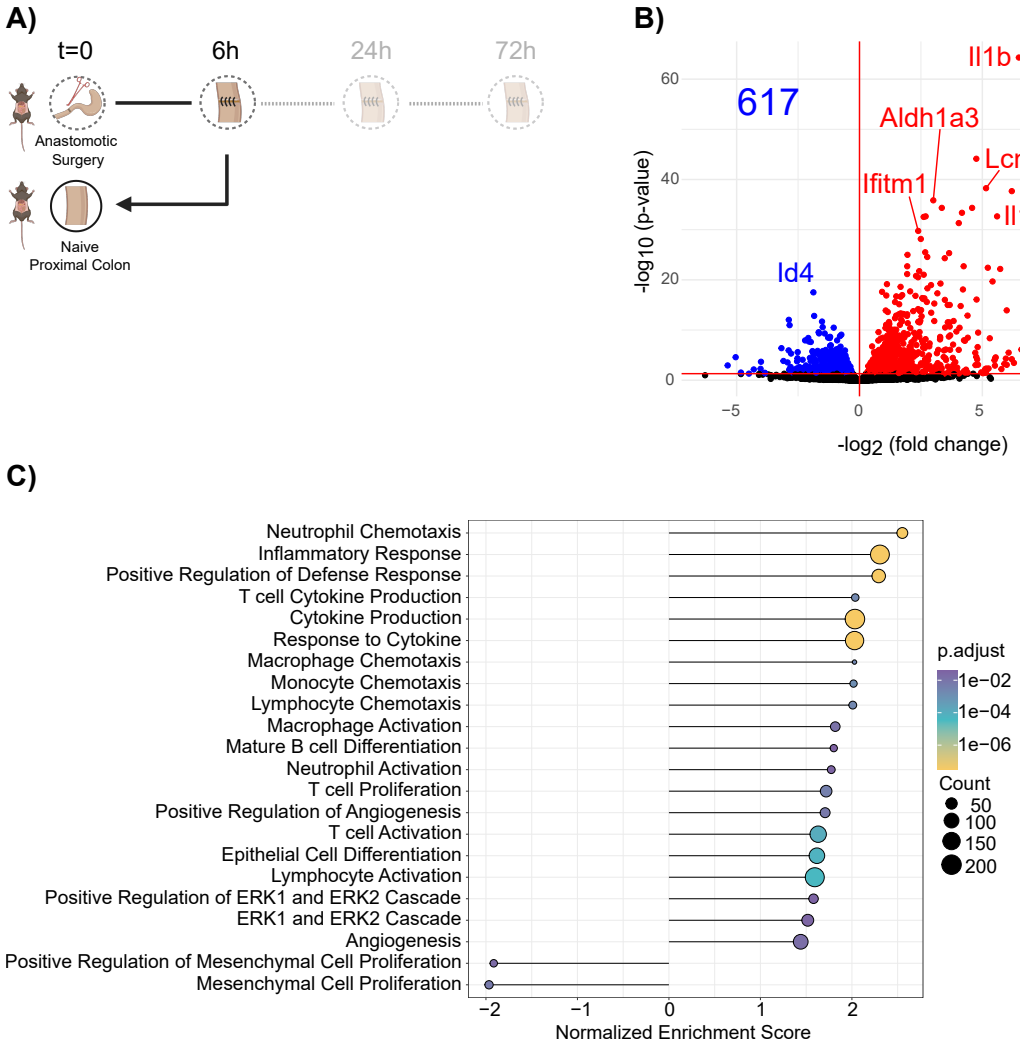

Fig 4: **Gene expression profile of the M/SM layer of the anastomotic tissue at 6h compared to naive controls. A)** Experimental setup. Direction of the arrow indicates the comparisons made **B)** Volcano plot of DEGs (red and blue shows up-/downregulated genes, respectively) in the M/SM layer of anastomotic tissue collected at 6h compared to naive tissue **C)** Selected significantly enriched pathways in the M/SM layer of anastomotic tissue at 6 h compared to the naive tissue based on GSEA.

A comparison of the expression levels of the genes detected in both M/SM and ME showed that the transcriptional profiles of the M/SM and ME positively correlate **(Figure 5A)**. In line with this, GSEA indicated that ME was also enriched in innate and adaptive immune cell response, angiogenesis, and defense response 6 h after surgery **(Figure 5B)**. These findings show that transcriptional pathways in the ME and M/SM overlap substantially in the early postoperative period.

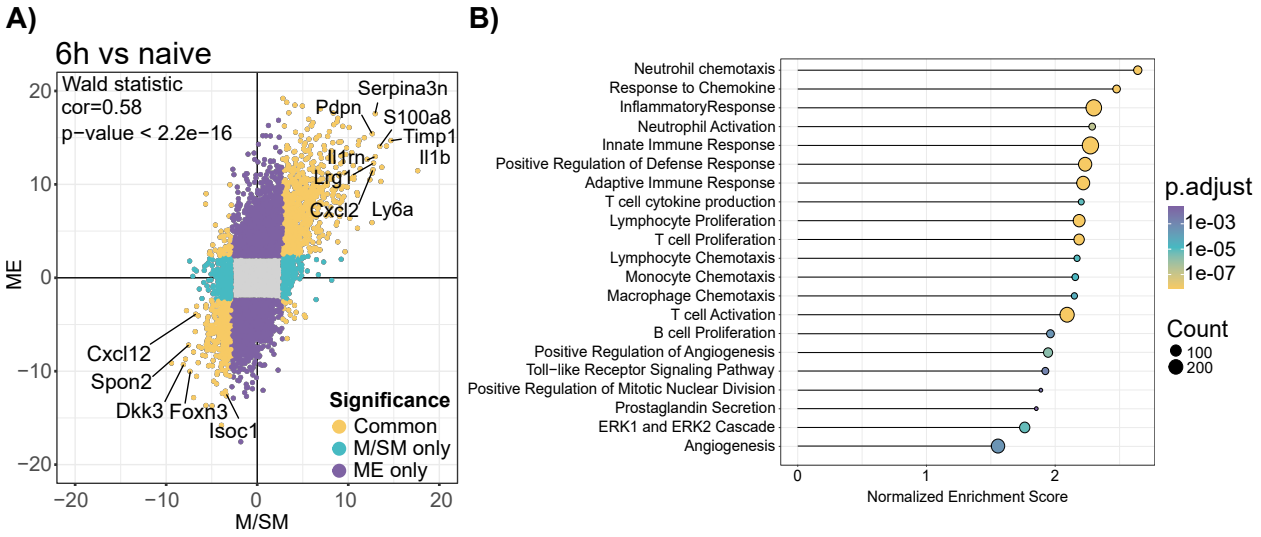

Fig 5: **Analysis of healing pathways in the ME layer at 6 h time point. A)** Correlation plot based on the Wald statistics of the genes shared between M/SM and ME layer at 6h after surgery compared to their corresponding naive controls. **B)** Selected enriched gene sets in the ME of anastomosis at 6 h time point compared to the naive tissue.

3.1.1.3 The proliferation phase starts 24 h after surgery

We then characterized the transcriptional changes between the 6 h and 24 h time points **(Figure 6A)**. In the M/SM, we detected 633 and 684 genes that were significantly up-/downregulated at 24 h, respectively **(Figure 6B)**. GSEA revealed that pathways involved in cell proliferation such as regulation of chromosome segregation, nuclear division, DNA replication, and cell cycle transition were enriched at 24 h. Therefore, the 24 h time point can be characterized as the proliferation phase of the CAH **(Figure 6C)**. Interestingly, negative regulation of cell division was also significantly enriched, which might be indicative of cell-specific regulation of proliferation.

We also observed a significant downregulation of the innate and adaptive immune responses, cytokine response, and host defense at the 24 h time point indicating that in the M/SM layer the host´s immune response within the first 24 h is predominantly activated in the immediate postoperative phase.

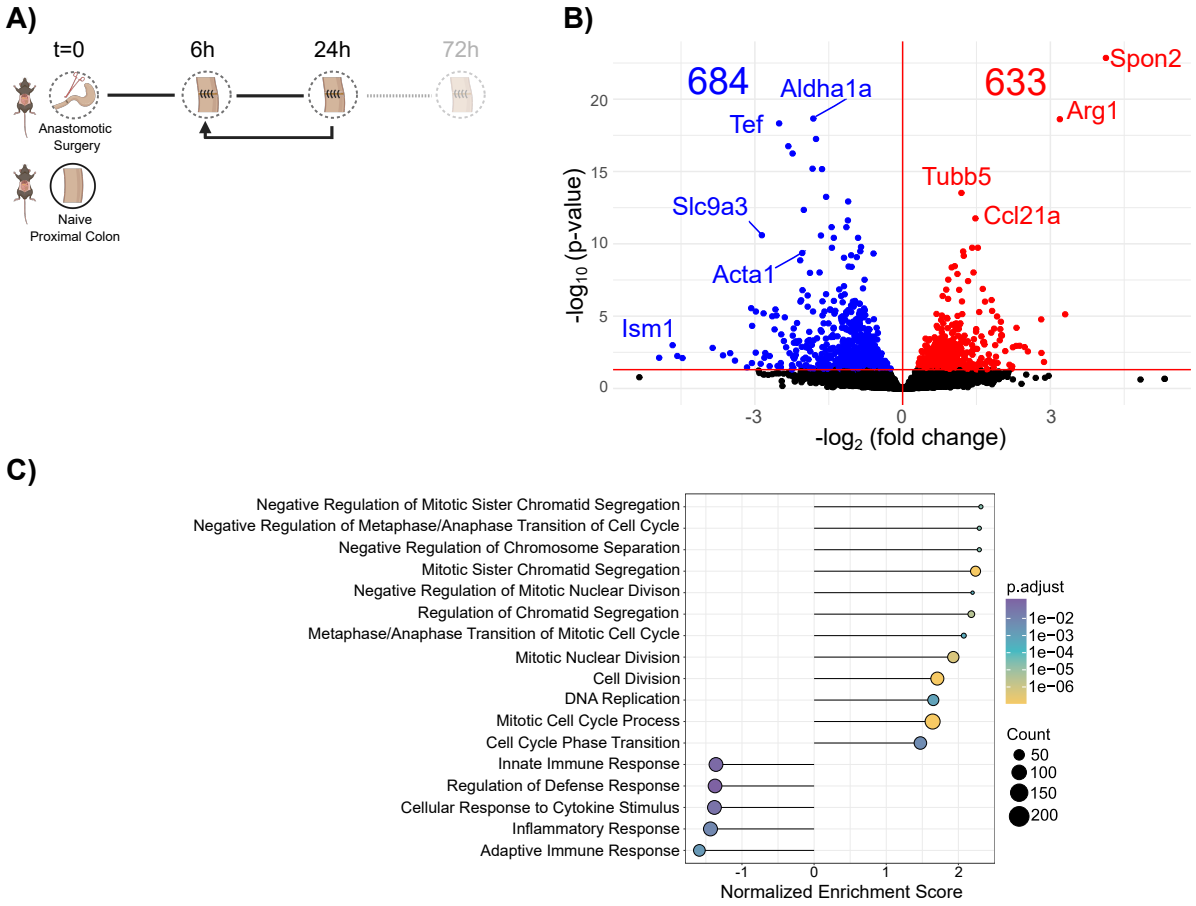

Fig 6: **Gene expression profile of the M/SM layer of the anastomotic tissue at 24h compared to 6h. A)** Experimental setup. Direction of the arrow indicated the comparisons made in this section **B)** Volcano plot of DEGs (red and blue shows up-/downregulated genes, respectively) in M/SM layer of anastomotic tissue collected at 24 h compared to 6 h. **C)** Selected significantly enriched pathways in the M/SM layer of anastomotic tissue at 24 h compared to 6h based on GSEA.

Correlation analysis using the DEGs shared between M/SM and ME at 24 h compared to 6 h showed a significant positive correlation between these layers **(Figure 7A)**. In line with this, GSEA showed that ME also undergoes the proliferation stage at 24 h time point **(Figure 7B)**, indicating that both layers move simultaneously through the stages of wound healing. Interestingly as opposed to the M/SM, in the ME, inflammation-related pathways (e.g., leukocyte and lymphocyte proliferation, and adaptive immune response) were significantly enriched at 24 h. These data indicate that the initial wound healing stages in the M/SM and the ME are mostly synchronized, except for the inflammation-related pathways, which appeared to be significantly downregulated in the M/SM but upregulated in the ME.

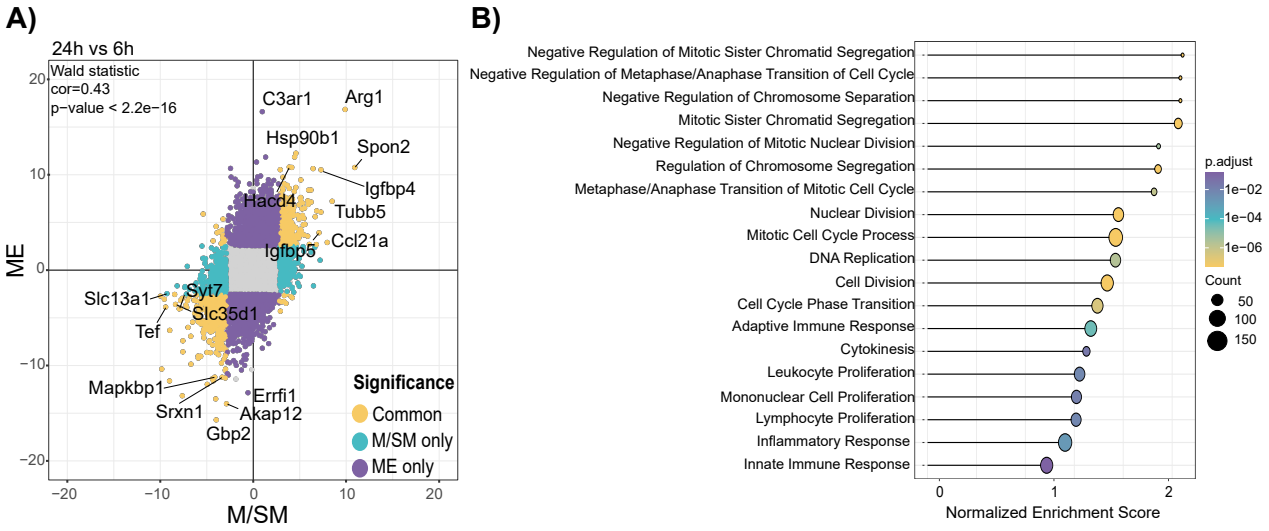

Fig 7: **Analysis of healing pathways in the ME layer at 24 h time point. A)** Correlation plot based on the Wald statistics of the genes shared between M/SM and ME layer at 24h after surgery compared to 6h. **B)** Selected significantly enriched pathways in the ME at 24h time point compared to 6h.

3.1.1.4 Extracellular matrix remodelling starts at 72 h after surgery.

Finally, we investigated the healing pathways specific for 72 h time point in M/SM and ME of anastomotic tissues in comparison to the 24 h time point **(Figure 8A)**. Notably, at 72 h the clinical scoring identified two groups based on ACS **(Figure 3B)**. For the analysis of healing pathways, we focused on the group with ACS<3 while the samples with ACS≥3 were separately analyzed afterward.

We identified 132 and 136 genes that were significantly up-/downregulated at 72 h compared to 24 h, respectively, in the anastomotic M/SM **(Figure 8B)**. GSEA showed an enrichment of extracellular matrix (ECM) remodelling-related pathways **(Figure 8C)**. We observed that most genes associated with ECM remodelling reached their peak expression at 72 h suggesting that the remodelling phase starts at 72 h **(Figure 8D)**.

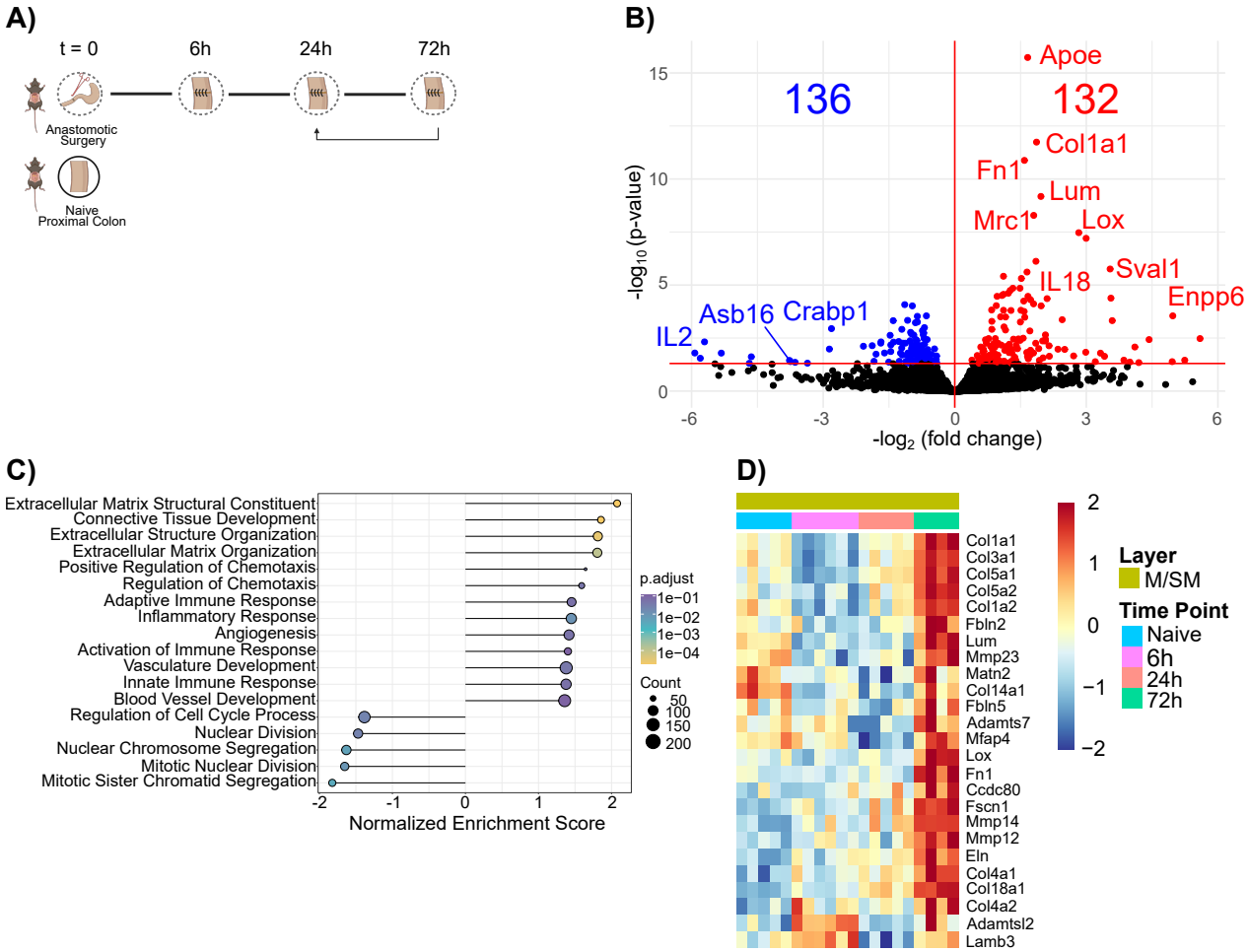

Fig 8: **Gene expression profile of the M/SM layer of the anastomotic tissue at 72 h compared to 24 h. A)** Experimental setup. Direction of the arrow indicated the comparisons made in this section. **B)** Volcano plot of DEGs (red and blue shows up-/downregulated genes, respectively) in the M/SM layer of anastomotic tissue collected at 72 h compared to 24 h. **C)** Selected significantly pathways in M/SM the layer of anastomotic tissue at 72 h compared to 24 h based on GSEA. **D)** Heatmap showing the expression pattern of genes related to ECM modelling in the M/SM layer of naive and anastomotic samples collected at 6 h, 24 h and 72h.

Correlation analysis based on the common DEGs in both M/SM and ME layers showed a significantly positive correlation **(Figure 9A)** and GSEA indicated that ECM remodelling-related pathways were also upregulated in ME **(Figure 9B)**.

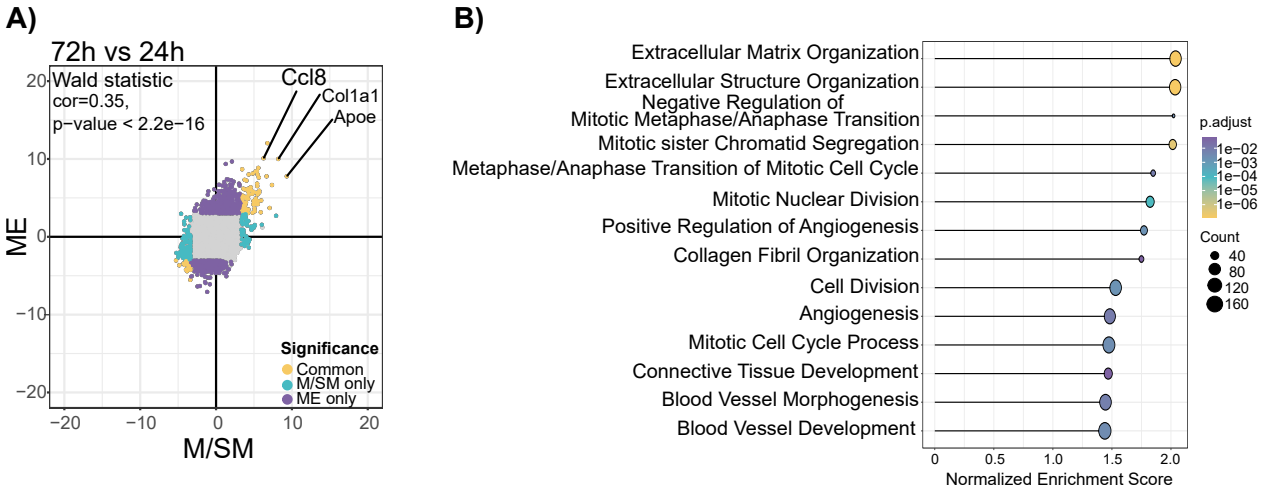

Fig 9: **Analysis of healing pathways in the ME layer at 72 h time point. A)** Correlation plot based on the Wald statistics of the genes shared between M/SM and ME layer at 72 h after surgery compared to 24 h. **B)** Selected significantly enriched pathways in the ME at 72 h time point compared to 24 h.

Our GSEA analysis also showed a significant enrichment in inflammatory and angiogenesis pathways at 72 h compared to 24 h in M/SM **(Figure 8C)** suggesting that there might be a second wave of these pathways in the M/SM following the proliferation phase. In the ME, the inflammation-related pathways did not significantly differ between 72 h and 24 h time point, while angiogenesis was enriched **(Figure 9B)**.

Overall, these data present transcriptional changes of murine CAH in its initial stages. Both ME and M/SM went through different transcriptional processes mostly synchronously. Inflammation, angiogenesis, and defense response activated within the first 6 h of anastomotic surgery. The proliferation phase starts at 24 h and ECM remodelling starts around 72 h after surgery.

3.1.2 Analysis of transcriptional pathways within M/SM and ME layers in tissue with CAL

As shown in Figure 3, at 72 h, 50 % of the mice developed CAL. Next, we compared the transcriptional profiles of CAH (ASC<3) and CAL (ACS≥3) samples collected at 72h. Principal component analysis (PCA) showed that ME of the CAL and CAH samples clustered together **(Figure 10A)**, which was corroborated by the lack of any detectable DEGs be-

tween the CAL and CAH samples, indicating that CAH and CAL cannot be distinguished based on the ME´s transcriptional profile. In contrast, M/SM samples of CAH and CAL tissues clustered separately, and DEG analysis showed 383 and 186 significantly up/-downregulated, respectively, in CAL **(Figure 10A+B)**.

We then analyzed the differentially regulated pathways between CAH and CAL at 72 h in their M/SM layers by performing Gene Ontology (GO) term analysis. Whilst the analysis of the upregulated CAL genes did not result in any enriched pathways, the downregulated genes in the CAL tissues were related to numerous GOterms. We then focused on the top 25 terms most significant GOterms and observed that CAL-associated downregulated genes were associated with ECM remodelling and its components such as collagens, wound healing, and cell migration **(Figure 10C)**.

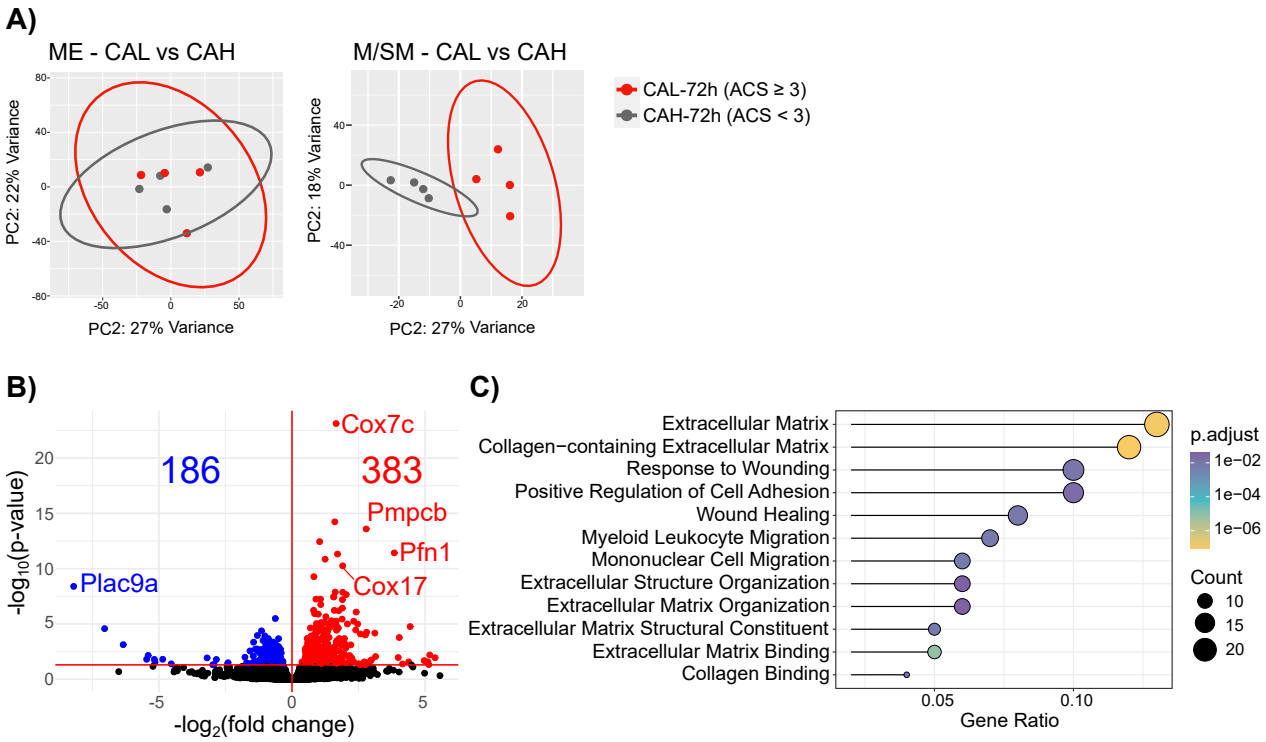

Fig. 10: Transcriptome of the M/SM at 72h distinguishes CAL and CAH. Mice underwent **A)** Principal component analysis (PCA) of ME and M/SM in CAL and CAH **B)** Volcano plot of DEGs (red and blue shows up-/downregulated genes, respectively) in the M/SM layer in CAL compared to CAH **C)** GOterms associated with the significantly downregulated genes in CAL compared to CAH.

Of the downregulated pathways in CAL tissue, we focused on the two most relevant pathways in CAL development, namely wound healing, and ECM remodelling. To investigate if these pathways were only enriched in CAH and not in CAL tissue, we incorporated the M/SM of the naive colon into the analysis. A comparison of CAH and CAL samples with naive tissues showed that there were 627 and 552 significantly up-/downregulated genes, respectively, that are common between CAH and CAL **(Figure 11A)**. Our GOterm analysis showed that upregulated genes shared between CAH and CAL were related to wound healing, and ECM remodelling pathways (data not shown) suggesting that the M/SM of CAL also had enriched these pathways, however, it lacked specific genes that are involved in these pathways.

We then proceeded to identify the genes that were enriched in CAH but not in CAL tissue. Our analysis showed 37 ECM remodelling-associated genes whose levels remained lower than and comparable to the naive tissue in CAL, whereas their expression was higher in the CAH tissue compared to the naive. Among these genes, 11 of them including *Col18a1* and *Col16a1* were significantly higher in the CAH compared to CAL **(Figure 11B)**. Analysis of wound healing-associated genes identified 29 genes with low levels in the CAL tissue and 15 of those, including *Pdpn* (gp38) (fibroblast marker), *Timp1* (MMP inhibitor), and *Fcer1g* (involved in anti-microbial immunity) significantly different between CAH and CAL **(Figure 11C)**.

Finally, we followed the expression pattern of the CAL-associated genes throughout the healing process in the M/SM of the samples with ACS<3 and observed that the expression of these genes exhibits different dynamics. Interestingly, the above-mentioned CAL-associated genes *Pdpn*, *Timp1*, and *Fcer1g* were upregulated as early as 6 h and maintained higher levels throughout the healing. On the other hand, *Kng2*, *Serpine2*, and *C3* were upregulated specifically at 72 h **(Figure 12)**.

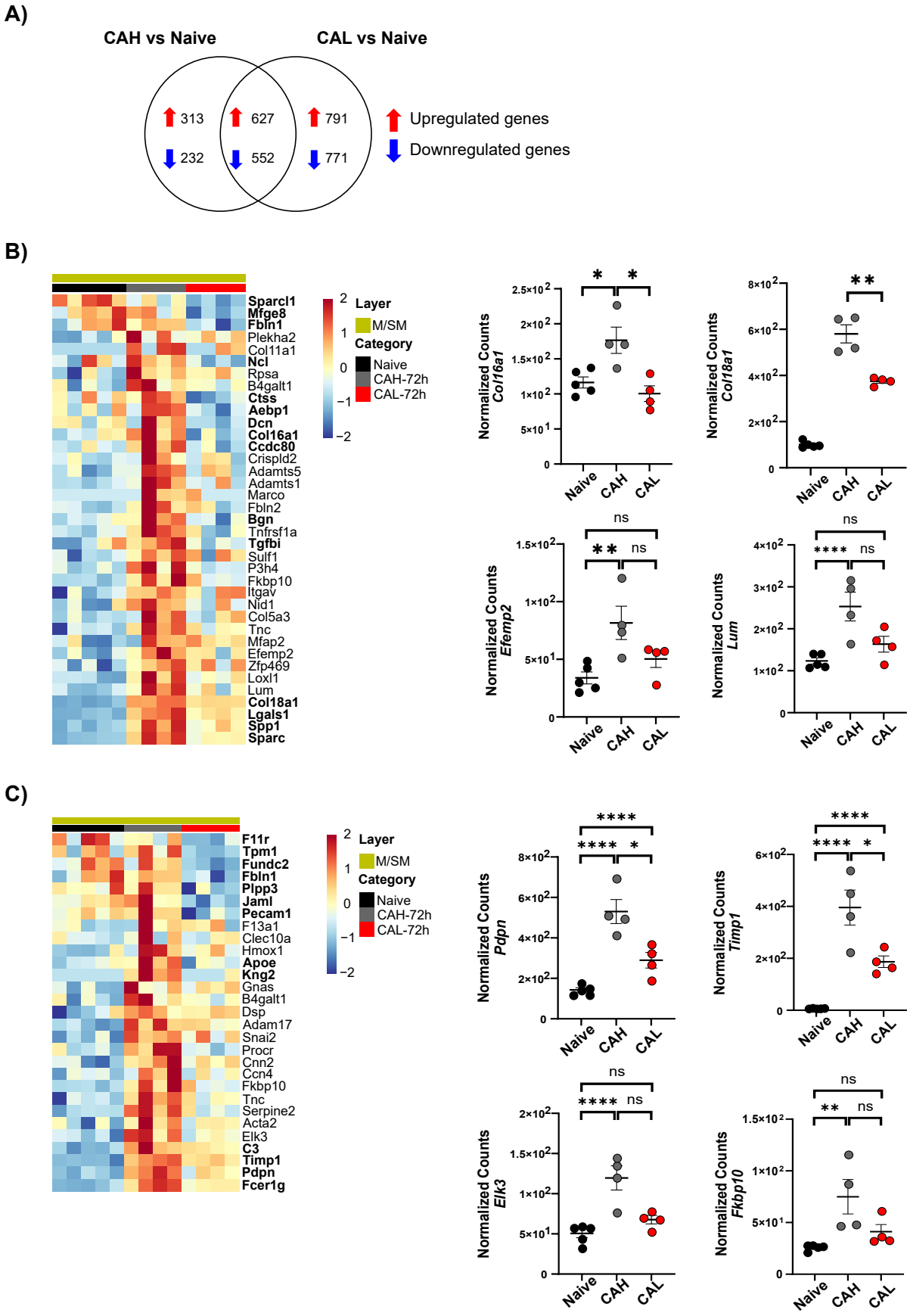
A)
CAH vs Naive
CAL vs Naive
313
232
627
552
791
771
Upregulated genes
Downregulated genes
B)
Sparcl1
Mfge8
Fbln1
Plekha2
Col11a1
Ncl
Rpsa
B4galt1
Ctss
Aebp1
Dcn
Col16a1
Ccdc80
Crispld2
Adamts5
Adamts1
Marco
Fbln2
Bgn
Tnfrsf1a
Tgfbi
Sulf1
P3h4
Fkbp10
Itgav
Nid1
Col5a3
Tnc
Mfap2
Efemp2
Zfp469
Loxl1
Lum
Col18a1
Lgals1
Spp1
Sparc
Layer
M/SM
Category
Naive
CAH-72h
CAL-72h
Normalized Counts Col16a1
Normalized Counts Col18a1
Normalized Counts Efemp2
Normalized Counts Lum
Naive
CAH
CAL
ns
C)
F11r
Tpm1
Fundc2
Fbln1
Plpp3
Jaml
Pecam1
F13a1
Clec10a
Hmox1
Apoe
Kng2
Gnas
B4galt1
Dsp
Adam17
Snai2
Procr
Cnn2
Ccn4
Fkbp10
Tnc
Serpine2
Acta2
Elk3
C3
Timp1
Pdpn
Fcer1g
Normalized Counts Pdpn
Normalized Counts Timp1
Normalized Counts Elk3
Normalized Counts Fkbp10

Fig. 11: M/SM of CAL lacks certain ECM remodelling- and wound healing- associated gene expression. A) Venn diagram showing the number of genes unique to and shared between CAH and CAL. **B)** Heatmap showing the gene expression of CAL-associated genes involved in ECM-remodelling and bar plots showing differences in expression levels of *Col16a1*, *Col18a1*, *Efemp2* and *Lum* in the M/SM layer of naive, CAH and CAL tissue. **C)** Heatmap showing the gene expression of CAL-associated genes involved in wound healing and bar plots showing differences in expression levels of *Pdpn*, *Timp1*, *Elk3* and *Fkbp10* in the M/SM layer of naive, CAH and CAL tissue. Genes differed significantly between CAH and CAL tissues were indicated in bold. n=4-5, Wald test with Benjamin-Hochberg correction, ns: not significant; *padj ≤ 0.05; **padj ≤ 0.01; ****padj ≤ 0.0001.

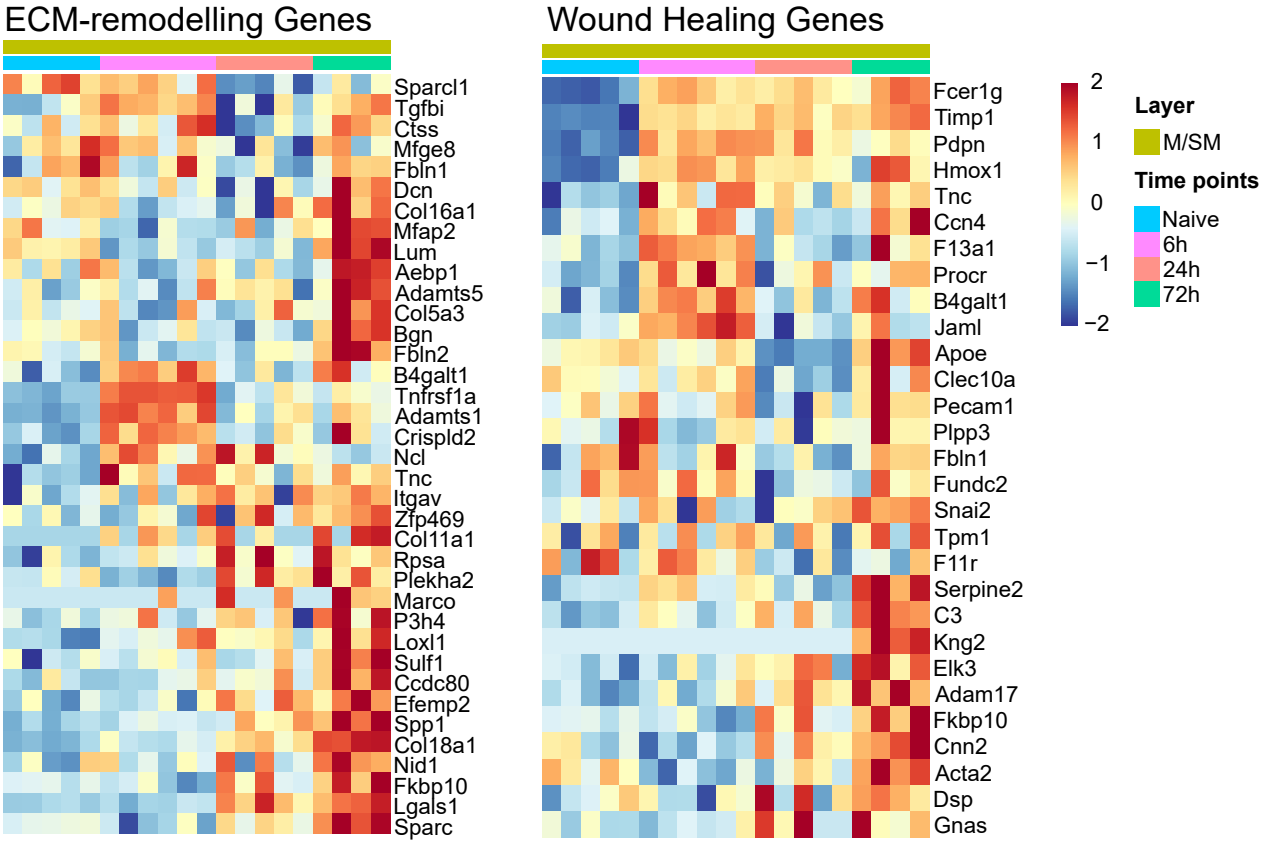

Fig. 12: Heatmap of ECM-remodelling- and wound healing associated gene expression in the M/SM layer in naive and anastomotic tissues collected at 6h, 24h, and 72h

Overall, our data suggests that CAL might develop due to disturbances in the M/SM healing rather than ME. We identified genes that CAL tissue lacked suggesting that these genes might be crucial for successful healing. We also showed that the expression level of these genes is highly dependent on the healing phase; therefore, the time of tissue collection is very critical when evaluating the potential use of a gene set as a biomarker.

3.2 Investigation of Molecular Mechanisms behind NSAID-induced CAL

Having achieved the first aim of this study, we then studied the biological pathways behind one of the well-recognized risk factors for CAL development, i.e. postoperative non-steroidal anti-inflammatory drugs (NSAIDs) administration.

3.2.1 Identification of causative pathways involved in NSAID-related CAL

3.2.1.1 Diclofenac sodium administration causes CAL in mice

We first tested the effects of postoperative NSAID administration by using our mouse model in which an 8-suture end-to-end proximal colon anastomosis is constructed. The mice were injected with 10 mg/kg diclofenac sodium (DCF), which is a non-selective NSAID and hence block both COX1 and COX2, bidaily (b.i.d), starting from one day before surgery until the end of the experiment **(Figure 13A)**. To identify the time point when the effect of DCF on CAH becomes apparent, we assessed the tissues daily after surgery. On postoperative day (POD1), we did not observe differences between DCF- and vehicle-treated mice. However, at POD2 all DCF-treated mice showed moderate CAL with ACS 3-4 whilst the vehicle-treated mice did not show any abnormalities **(Figure 13B+C)**. At POD3 70 % of the DCF-treated mice developed severe CAL with ACS 5-6 but the remaining 30 % had moderate CAL. On the other hand, only 1 % of the vehicle-treated mice showed moderate CAL at POD3 **(Figure 13C)**. On POD5 all DCF-treated mice reached the humane endpoint due to CAL development while the vehicle-treated mice survived without complications until the end of the experiment at POD5 **(Figure 13D)**. Overall, these results show that DCF administration results in CAL development in mice within 3 days after surgery.

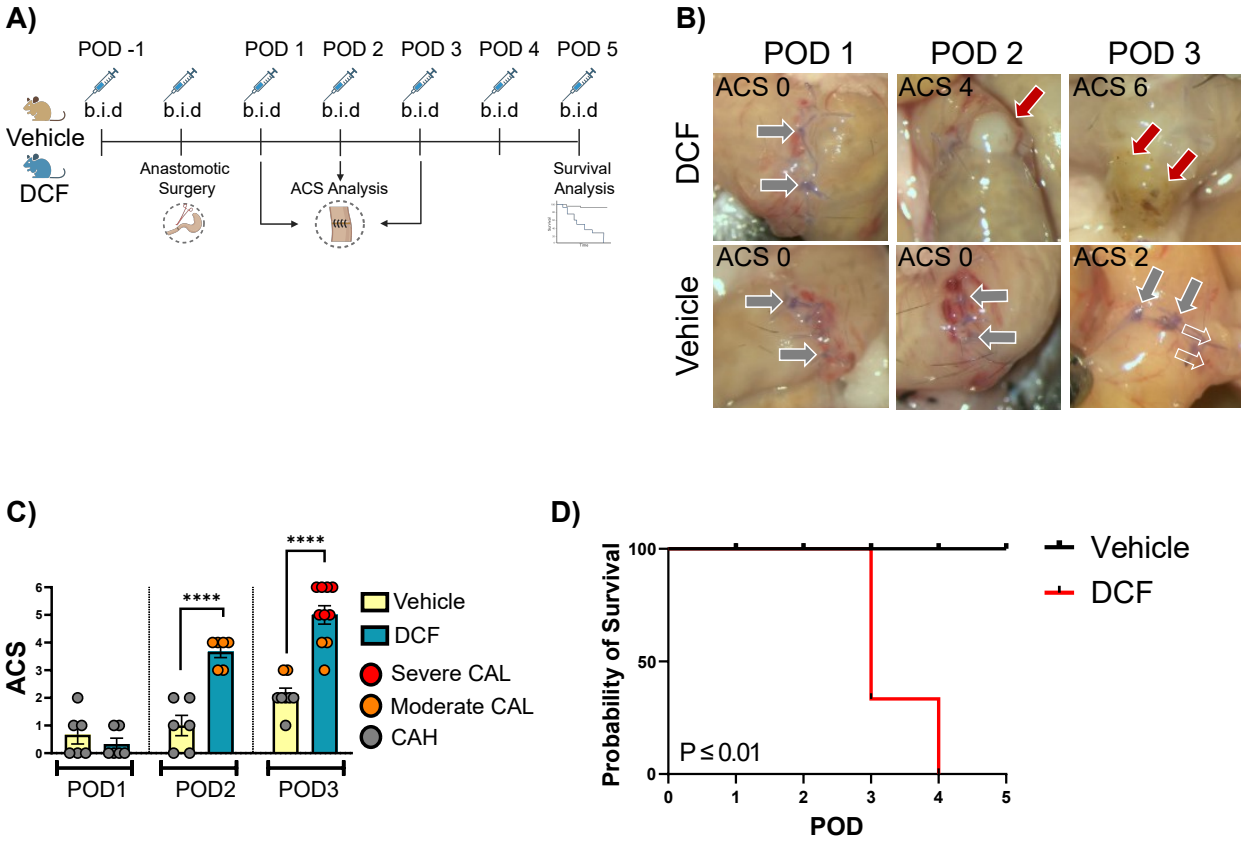

Fig. 13: Analysis of the effect of DCF on proximal CAH A) Experimental setup **B)** Representative images for anastomotic complications observed in vehicle- and DCF-treated mice at POD1, POD2, and POD3. Arrows point towards single sutures (grey), abscesses and peritonitis (red), and adhesions (clear). **C)** ACS of the vehicle- and DCF-treated mice at POD1, POD2 and POD3. **D)** Survival analysis of vehicle- and DCF-treated mice until POD5. b.i.d: bidaily, n=6-10, Unpaired t-test and Mantel-COX test, ****p ≤ 0.0001

3.2.1.2 DCF administration prevents PGE2 production in the anastomotic tissues

NSAIDs are well known to prevent prostaglandin (PG) production induced by inflammation (Hakkarainen et al. 2015). As anastomotic healing is accompanied by a strong immune response, we speculated that local PG levels would drop with DCF treatment. To measure anastomotic PG levels, we used two different approaches. First, we visualized lipid mediators including arachidonic acid (AA), PGE2 isomers (PGE2 and PGD2) and PGF2α using nanospray desorption electrospray ionization mass spectrometry imaging (nano-DESI MSI) in the mouse anastomotic tissues collected at POD1. Tissue images showed that

while AA is widely produced in the injured tissue, PGE2 isomers and PGF2α are highly concentrated in the anastomotic region **(Figure 14A)**. To measure the concentration of these mediators in the visualized sections, we identified multiple regions of interest in the unaffected, i.e. not operated part of the tissue, ME and M/SM layers as well as in the anastomotic region, in which a separation between both layers was not possible. Confirming the visualization, fold change analysis of the measured concentrations showed that the levels of PGE2 isomers and PGF2α are considerably higher in the anastomotic region compared to the unaffected parts of the tissue **(Figure 14B)**. PGE2 and PGD2 cannot be separated by nano-DESI MSI since they share the same chemical formula (Mavroudakis and Lanekoff 2023). Hence, we used ELISA measurement to determine the PGE2 concentration in the naive colon and anastomotic tissues obtained from the vehicle- and DCF-treated. We observed a significant increase in PGE2 levels in the anastomotic tissues compared to naive controls at POD2 **(Figure 14C)**. As expected, the DCF administration significantly reduced PGE2 in the anastomotic tissues **(Figure 14C)**. Together, these data indicate that DCF treatment prevents the increase in PGE2 during healing.

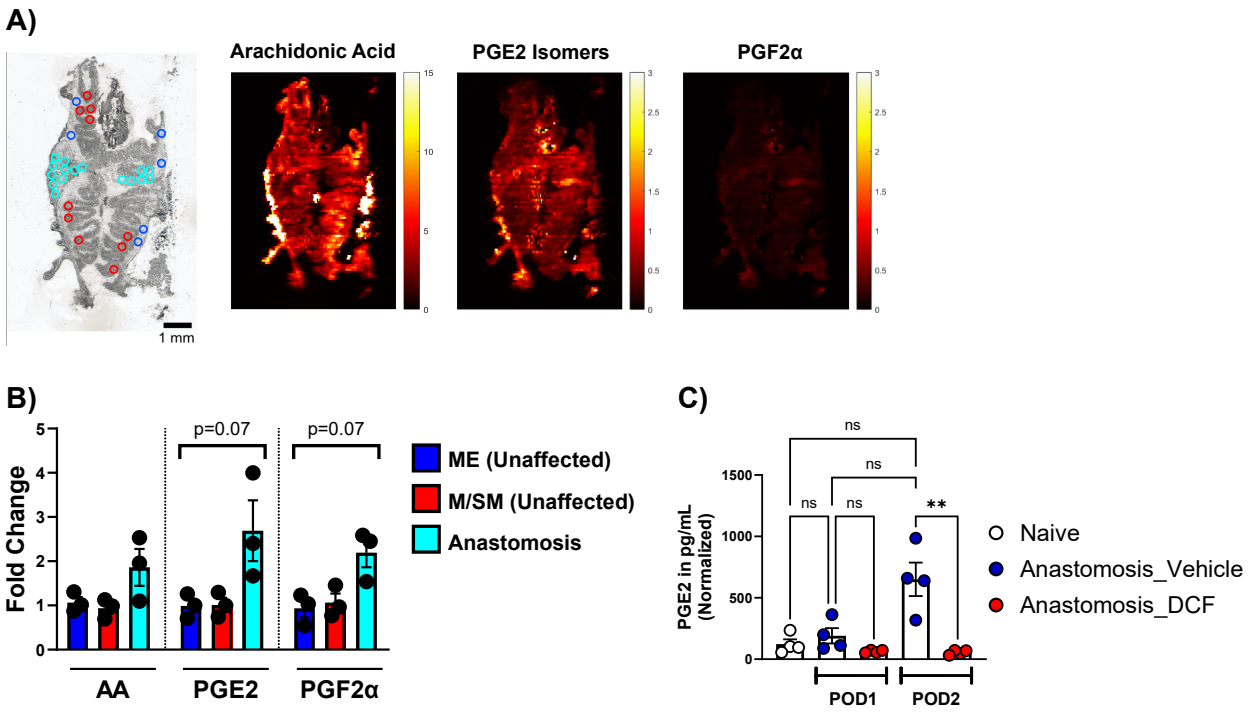

Fig. 14: Analysis of prostaglandin concentrations in the anastomotic tissue A) Microscopy images of an anastomotic section (left). Regions of interest within unaffected ME, M/SM, and anastomotic regions are shown in dark blue, red, and light blue, respectively. nano-DESI MS images of the same anastomotic section showing the localization of AA,

PGE2 isomers, and PGF2α. Colormap scales represent the concentrations in micromolar. **B)** The changes in AA, PGE2, and PGF2α levels within the anastomosis relative to ME and M/SM represented by the fold change analysis based on normalized average signal intensities measured using nano-DESI MSI. **C)** Normalized PGE2 concentrations measured by ELISA in naive, and anastomotic colon tissues collected from vehicle- and DCF-treated mice. n=3-4, Kruskal-Wallis test with multiple comparison (B and C),**p ≤ 0.01

3.2.1.3 COX2-PGE2 pathway is affected by postoperative DCF administration.

The COX2-PGE2 pathway has been associated with intestinal wound healing including CAH (Cheng et al. 2021; Gilman and Limesand 2021). To identify healing pathways disturbed in the absence of PGE2 due to DCF treatment, we analyzed the anastomotic tissues collected from vehicle- and DCF-treated mice at POD2 with 3´ bulk RNA-Seq **(Figure 15A)** and included control tissues from sham-operated animals with only colon eventration to the analysis. We first analyzed the effect of the DCF administration on the COX pathway. Our results show that *Ptgs2* (COX2), but not *Ptgs1* (COX1), expression was significantly higher in both vehicle- and DCF-treated anastomotic tissues compared to their corresponding sham controls **(Figure 15B)**. We also looked at the expression of PGs-producing enzymes. Our analysis showed that the expression of PGE2- and thromboxane-generating enzymes *Ptges* and *Tbxas1*, respectively, was significantly higher in the anastomotic tissues of both vehicle- and DCF-treated mice compared to the sham controls **(Figure 15C)**. Notably, the expression of these enzymes was higher in the DCF-treated anastomotic tissues compared to the vehicle-treated samples. Interestingly, we did not observe any changes in enzymes involved in the production of other PGs **(Figure 15C)**. We then looked at the expression of the PGE2 receptors, namely *Ptger1* (EP1), *Ptger2* (EP2), *Ptger3* (EP3), and *Ptger4* (EP4) **(Figure 15D)**, and saw a trend towards an increase in the *Ptger2* expression in the DCF-treated anastomotic tissues. Although *Ptger4* levels did not differ between all groups, it was the most highly expressed PGE2 receptor confirming a previous report (Crittenden et al. 2021). Overall, these data suggest that reduction in PGE2 levels in anastomosis due to DCF treatment results in a simultaneous induction of its producing enzyme (*Ptges*) and detecting receptor EP2 (*Ptger2*) gene expression.

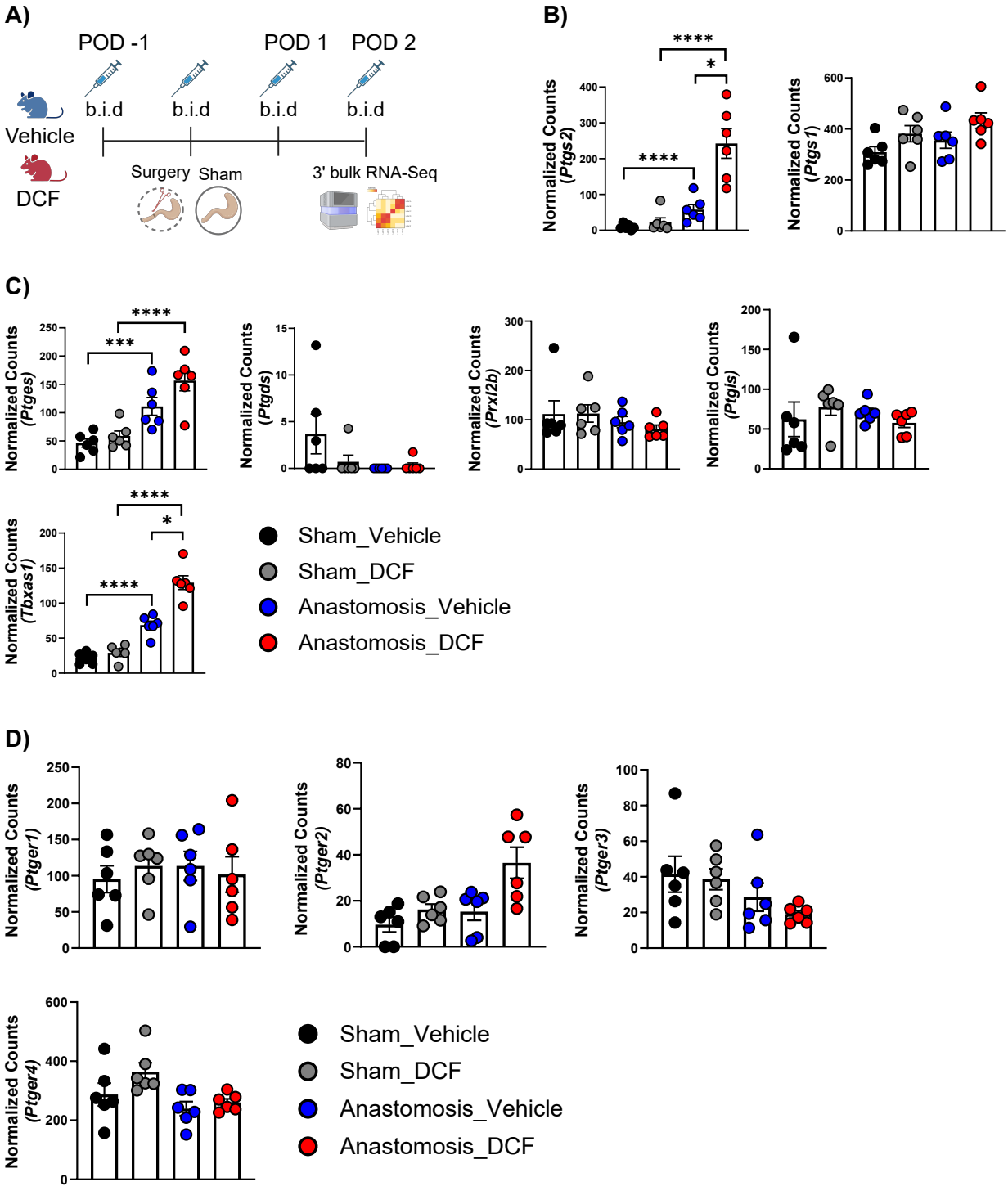

Fig. 15: Analysis of the genes in the COX pathway. **A)** Experimental setup. Expression levels of **B)** *Ptgs1*, *Ptgs2*, **C)** *Ptges*, *Ptgds*, *Prxl2b*, *Ptgis*, *Tbxas1*, **D)** *Ptger1*, *Ptger2*, *Ptger3*, and *Ptger4* in vehicle- and DCF-treated sham and anastomotic tissues. b.i.d: bidaily. n=6, Wald test with Benjamin-Hochberg correction, *padj ≤ 0.5, ***padj ≤ 0.001, ****padj ≤ 0.0001

3.2.1.4 Postoperative DCF treatment results in higher immune response at POD2

We then analyzed the pathways affected by the DCF treatment after surgery using our 3' bulk RNA-Seq data **(Figure 15A)**. PCA showed that while the sham-operated mice that received either vehicle or DCF treatment clustered together, vehicle- and DCF-treated anastomotic tissues clustered separately **(Figure 16A)**. Moreover, we identified 357 and 245 significantly up- and down-regulated DEGs in the DCF-treated anastomotic tissues compared to the vehicle-treated anastomotic samples **(Figure 16B)**.

GOterm analysis showed that upregulated genes in the DCF-treated anastomotic samples were related to myeloid cell-related pathways such as myeloid cell differentiation and neutrophil migration. Adaptive immune responses including B cell activation, type II IFN response and T-cell mediated immunity were also enriched in the in the DCF-treated samples **(Figure 16C)**.

We also performed GOterm analysis with the significantly downregulated genes in the DCF-treated anastomotic samples **(Figure 16B)**. Our results showed that these genes were primarily associated with several metabolic pathways including xenobiotic response and particularly glutathione-related processes, as well as peroxidase oxidoreductase activities **(Figure 16D)**.

3.2.1.5 *Rag1*$^{-/-}$ mice are protected from DCF-induced CAL

Given that GO analyses pointed towards a pronounced IFN response and T-cell-mediated immunity in anastomosis of the DCF-treated mice, we hypothesized that higher T-cell responses might worsen intestinal healing and could be a causative factor for the DCF-related CAL development. To test this, we subjected *Rag1*$^{-/-}$, which lack T and B cells, and *Rag1*$^{+/+}$ mice to the established DCF treatment regime and analyzed the anastomotic healing at POD2 **(Figure 17A)**. ACS analysis showed that *Rag1*$^{-/-}$ mice had significantly lower ACS compared to the *Rag1*$^{+/+}$ mice, corresponding to a 36 % reduction in CAL rates **(Figure 17B)**.

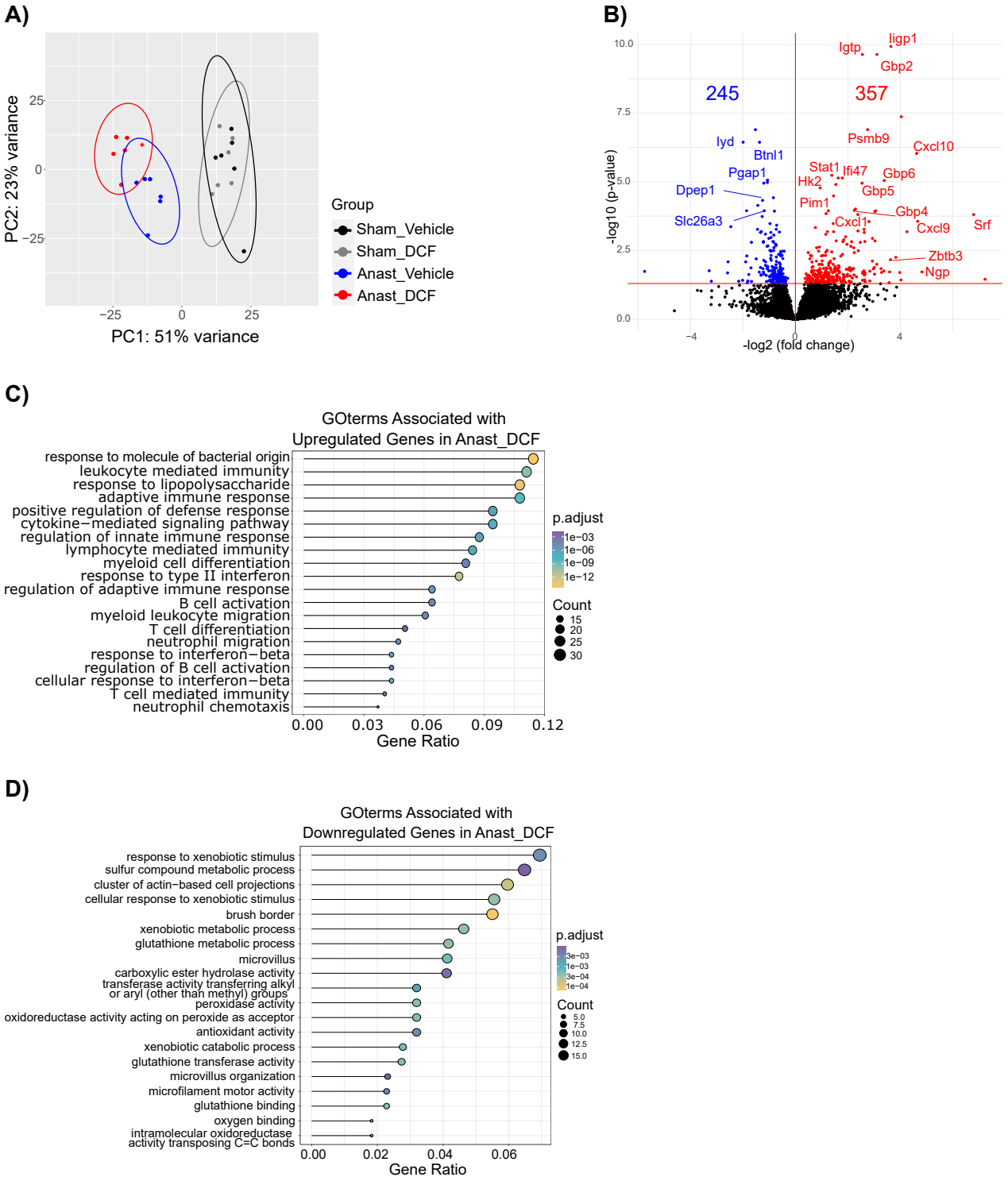

Fig. 16: Gene expression profile of sham and anastomotic tissues collected from vehicle- and DCF-treated mice. **A)** PCA plot of vehicle- and DCF-treated sham and anastomotic tissue. **B)** Volcano plot of DEGs (red and blue shows up-/downregulated genes, respectively) in the Anast-DCF samples compared to Anast-Vehicle samples. **C)** Selected GO terms associated with the upregulated genes in the Anast-DCF samples. **D)** Selected downregulated pathways in the Anast-DCF samples based on GOterm analysis.

To identify the difference between the DCF-treated *Rag1*$^{-/-}$ and *Rag1*$^{+/+}$ mice, we performed 3´bulk RNA-Seq in the anastomotic tissues. PCA analysis showed separate clustering of *Rag1*$^{-/-}$and *Rag1*$^{+/+}$ mice **(Figure 17C)** and we found 485 and 670 up- and downregulated DEGs, respectively, in the *Rag1*$^{-/-}$ mice compared to *Rag1*$^{+/+}$ controls **(Figure 17D)**. GOterm analysis on the significantly downregulated DEGs indicated that the *Rag1*$^{-/-}$ mice had lower immune and defense responses as well as lower type II and type I IFN responses **(Figure 17E)** suggesting that T-cells are a significant source of IFNs in anastomotic tissue. On the other hand, GOterm analysis with the significantly upregulated DEGs indicated that ECM and collagen-related pathways as well as tissue remodelling were significantly enriched in the *Rag1*$^{-/-}$ mice **(Figure 17F+G)**. Correspondingly, expression levels of 9 collagens, e.g. *Col1a1*, *Col3a1*, *Col5a1*, and *Col16a1*, were significantly higher in the *Rag1*$^{-/-}$ mice compared to the *Rag1*$^{+/+}$ controls **(Figure 17G)**. These data suggest that exaggerated T-cell activation is detrimental to anastomotic healing and linked to impaired extracellular matrix and tissue remodelling.

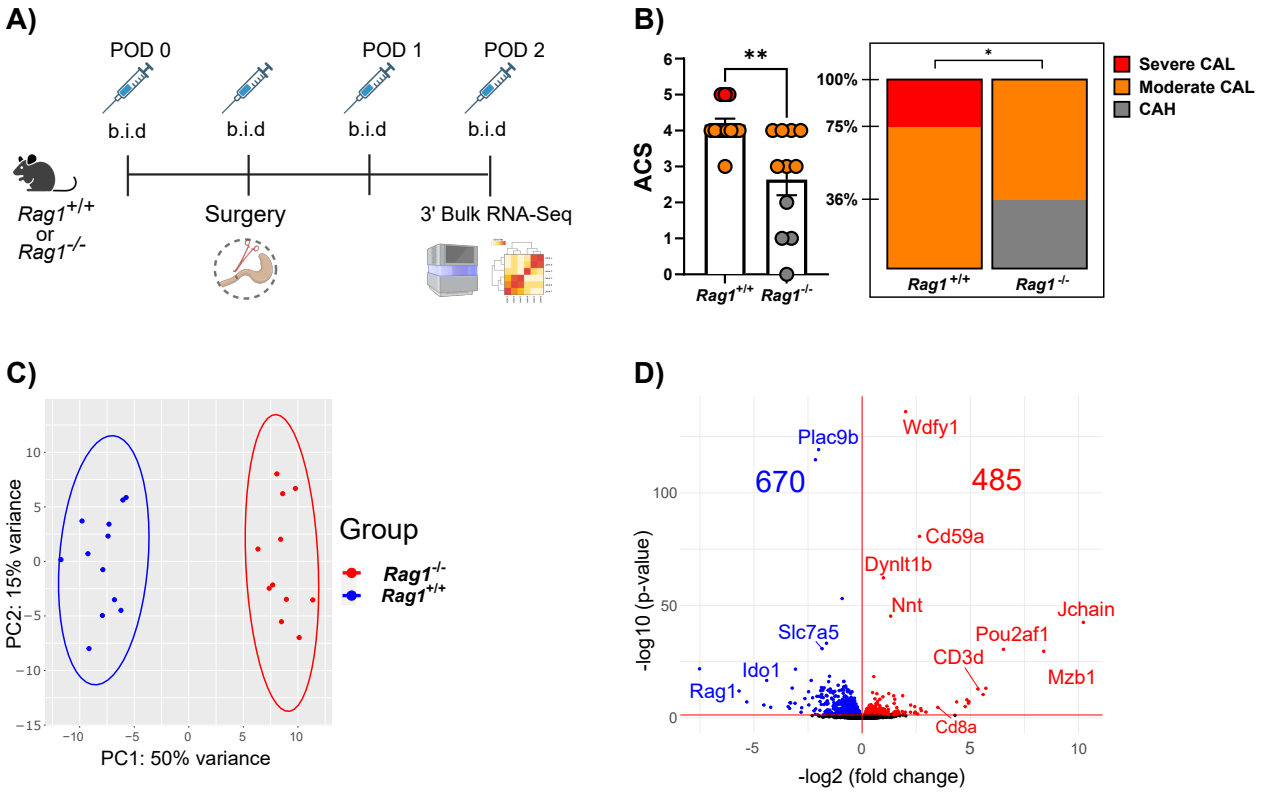

E)

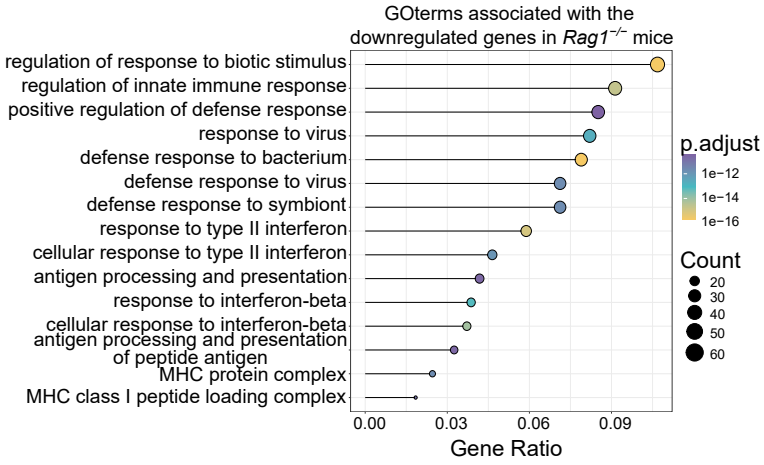
GOterms associated with the downregulated genes in Rag1−/− mice
regulation of response to biotic stimulus
regulation of innate immune response
positive regulation of defense response
response to virus
defense response to bacterium
defense response to virus
defense response to symbiont
response to type II interferon
cellular response to type II interferon
antigen processing and presentation
response to interferon-beta
cellular response to interferon-beta
antigen processing and presentation of peptide antigen
MHC protein complex
MHC class I peptide loading complex
0.00
0.03
0.06
0.09
Gene Ratio
p.adjust
1e−12
1e−14
1e−16
Count
20
30
40
50
60

F)

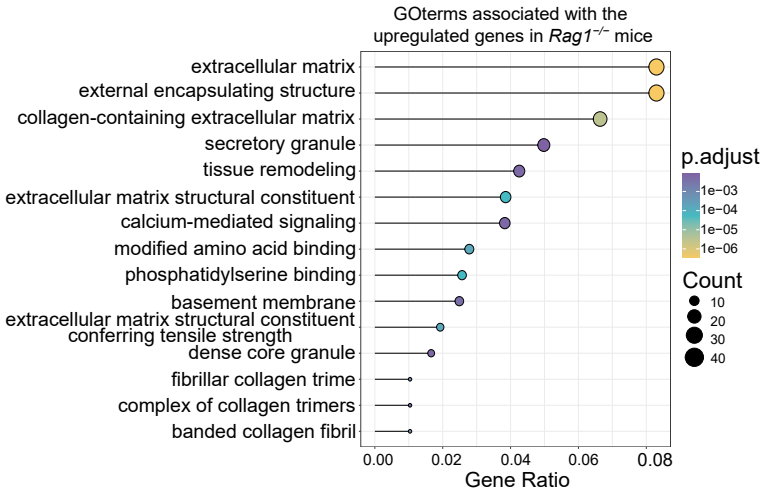
GOterms associated with the upregulated genes in Rag1−/− mice
extracellular matrix
external encapsulating structure
collagen-containing extracellular matrix
secretory granule
tissue remodeling
extracellular matrix structural constituent
calcium-mediated signaling
modified amino acid binding
phosphatidylserine binding
basement membrane
extracellular matrix structural constituent conferring tensile strength
dense core granule
fibrillar collagen trime
complex of collagen trimers
banded collagen fibril
0.00
0.02
0.04
0.06
0.08
Gene Ratio
p.adjust
1e−03
1e−04
1e−05
1e−06
Count
10
20
30
40

G)

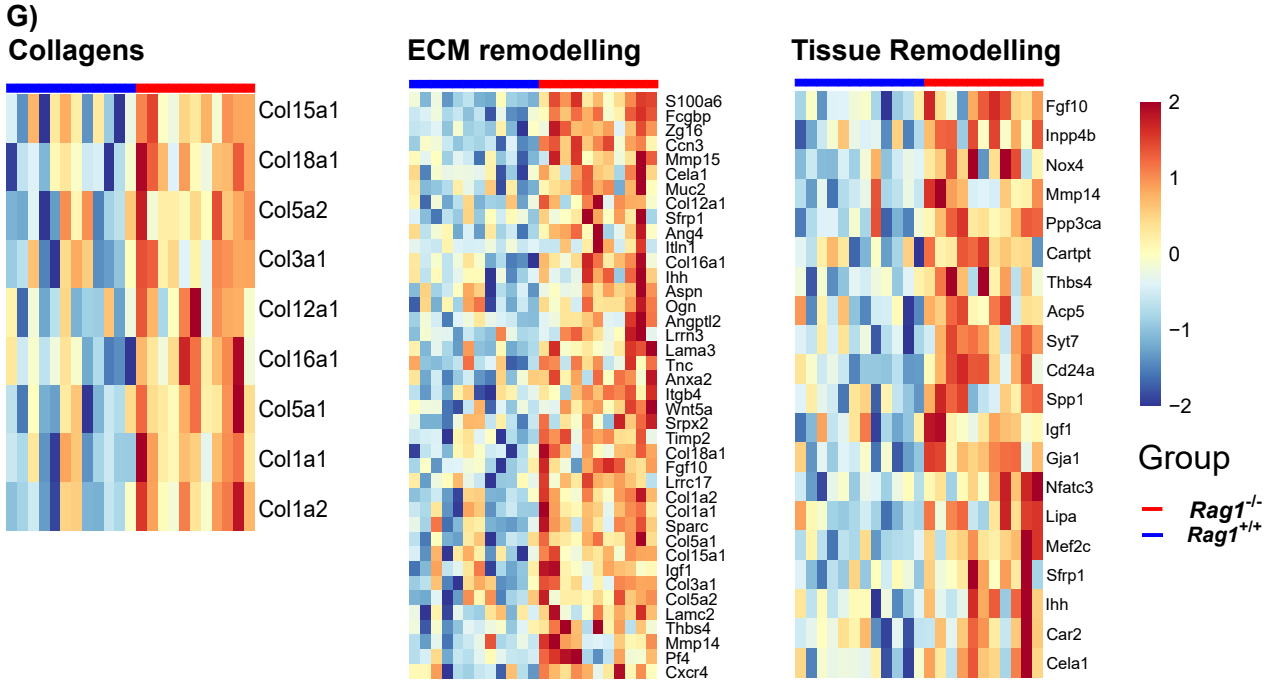
Collagens
Col15a1
Col18a1
Col5a2
Col3a1
Col12a1
Col16a1
Col5a1
Col1a1
Col1a2
ECM remodelling
S100a6
Fcgbp
Zg16
Ccn3
Mmp15
Cela1
Muc2
Col12a1
Sfrp1
Ang4
Itln1
Col16a1
Ihh
Aspn
Ogn
Angptl2
Lrrn3
Lama3
Tnc
Anxa2
Itgb4
Wnt5a
Srpx2
Timp2
Col18a1
Fgf10
Lrrc17
Col1a2
Col1a1
Sparc
Col5a1
Col15a1
Igf1
Col3a1
Col5a2
Lamc2
Thbs4
Mmp14
Pf4
Cxcr4
Tissue Remodelling
Fgf10
Inpp4b
Nox4
Mmp14
Ppp3ca
Cartpt
Thbs4
Acp5
Syt7
Cd24a
Spp1
Igf1
Gja1
Nfatc3
Lipa
Mef2c
Sfrp1
Ihh
Car2
Cela1
2
1
0
−1
−2
Group
Rag1-/-
Rag1+/+

Fig. 17: Gene expression analysis of the anastomotic tissues collected from DCF-treated *Rag1*$^{-/-}$ and *Rag1*$^{+/+}$ mice at POD2 A) Experimental design. **B)** ACS and ratios of CAH, moderate CAL, and severe CAL in DCF-treated *Rag1*$^{-/-}$ and *Rag1*$^{+/+}$ mice at POD2. **C)** PCA of anastomotic tissues collected from DCF-treated *Rag1*$^{-/-}$ (red) and *Rag1*$^{+/+}$ mice (blue) **D)** Volcano plot of DEGs (red and blue shows up-/downregulated genes, respectively) in *Rag1*$^{-/-}$ mice compared to *Rag1*$^{+/+}$ mice **E)** Top15 GOterms associated with the downregulated genes in *Rag1*$^{-/-}$ mice. **F)** Top15 GOterms associated with the upregulated genes in *Rag1*$^{-/-}$ mice. **G)** Heatmap of collagens, ECM remodelling- and tissue remodelling-associated genes in *Rag1*$^{-/-}$ (red) and *Rag1*$^{+/+}$ (blue) mice. n=11-12, Unpaired t-test, Chi-square test, and Wald statistics were used for ACS, CAH and CAL ratio, and 3' bulk RNA-Seq analysis, respectively. b.i.d: bidaily, *p ≤ 0.05, **p ≤ 0.01

3.2.1.6 T- and B-cell abundance is not affected by the DCF treatment

Having shown a detrimental effect of adaptive immune response in the DCF-related CAL, we analyzed if the abundance of T- and B cells changes in the DCF-treated mice after surgery using flow cytometry. We particularly focused on CD19$^+$ B cells, CD8$^+$, CD4$^+$, and NK1.1$^+$ NK-T cell populations. Additionally, we analyzed the expression level of EP2 and EP4 receptors within these cells since EP2 expression was induced in DCF-treated mice and EP4 was the highest expressed receptor in the anastomotic tissues. We observed that in the anastomotic tissues, about 15 % of CD45$^+$ are CD3$^+$ T-cells and 3-4 % of them are CD19$^+$ B cells **(Figure 18A)**. Of CD45$^+$CD3$^+$ T-cells, 10 % of are CD4$^+$ cells, 60 % are CD8$^+$, and the remaining 30 % are NK1.1$^+$ NK-T cells **(Figure 18B)**. Of these populations, only CD4$^+$ abundance significantly increased after surgery compared to naive control tissue **(Figure 18B)**. Interestingly, the expression level of EP2/4 receptors as measured by the geometric mean fluorescent intensity (GeoMFI) within the T- and B-cell populations did not differ between DCF- and vehicle-treated mice **(Figure 18C)**.

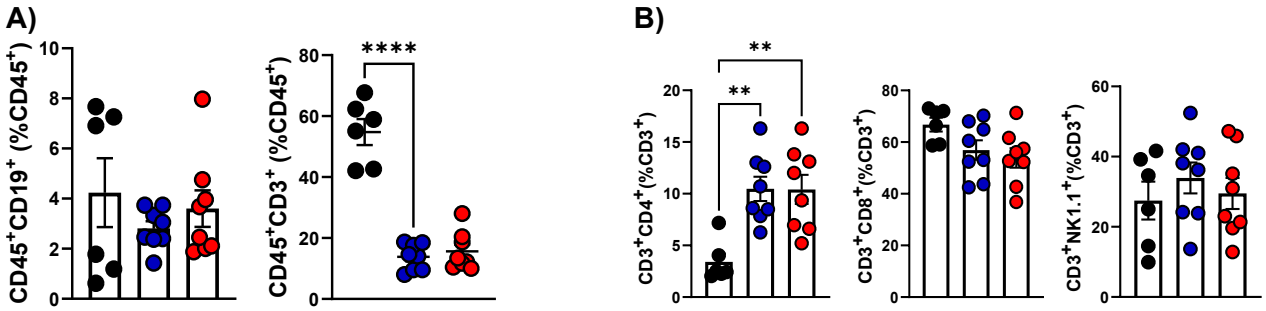

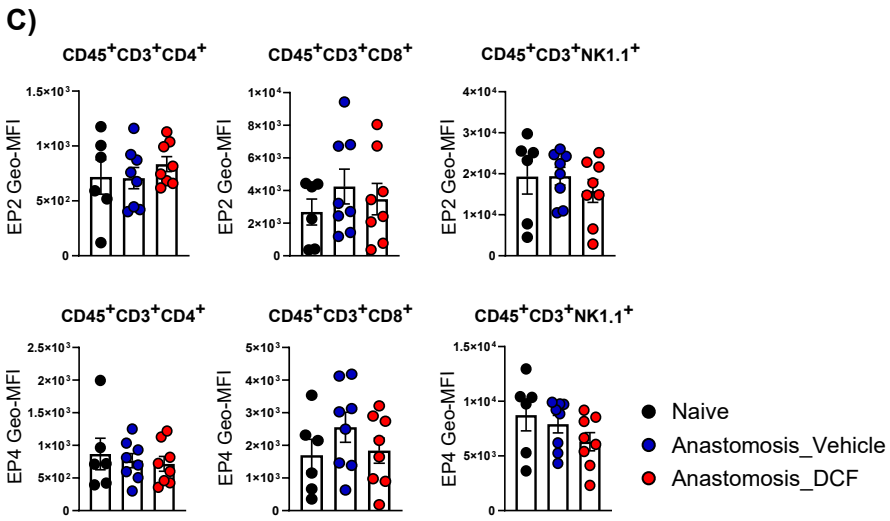

Fig. 18: Flow cytometry analysis of lymphocytes within naive, and vehicle- and DCF-treated anastomotic tissues at POD2 **A)** Percentage of $CD19^+$ B-cells and $CD3^+$ T-cells out of $CD45^+$ immune cells. **B)** Percentage of $CD45^+CD3^+CD4^+$, $CD45^+CD3^+CD8^+$, and $CD45^+CD3^+NK1.1^+$ T cells cells out of $CD45^+CD3^+$ population. **C)** EP2 and EP4 expression levels within $CD45^+CD3^+CD4^+$, $CD45^+CD3^+CD8^+$, and $CD45^+CD3^+NK1.1^+$ T cells shown as geometric mean fluorescent intensity (GeoMFI). n=6-8, One way ANOVA, $^{**}p \leq 0.01$, $^{****}p \leq 0.0001$

3.2.1.7 EP2/4 expression increases in neutrophils and infiltrating monocytes in DCF-induced CAL

As myeloid cells constitute a large portion of the immune response following injury and our 3' bulk RNA-Seq results showed enrichment in myeloid cell signatures in the anastomosis of DCF-treated mice, we next analyzed the changes in myeloid cell abundance and EP2/4 expression within them. We observed a significant increase in all tested myeloid cell populations, i.e. $F4/80^+Ly6C^+$ monocyte-derived and $F4/80^+Ly6C^-$ resident macrophages, $F4/80^-Ly6C^+Ly6G^+$ neutrophils, and $F4/80^-Ly6C^+Ly6G^-$ infiltrating monocytes, in the anastomotic tissues compared to the naive controls **(Figure 19A+B)**. Similar to the T cell population, there was no significant difference in the myeloid cell abundance between DCF- and vehicle-anastomotic tissues. However, there was a noticeable increase in the $F4/80^+Ly6C^+$ monocyte-derived macrophage population in the DCF-treated mice **(Figure 19C)**. Interestingly, GeoMFI of EP2 was significantly higher within the neutrophils and infiltrating monocytes, and GeoMFI of EP4 was higher within the infiltrating monocytes in the DCF-treated mice compared to vehicle controls **(Figure 19C)**.

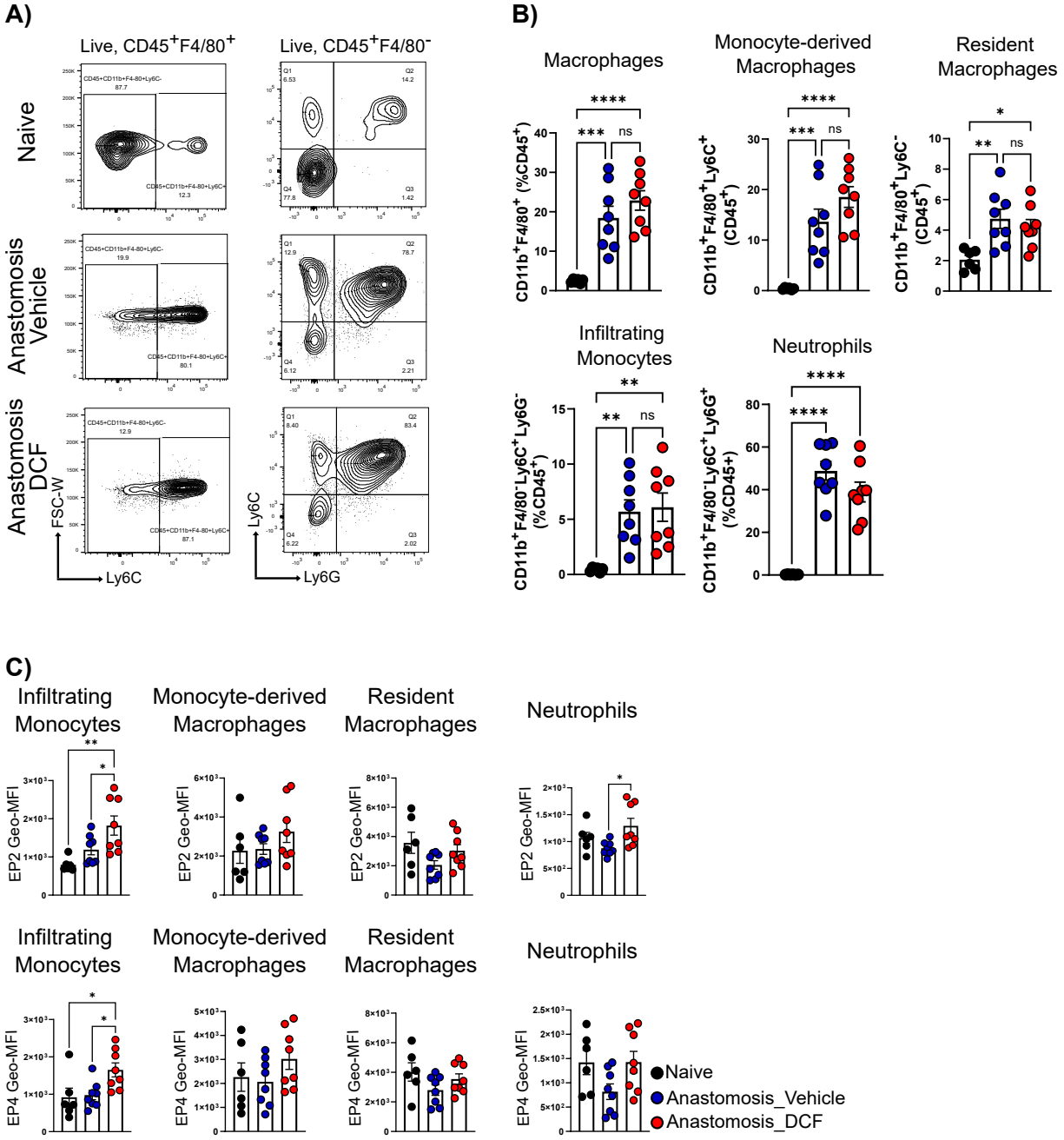

Fig. 19: Flow cytometry analysis of myeloid cells within naive, and vehicle- and DCF-treated anastomotic tissues at POD2 A) Gating strategy for identification of monocyte-derived macrophages ($CD45^+Cd11b^+F4/80^+Ly6C^+$), resident macrophages ($CD45^+Cd11b^+F4/80^+Ly6C^-$), infiltrating monocytes ($CD45^+Cd11b^+F4/80^-Ly6C^+Ly6G^-$), and neutrophils ($CD45^+Cd11b^+F4/80^-Ly6C^+Ly6G^+$). **B)** Percentages of macrophages, monocyte-derived and resident macrophages, infiltrating monocytes, and neutrophils within $CD45^+$ immune cells. **C)** EP2 and EP4 expression levels within monocyte-derived and resident macrophages, infiltrating monocytes, and neutrophils shown as geometric mean fluorescent intensity (GeoMFI). b.i.d: bidaily, n=6-8, One way ANOVA, *p ≤ 0.05, **p ≤ 0.01, ***p ≤ 0.001, ****p ≤ 0.0001

Overall, these results show that the DCF treatment did not influence the abundance of the analyzed myeloid and lymphoid cells. Enrichment of innate and adaptive immunity-associated pathways detected in RNA-Seq analysis and changes in EP2/4 expression within myeloid cells might suggest that the metabolism of the myeloid and lymphoid cells instead of their infiltration and/or proliferation might be affected by the lack of PGE2 signalling pathway.

3.2.2 Testing the role of PGE2 in preventing NSAID-(un)related CAL

3.2.2.1 PGE2 supplementation does not prevent DCF-induced CAL

Our results demonstrated that PGE2 is the main PG in the anastomotic tissues. Moreover, a previous study has shown a reduction in CAL rates in *Cox2*$^{-/-}$ mice upon PGE2 supplementation (Reisinger et al. 2017). Therefore, we finally tested if PGE2 supplementation prevents DCF-induced CAL mice by injecting DCF-treated mice with 100 ug/kg 16,16-Dimethyl Prostaglandin E2 (dmPGE2) or vehicle **(Figure 20A)**. Evaluation of the anastomotic tissue at POD3 showed that this treatment strategy did not result in any changes in the ACS **(Figure 20B)**. As the effect of dmPGE2 may not be strong or long enough to overcome the detrimental actions of DCF in this model, we used an additional approach to test if PGE2 signalling protects mice from CAL.

3.2.2.2 PGE2 supplementation reduces spontaneously occurring CAL rates

Herein we used a spontaneous anastomotic leakage model based on anastomosis construction with six instead of eight sutures. Mice with the reduced number of sutures were treated b.i.d with 2.5 mg/kg, 5 mg/kg, or 10 mg/kg of SW033291, which increases PGE2 levels by blocking PG-degrading enzyme 15-PGDH, or vehicle **(Figure 20C)**. Assessment of the tissues at POD5 showed that while 2.5 mg/kg dosing did not have any effect on ACS, 5 mg/kg dosing led to an almost significant decrease in the CAL rates in the SW033291-treated group **(Figure 20E)**. In 10 mg/kg dosing, PGE2 levels in the anastomotic tissue

were increased **(Figure 20D)** and the ACS was significantly lower in the SW003291-treated mice compared to the vehicle controls, which corresponds to a 45 % increase in the CAH rates **(Figure 20E)**. Moreover, our analysis using the anastomotic tissues collected from vehicle- and SW033291-treated mice in 10 mg/kg dosing showed a significant inverse correlation between tissue PGE2 levels and the severity of the leakage indicating that PGE2 might promote healing **(Figure 20F)**.

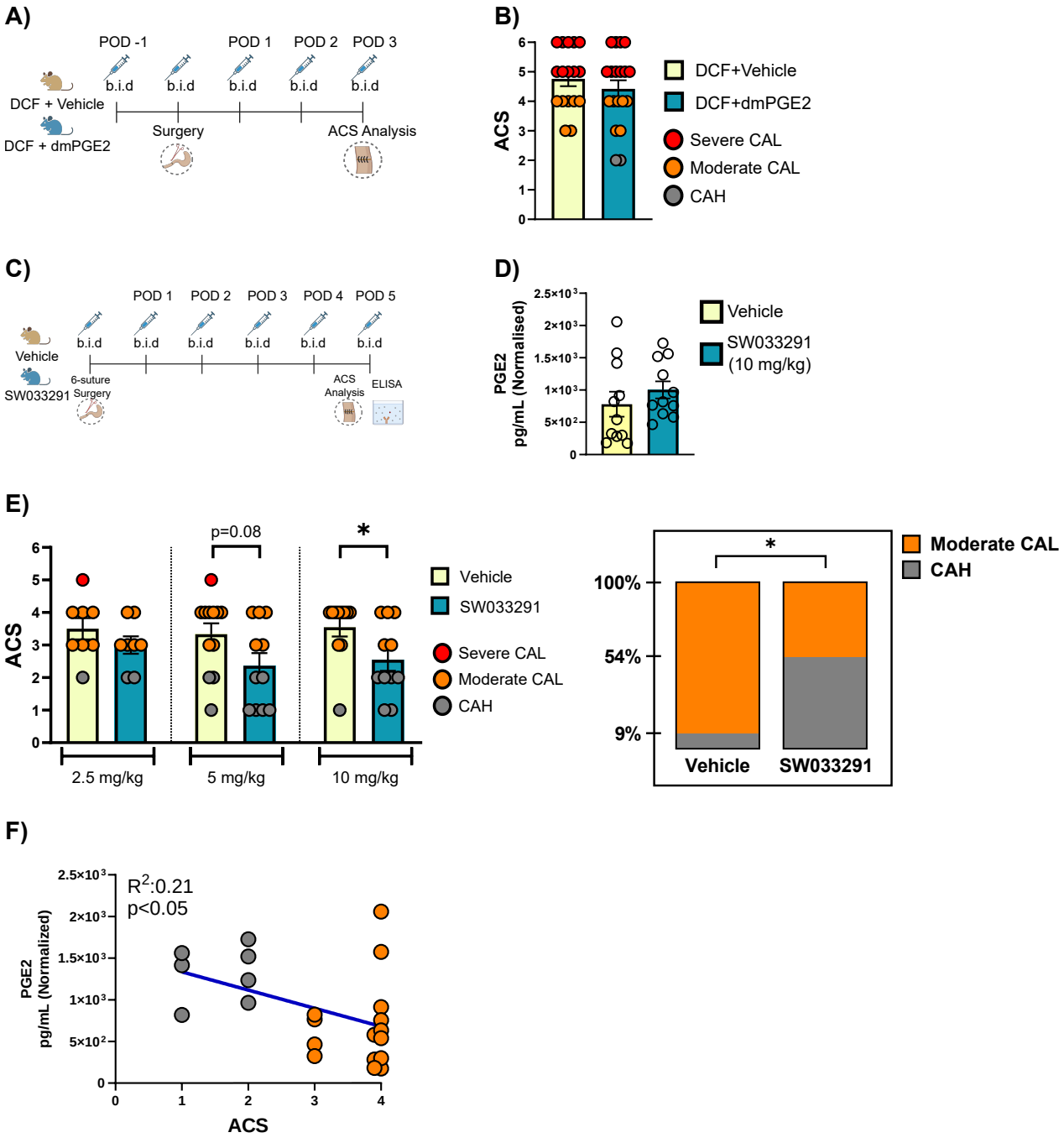

Fig. 20: Effect of PGE2 in preventing DCF-induced and spontaneously occurring CAL. **A)** Experimental design for testing the effect of dmPGE2 supplementation on DCF-induced CAL. **B)** ACS of DCF+Vehicle- (n=17) and DCF+dmPGE2-treated (n=19) mice at POD3 **C)** Experimental design for testing the effect of increasing endogenous PGE2 levels with SW033291 treatment on insufficient suture CAL model. **D)** Normalized PGE2 levels in anastomotic tissues collected from 10 mg/kg SW033291- and vehicle-treated mice at POD5. **E)** Bar graph on the left showing the ACS of SW032291- and vehicle-treated mice at POD5 in 2.5 mg/kg (n=8), 5 mg/kg (n=11-12), and 10 mg/kg (n=11) dosing. Stacked bar charts on the right shows moderate CAL and CAH ratios in 10 mg/kg SW032291- and vehicle-treated mice at POD5. **F)** Correlation analysis between normalized PGE2 levels and ACS score based on the within anastomotic tissues collected from 10 mg/kg SW033291- and vehicle-treated mice at POD5. Data points were jittered to ensure the visibility of data points. Unpaired t-test, Chi-square and correlation tests were applied. *$p \leq 0.05$

In summary, our data show that PGE2 is a key mediator of CAH. Supporting its endogenous production or inhibiting PGE2 degradation might be a suitable strategy to support CAH in patients at risk of developing CAL. At the cellular level, multiple immune cell populations have been shown to switch into a detrimental state in the absence of PGE2 (Cheng et al. 2021), making it an interesting target for future studies aiming to understand the full mechanism of PGE2 action in anastomotic leakage.

4 Discussion

4.1 Identification of Layer-specific Transcriptional Signatures in CAH Mouse model

CAH is a well-orchestrated process that follows three distinct stages, namely inflammation, proliferation, and remodelling (Morgan and Shogan 2022). Each stage involves multiple cell types and biological pathways whose fined-tuned regulation plays an important role in successful CAH (Bosmans et al. 2015). Therefore, characterizing cellular and molecular mechanisms behind each stage of CAH is crucial. Moreover, wound healing is a dynamic process where its stages highly overlap, and different components of these phases come into play over time (Guo and DiPietro 2010). Cutaneous wound healing studies have become the major source of information for the regulation of these stages, however, many factors involved in healing differ between skin and colon (Bosmans et al. 2015; Chadi et al. 2016; Lam et al. 2020; Lee et al. 2018; Lundy 2014). Therefore, our current knowledge of CAH is still very limited, and detailed longitudinal analyses of anastomotic tissues are needed to fully characterize CAH.

Another important factor to consider in CAH is the different layers of the bowel wall. In the case of surgical manipulation exerted by handling of the bowel without transection, the ME layer has been the focus of many studies (Schneider et al. 2021; Schneider et al. 2022; Stoffels et al. 2014). However, in the case of anastomotic injury, which involves complete bowel wall transection, transmural healing is required that involves ME and M/SM, which might have distinct roles. M/SM is considered critical since the mucosal surface provides a barrier and protects the epithelial cells against pathogens and toxins (Linden et al. 2008). Moreover, collagens in the submucosa provide strength in the tissue (Bosmans et al. 2017; Rosendorf et al. 2022). Collagens also reside in the muscularis propria making the ME layer an important component of CAH (Thompson et al. 2006). However, transcriptional profiles of the intestinal layers throughout CAH stages have not been studied before.

To this end, the first aim of this project was to provide a detailed transcriptional description of the M/SM and ME layers of the anastomotic tissues throughout CAH using a mouse anastomosis model.

Our findings show that both layers follow the common stages of wound healing, namely inflammation, proliferation, and remodelling. Correlation analyses of the transcriptional profile of M/SM and ME at 6 h, 24 h, and 72 h further indicated that these layers follow the wound healing stages mostly in synchronization.

Analysis of the 6 h time point showed that inflammation starts immediately after surgery in both layers, and it is mainly dominated by the innate immune response as shown by the enrichment of neutrophils, macrophages, and monocytes signatures. Additionally, our data indicated that adaptive immune responses were enriched in CAH as well, which was also shown by van Helsdingen et al. recently in a rat anastomosis model (van Helsdingen et al. 2023). Interestingly, inflammation appeared to decrease at 24 h and then significantly increase again at 72 h time point at the M/SM layer. However, inflammatory responses were significantly upregulated at 24 h compared to 6 h and remained the same at 72 h time point in the ME layer. This observation could be because the granulation tissue, which carries a large portion of the immune cells remained in the ME layer after separation.

Together with inflammation and defense responses, angiogenesis was also simultaneously triggered in the early postoperative M/SM and ME. Previous studies have associated angiogenesis with the proliferation stage of wound healing (Zhang et al. 2020). However, our data showed that transcriptional initiation of the angiogenesis coincides with the inflammation phase. Recently, based on the histological evaluation of the anastomotic tissue, neoangiogenesis was reported to start 3 days after surgery in an anastomosis rat model (van Helsdingen et al. 2023). Interestingly, we also found a further enrichment of angiogenesis-related genes at 72 h within both the M/SM and ME layer indicating that there might be another phase of angiogenesis in the later stages of CAH.

Additionally, our results showed that the proliferation phase predominantly starts 24 h after surgery in both layers. Interestingly, GSEA showed both positive and negative regulation of proliferation. This suggests that the regulation of proliferation is cell-type dependent. Notably, we also observed a reduction in mesenchymal cell proliferation at 6 h, further supporting that regulation of proliferation might be cell-specific and can begin immediately after surgery. Interestingly, the proliferation phases are not fully synchronized between the

M/SM and ME. While proliferation gene signatures become already downregulated at 72 h in the M/SM, their levels become higher at the 72 h time point compared to the 24 h in the ME. This might be also due to different cell populations present in both layers.

Due to high microbial load of the colon, sufficient and quick healing of anastomoses is very critical to prevent the organism from infections. Therefore, CAH needs to be completed in a short time (Morgan and Shogan 2022). In line with this, we observed enrichment of epithelial cell proliferation at 6 h and ECM remodelling at 72 h, which suggests that the transcriptional initiation of re-epithelization and tissue remodelling of the anastomotic wound might occur earlier than previously thought (Morgan and Shogan 2022). As a relevant example for the early onset of remodelling, we found collagen type I-III and V, which has been reported to be prominent in anastomotic healing (Morgan and Shogan 2022) are already highly induced at 72 h while other remodelling-associated collagens such as *Col16a1*, which supports strength but also cell invasion (Jensen et al. 2018), and *Col18a1*, which are required for remodelling of the enteric nervous system (Nagy et al. 2018), are also induced. A switch from collagen type III to collagen type I in the remodelling stage of the skin wound healing was reported before (Lam et al. 2020; Lundy 2014). Interestingly, transcription of the genes encoding these two collagens, namely *Col1a1* and *Col3a1*, were induced simultaneously in the anastomotic tissue at 72 h time point. However, expression of *Mmp8*, which degrades collagen type I (Biel et al. 2024), is significantly lowered at 72 h compared to 6 h, which might be indicative of changes in collagen content. Having said this measurement of these collagens on protein level and their microscopic visualization will be needed in future studies to demonstrate if such change in collagen content takes place in the anastomotic tissues.

To sum up, our results indicate that CAH is a very dynamic process already within the first 72 h. Whilst different wound healing stages are sequentially initiated, there is a substantial overlap between these stages in both layers. As our study did not include time points after 72 h, it remains unclear when these phases will be resolved. A recent finding indicated that the inflammation was still present 7 days after surgery (van Helsdingen et al. 2023), which is longer than previously thought (Morgan and Shogan 2022). Overall, our data indicate that the wound healing phases are transcriptionally overlapping and not strongly separated

as indicated in a scheme shown in a recent study (Winter et al. 2023). Furthermore, our study shows that the first 72 h after surgery, which has been previously referred to as the “inflammatory phase” (Winter et al. 2023), involves elements of all wound healing stages. Future studies are required to clarify if these quick transcriptional changes correspond to changes in protein levels and cellular compositions.

4.2 Transcriptional Signatures of CAL in M/SM and ME Layers of Anastomotic Tissue

Although research on CAL has increased in the last decade, our understanding of its underlying pathology remains limited due to several knowledge gaps one of which is the role of the different intestinal layers in CAL development (Bosmans et al. 2015). Therefore, another aim of this study was to analyze transcriptional changes in M/SM and ME layers in CAL.

We observed that on the transcriptional level, M/SM, but not ME, differs between CAL and CAH. In line with previous research, we observed that M/SM of CAL tissues had a reduction in ECM remodelling- and collagen-associated pathways (Shogan et al. 2016). Additionally, our data shows that CAL mechanisms may not be limited to these pathways as we observed changes in various other processes such as cell migration and adhesion. However, since this analysis is based on tissues that already had leakage, it remains unknown whether these differences were the cause of CAL, or they were a result of other causative factors that might have taken place in earlier stages of the healing. Also, it is important to note that the statistical power of this analysis was low due to the limited sample size. Hence, future studies with higher power will be needed to validate our findings, which might also reveal the important pathways that we may have missed in this study. Nonetheless, here we provide a list of CAL-associated genes that might be used as leakage markers in mice in addition to other surrogate markers such as bursting pressure and histological examination of inflammatory cell infiltration, fibroblast activity, and collagen deposition. Importantly we identified the CAL pathways in the pre-operatively healthy intestine. For use in humans, other patient-related factors, such as the presence of cancer or intestinal inflammation, should be incorporated in future studies to validate if the genes we identified

can serve as biomarkers for CAL. Due to the newly developed digital rigid sigmoidoscope with the ability to biopsy for surgical rectal assessments (Lewis et al. 2021), the gene list we provide might be useful to identify perianastomotic mucosal CAL signatures in patients at risk of developing CAL. Proteins of some of these CAL–related genes, such as Anxa1, Ccn1, and Krt10, have been previously detected in the circulation and therefore might serve as blood markers for CAL (Han et al. 2018; Lin et al. 2015; Signorelli et al. 2020).

4.3 Concluding Remarks for First Aim of the Project

In conclusion, our study establishes a transcriptional framework of CAH and CAL in mice and provides an inventory of genes associated with various pathways related to both processes. While our findings are on one hand useful for future CAH and CAL studies to identify the right scientific endpoint with appropriate gene sets, they also provide the first insight into target genes that will be further investigated as potential predictors of CAL.

4.4 Investigation of Molecular Mechanisms Behind NSAID-induced CAL

CAL is still a feared complication following colorectal surgery, therefore, there has been an increase in efforts to identify the predictive factors for CAL and postoperative NSAID administration has been recognized as a potential risk factor (Zarnescu et al. 2021; Tsalikidis et al. 2023). Due to the serious side effects of opioids, ERAS protocols recommend NSAID treatment to manage postoperative pain, fever, and inflammation after surgery (Gelman et al. 2018). However, several meta-analyses have found an association between NSAID use and CAL development (Modasi et al. 2019; Huang et al. 2018; Jamjittrong et al. 2020; Smith et al. 2016; Chen et al. 2022). Although these findings have been mostly replicated over the last couple of years, there are contradicting results as well (EuroSurg Collaborative 2020; Arron et al. 2020). Therefore, even though the safety of NSAID administration after colorectal surgery is being questioned, the use of NSAIDs is not avoided worldwide. Previous studies have shown that the pathophysiology of NSAID-induced CAL is multifactorial necessitating an in-depth investigation of pathways affected by the postoperative

NSAID treatment (Reisinger et al. 2017; Inan et al. 2006; Yauw et al. 2018a; Yauw et al. 2018b). Hence, the second aim of this study was to unravel cellular and molecular mechanisms of NSAID-induced CAL with a focus on the COX pathway.

4.5 Effect of Postoperative DCF Administration on COX pathway

To investigate how NSAIDs affect the healing pathways after surgery, we treated mice with diclofenac sodium (DCF), which is a non-selective NSAID, after anastomotic surgery. Our results confirmed the previous findings that DCF treatment leads to CAL development in the proximal colon (Reisinger et al. 2017; Yauw et al. 2015). We observed the first signs of wound healing deficiencies at POD2, which resulted in peritonitis by POD3-POD4 indicating that DCF interferes with the early wound healing processes within the first 48h after surgery.

To gain mechanistic insights into DCF-induced CAL, we performed 3' bulk RNA-seq and first analyzed how the components of the COX pathway, which is blocked by the DCF, were affected by surgical injury with and without drug treatment. We observed that while the anastomotic injury did not influence the levels of *Ptgs1* (COX1), the *Ptgs2* (COX2) expression was significantly upregulated after surgery. This is in line with the previous research that COX1 is constitutively active whereas COX2 is induced upon injury (Funk 2001). Interestingly, there was a significant difference in *Ptgs2* but not in *Ptgs1* levels between vehicle- and DCF-treated mice after surgery, which could be due to a feedback loop where the lack of PGs in the tissue might have resulted in the upregulation of *Ptgs2* expression. We also analyzed the expression of enzymes that derive PGs and observed that only PGE2- and thromboxane A2-producing enzymes (*Ptges* and *Tbxas1*, respectively) were significantly induced upon anastomotic surgery and their levels were even higher in tissues collected from DCF-treated mice. This again might be indicative of a feedback loop where the reduction of PGs caused by DCF treatment in the anastomotic tissue might trigger the expression of these enzymes. Interestingly, this effect was limited to *Ptges* and *Tbxas1* as the expression of the enzymes that derive PGI2, PGD2, and PGF2α were not affected neither by the anastomotic injury nor by the DCF administration. Additionally, dif-

ferences in *Ptgs2*, *Ptges*, and *Tbxas1* expression between vehicle- and DCF-treated mice after surgery were not observed between their corresponding sham-operated controls suggesting that the effect of the DCF on the expression of these enzymes is associated with the injury. Similarly, Maseda et al. reported an increase in *Ptgs2* and *Ptges* expression upon NSAID treatment in mice with C. difficile infection (Maseda et al. 2019). On the contrary, *in vitro* studies investigating the feedback loops within the COX pathway showed that in immune and colon cancer cell lines *Ptgs2* expression increases upon stimulation with PGE2 under non-inflammatory conditions (Hsu et al. 2017; Obermajer et al. 2011; Neuschäfer-Rube et al. 2023). This suggests that the increase we observed in *Ptgs2*, *Ptges*, and *Tbxas1* in DCF-treated mice might be due to other molecular changes induced by the drug or there might an undiscovered feedback loop mechanisms regulating the PG levels under inflammatory conditions. Nonetheless, although the expression of these enzymes was upregulated, production of the PGs was successfully inhibited by DCF as shown by the significant reduction of PGE2 levels measured with ELISA in the anastomotic tissues collected from the DCF-treated mice.

Since PGE2 has been associated with the maintenance of the gut epithelium, protection against acute damage, and regeneration after injury, in this study we paid special attention to PGE2 signalling (Kabashima et al. 2002; Duffin et al. 2016; Zhang et al. 2015). PGE2 signals through four different receptors, namely EP1, EP2, EP3, and EP4 (Funk 2001). Among these EP2 and EP4 have been associated with gut wound healing and regulation of immune responses (Gilman and Limesand 2021). Our RNA-Seq data did not show a difference in *Ptger1* (EP1) and *Ptger3* (EP3) expression after surgery with or without DCF administration. At the same time, *Ptger2* (EP2) levels were substantially elevated in the anastomotic tissues collected from DCF-treated mice. Confirming this, our flow cytometry analysis showed an increase in EP2 expression within neutrophils and infiltrating monocytes in the DCF-treated CAL model. However, EP2 is also expressed by other immune and intestinal cells which were not analyzed in this study (Sun and Li 2018; Olsen Hult et al. 2011; Thumkeo et al. 2022), therefore elevated EP2 expression we observed in RNA-Seq analysis might be driven by other cell types as well. For EP4, previous studies identified it as the highest expressed EP receptor in the colon (Crittenden et al. 2021) and

in line with this we found a ~20-times higher expression in anastomotic tissue than EP2, however, we did not observe a change in *Ptger4* (EP4) expression due to surgical injury and/or DCF administration. Having said this, flow cytometry analysis showed a significant increase in EP4 signal within infiltrating monocytes in the DCF-treated mice showing that the effect of the DCF on the expression of these receptors should be analyzed on a cellular level. Therefore, future studies might employ single-cell RNA-Seq or CyTOF technologies to map EP2 and EP4 expression on the anastomotic tissue and how it changes upon DCF treatment.

4.6 Analysis of Localization and Concentration of PGs in Anastomotic Tissues

PGs, which are arachidonic acid derivatives, are lipid molecules that cannot be visualized by traditional microscopy techniques. To detect the PGs, we performed a spatial analysis by using nanospray desorption electrospray ionization mass spectrometry imaging (nano-DESI MSI) (Duncan et al. 2018). Visualization of the anastomotic tissues collected at POD1 showed that the PGE2 isomers and PGF2α are highly localized in the anastomotic region indicating that production of PGs is spatially regulated. Using light microscopy images of the anastomotic tissues, we identified unaffected, i.e. not operated, regions in ME and M/SM layers as well as anastomotic regions of interest. Fold change analysis of AA, PGE2 isomers, and PGF2α in the anastomotic region compared to unaffected ME and M/SM confirmed the visualization data that whilst AA is produced widely both in the anastomotic region and neighboring parts, PGE2 isomers and PGF2α were substantially increased specifically in the anastomotic region. The colormap scale, which depicts the detected concentration, of the images shows that PGE2 isomer concentrations are much higher than that of PGF2α suggesting that PGE2 isomers are the most abundant PG in the anastomotic tissue. PGE2 isomers include both PGD2 and PGE2, which could not be separated by nano-DESI MSI since they have the same chemical formula (Mavroudakis and Lanekoff 2023). However, our RNA-Seq analysis showed low to no expression in the PGD2-deriving enzyme *Pgds*. Because of this, we infer that PGE2 isomers visualized in the anastomotic tissue mostly contain PGE2 rather than PGD2, hence PGE2 is

the most abundant PG in the anastomotic tissue. To determine the PGE2 concentration in anastomotic tissues, we also performed ELISA and observed an increase in its levels in anastomotic tissues compared to naive colon samples reaching significance at POD2. As opposed to our observations, Jain et al showed that PGE2 reaches its highest levels immediately after injury and declines gradually over time (Jain et al. 2018) suggesting that the dynamics of PGE2 regulation might be dependent on the type of injury.

4.7 Effect of DCF Administration on Inflammatory Responses After Surgery

4.7.1 Effect of DCF on Adaptive Immune Responses After Surgery

We further delved into the molecular mechanisms behind DCF-induced CAL by analyzing transcriptional changes induced by DCF treatment after surgery. PCA analysis showed that in the case of sham operation, vehicle- and DCF-treated mice clustered together indicating that three days of DCF administration alone does not result in transcriptional changes in the proximal colon. However, samples collected from vehicle- and DCF-treated mice 48h after anastomotic surgery clustered separately indicating that the effect of the DCF on the tissue is injury-related.

Analysis of the genes upregulated in the anastomotic tissues of the DCF-treated mice compared to the vehicle-treated controls showed a significant enrichment of the immune responses involving both myeloid and lymphoid cells in the DCF-treated mice indicating a higher level of inflammation. This was an interesting observation because NSAIDs are categorized as anti-inflammatory drugs, however, in some *in vivo* and *in vitro* models of intestinal inflammation, NSAIDs have been shown to exacerbate immune reaction with higher T-cell response. (Chen et al. 2021; Berg et al. 2002). Interestingly our flow cytometry analysis did not show any significant difference in $CD8^+$, $CD4^+$, $NK1.1^+$ NK-T, and $CD19^+$ B cell abundance between vehicle- and DCF-treated mice after anastomotic surgery. Overall, these results show that in the case of anastomotic surgery, DCF can lead to higher inflammation including adaptive immune responses, however, this does not result from an increased abundance of T/B cells suggesting that DCF administration affects

the cell metabolism rather than their proliferation and/or infiltration.

Flow cytometry analysis showed that even though percentage of $CD4^+$ increases after anastomotic surgery, $CD8^+$ cells are the most abundant type of T cells in the anastomotic tissue which is followed by $NK1.1^+$ NK-T cells. Whilst both $CD8^+$ and NK-T cells can react to wounding fast upon stimulation, $CD4^+$ cells need to be differentiated into Th cells for IFN secretion, which might take longer than 48 h (Zheng et al. 2023; Zhu and Zhu 2020). While this makes $CD8^+$ and NK-T cells a likely source for the higher levels of IFN in the early phases of anastomotic injury, future studies are needed to identify the cause of enriched IFN response in the DCF-treated anastomotic tissues given that other immune cell types such as dendritic cells can also produce IFNs (Hochrein et al. 2001).

Another important finding of this study is that adaptive immune responses are partially responsible for DCF-induced CAL. *Rag1*$^{-/-}$ mice, which lack T and B cells, had significantly reduced CAL rates. Better wound healing in the *Rag1*$^{-/-}$ mice was also proven with the transcriptional signatures of healing where the levels of collagen- and ECM remodelling-associated pathways were significantly enriched. Overall, this suggests that elevated T- and/or B-cell activity due to DCF treatment after surgery leads to CAL by disturbing ECM and tissue remodelling. Previous studies showed that T-cell mediated cytokines can lead to a reduction in colon barrier integrity, and higher levels of IFNγ and IL17 were measured in the colonic mucosa and peritoneal cavity of the patients with CAL (Ito et al. 2006; Langer et al. 2019; Hajjar et al. 2023; Qi et al. 2023). Moreover, our flow cytometry analysis showed that $CD19^+$ B cells only constitute 3-4 % of the $CD45^+$ immune cells, whereas the abundance of $CD45^+CD3^+$ is around 15 % in the anastomotic tissues. Altogether, these suggest that the lack of T-cell rather than B-cell activity might be the reason for better healing in the *Rag1*$^{-/-}$ mice, which needs to be confirmed by future studies. Conditional IFN receptor knockout mice, e.g. $CD8^{Cre+}$*Ifnar1*$^{fl/fl}$ and/or $CD8^{Cre+}$*Ifng*$^{fl/fl}$ might be used to identify the roles of specific T-cell responses in DCF-induced CAL development.

While we demonstrated that higher levels of adaptive immune response were a causative factor for DCF-induced CAL, the reason for the dysregulation of these responses remains unknown. It is important to note that adaptive immune responses are also observed in the

case of CAH, however, its higher levels are associated with CAL development indicating that T- and B-cell responses need to be tightly regulated. Interestingly, recent studies have identified PGE2 as one of the regulators of T-cell response where IFN secretion by the T cells was suppressed when treated with either PGE2 or EP2/4 agonists *in vivo* and *in vitro* (Kabashima et al. 2002; Thumkeo et al. 2022; Mehta et al. 2023; Boniface et al. 2009). Since we could partially prevent DCF-induced CAL by removing adaptive immune responses, the lack of PGE2-EP2/4 signalling in the DCF-induced CAL model might be the underlying reason for exacerbated T-cell response. However, given that DCF-treated mice show signs of CAL already at POD2, the elevated immune response observed at this time point might also be due to an already broken epithelial barrier. Future studies should focus on earlier time points to identify the cause of higher IFN response. Additionally, EP2 and EP4 knockout mice can be used to investigate if the absence of EP2/4 signalling would result in elevated IFN response after surgery and to identify the cell types affected by the lack of EP2/4 signalling.

4.7.2 Effect of DCF on Innate Immune Responses After Surgery

Our RNA-Seq data also showed an enrichment of innate immune responses such as neutrophil migration and myeloid cell differentiation in the DCF-treated mice at POD2. Therefore, we analyzed changes in myeloid cell composition after surgery by flow cytometry. Interestingly, albeit not significant, there was a noticeable increase in the percentage of macrophages in the DCF-treated mice, which could be mostly caused by the increase in monocyte-derived macrophages. We did not observe any difference in other myeloid cell types. Having said this, we observed that within neutrophils EP2 expression and within infiltrating monocytes both EP2 and EP4 expression was significantly higher in the DCF-treated mice. Interestingly, a recent study showed that EP4-expressing intestinal macrophages promote the regeneration of the injured epithelium by supporting the intestinal stem cell niche (Na et al. 2021). Overall, these results show that myeloid cells might be susceptible to the lack of PGs in the tissue although their abundance does not change. Future studies are needed on how and if the metabolism of these cells changes and if this

is involved in CAL development.

4.8 The Role of PGE2 in DCF-induced CAL

Given the roles of PGE2-EP2/4 signalling in regulating T-cell response and gut wound healing, we hypothesized that DCF-induced CAL might be caused by the lack of PGE2. However, in our study co-administration of PGE2 with DCF did not reduce CAL rates in mice. This was interesting because Reisinger et al. reported a reduction in CAL development in *COX2*$^{-/-}$ mice with the same dosage and frequency of PGE2 supplementation (Reisinger et al. 2017). This could be because the treatment scheme required to reverse the CAL phenotype in *COX2*$^{-/-}$ mice may not be the same in the DCF-induced CAL model, in which both COX1 and COX2 activity were blocked. Moreover, the plasma half-life of PGE2 (~4.5 mins) is much shorter than that of DCF (~30 mins) (Wilson et al. 2018; Steffenrud 1980), therefore, more stable synthetic PGE2 and/or PGE2 receptor agonists or better delivery methods might be used to test this hypothesis (Cheng et al. 2021). Moving forward, our observation might also indicate that DCF-induced CAL may not be solely caused by the lack of PGE2, and the absence of other PGs might also disturb wound healing. This might be a likely explanation since PGE2 supplementation did not fully prevent CAL in *COX2*$^{-/-}$ mice either (Reisinger et al. 2017). Thus, even though NSAID-induced small intestinal damage has been associated with a lack of PGE2 (Kunikata et al. 2001; Tanaka et al. 2002; Kunikata et al. 2002), it remains unknown if the NSAID-induced CAL can be explained by the blockage of the COX-PGE2 pathway. Moreover, studies have found that inhibition of COX may not be the only mechanism involved in NSAID-induced intestinal damage. For example, Li et al reported that aspirin impairs gut barrier function via depleting important species of gut microbiota such as *P. goldsteinii*, which was associated with CAH (Hajjar et al. 2023; Li et al. 2024). Furthermore, analyses conducted by Lin et al indicated that disturbance in bile acid composition due to aspirin treatment leads to the activation of inflammatory pathways resulting in small intestinal damage (Lin et al. 2024). Similarly, Yauw et al. showed a disruption in bile metabolism due to diclofenac administration leading to anastomotic leakage (Yauw et al. 2018a; Yauw et al. 2018b). Studies

regarding microbiome and bile acid changes due to NSAID treatment might be of particular importance for CAL studies since it was shown that DCF treatment leads to CAL in the proximal colon but not in the distal colon (Yauw et al. 2015). Given that the ileum and proximal colon share similarities in their microbiome and bile composition, mechanisms associated with NSAID-induced small intestinal damage and proximal CAL might be more similar than currently recognized (Yauw et al. 2015). Hence, further studies would be needed to analyze the effect of NSAID-induced microbiome and bile composition changes on anastomotic healing.

Additionally, it is important to note that we observed numerous other changes in the DCF-treated mice that we could not investigate in this study. For example, GOterm analysis of the downregulated genes showed a reduction in antioxidant activity and glutathione metabolism in anastomotic tissue of the DCF-treated mice. Both mechanisms are involved in reducing the levels of reactive oxygen species (ROS) generated during wound healing, which is crucial for preventing ROS-mediated adverse effects (Wu et al. 2004; Wang et al. 2023).

To sum up, the detrimental effects of NSAIDs might be multi-factorial, and more research is needed to fully characterize the pathophysiology of NSAID-induced CAL. In this study, we chose to use DCF due to its reported effects on anastomotic healing, however, there are other types of NSAIDs such as ketorolac that are also associated with CAL (Chen et al. 2022). Hence, future investigations should also test if the mechanisms behind DCF-induced CAL are similar across different types of NSAIDs to develop preventative measures for NSAID-induced CAL.

4.9 The Role of PGE2 in Spontaneously Occurring CAL

Even though the role of PGE2 in NSAID-induced CAL is yet to be determined, the beneficial effects of the PGE2 pathway on gut wound healing have long been recognized (Patankar et al. 2021; Na et al. 2021; Lee et al. 2022; Kunikata et al. 2002). However, the half-life of PGE2 in vivo is extremely short and it causes unwanted systemic effects

such as headache and diarrhea, which limits its therapeutic use (Markovič et al. 2017). Therefore, an alternative drug, named SW033191, that increases PGE2 levels by blocking PGE2-degrading enzyme has been produced (Zhang et al. 2015). Previous studies have shown that SW033191 administration improves colon wound healing *in vivo* (Jain et al. 2018; Zhang et al. 2015). In line with these previous reports, we observed a dose-dependent effect of SW033291 where 10 mg/kg dosing resulted in a significant reduction in CAL in our insufficient suture CAL model, in which CAL develops spontaneously. We also observed an inverse correlation between ACS and PGE2 concentrations suggesting an association between PGE2 and successful wound CAH. While it remains unclear how PGE2 contributes to CAH, previous research has shown that PGE2 not only resolves inflammation but also promotes epithelial regeneration through stem cell expansion and suppression of epithelial cell necroptosis indicating that the beneficial effects of PGE2 in CAH should be explored from different angles in future studies (Miyoshi et al. 2017; Gao et al. 2021; Lee et al. 2022; Patankar et al. 2021). Whilst these studies made it clear that PGE2 is indispensable to achieve successful wound healing, it was also shown that prolonged PGE2 signalling can detriment epithelial regeneration (Jain et al. 2018; Li et al. 2018). Overall, this shows that PGE2 signalling should be tightly regulated, thus studies are needed to pinpoint when and at which concentrations PGE2 is needed to fulfill its supportive role in CAH. To unravel the PGE2-dependent CAH pathways, *Ptges*$^{-/-}$ mice could be utilized. Given that PGE2-EP2/4 has been associated with acute wound healing, pan- or conditional *Ptger2*$^{-/-}$ and *Ptger4*$^{-/-}$ mice can also be used to decipher when and how PGE2-EP2/4 signalling might be beneficial for successful CAH.

4.10 Concluding Remarks for the Second Aim of the Project

In the second part of this study, we used a clinically relevant CAL model and investigated mechanisms behind the detrimental effects of postoperative DCF use. We showed that DCF-induced CAL is caused by excessive adaptive immune responses, which is likely to be due to changes in T-cell activity since the abundance of these cells was not affected in the DCF-treated mice. To the best of our knowledge, this is the first report that links

elevated T-cell response to CAL development and future studies should characterize their subtypes and functions within the anastomotic tissues to better understand their role in NSAID-(un)related CAL development. In this research, we also showed that PGE2 is beneficial for preventing spontaneously occurring CAL providing potential novel targets for improving wound healing post-surgery. Though EP2/4 signalling has been associated with colon wound healing before, further investigations would be required to fully decipher the PGE2 signalling during anastomotic wound healing.

4.11 Final Conclusions

In this project, we aimed to fill important knowledge gaps in the field by adopting a top-down approach. By combining transcriptomics, imaging, and flow cytometry analyses we provided an in-depth investigation of CAH and CAL mechanisms. While our data can serve as a transcriptional inventory to guide researchers when selecting a time point of interest and CAL biomarkers in future mice studies, it also provides new targets that might allow modulating healing pathways to prevent CAL.

5 Abstract

Introduction

Colon anastomotic leakage (CAL) is a postoperative complication originating from disturbed colon anastomotic healing (CAH). Wound healing involves several well-coordinated stages, which have not been comprehensively studied for CAH or CAL. The first aim of this study was to provide transcriptional profiles of different intestinal layers of anastomotic tissues throughout distinct healing stages and to identify CAL-related genes.

Non-steroidal anti-inflammatory drugs (NSAIDs) prevent PGE2 production by inhibiting the COX pathway. Although postoperative NSAID treatment has been recognized as a risk factor for CAL, its molecular and cellular effects on the anastomotic tissue have not been investigated in detail. The second aim of this study was to identify the causative pathways behind NSAID-induced CAL while investigating the roles of PGE2 in CAH.

Methods

To achieve the first aim of this project, proximal colon anastomosis was constructed with 8 interrupted sutures in mice. 6 h, 24 h, and 72 h after surgery, anastomotic complications were assessed. Transcriptional profiles of the inner (mucosa and submucosa) and outer (muscularis externa) layers of the anastomotic and naive control tissues were analyzed with 3' bulk mRNA sequencing to identify the layer-specific healing and leakage pathways.

For the second aim of this project, mice were subjected to postoperative diclofenac sodium (DCF) treatment. Transcriptional and cellular changes induced by DCF treatment in anastomotic tissues were analyzed at postoperative day (POD) 2 with 3' bulk RNA-Seq and flow cytometry. Tissue level PGE2 concentration was determined with nano-DESI MS imaging and ELISA. For testing the beneficial effects of PGE2 on CAH, DCF-induced and insufficient suture CAL mouse models were treated with dmPGE2 and an inhibitor of PGE2-degrading enzyme named SW033291.

Results

Our data regarding the first aim of the project indicate that the mucosa/submucosa and muscularis externa enter the inflammation stage at 6 h, the proliferation stage at 24 h, and the tissue remodelling stage at 72 h during CAH. We observed that transcription profiles of the mucosa/submucosa, but not the muscularis externa, differ between CAH and CAL. Particularly, genes related to extracellular remodelling and wound healing showed lower expression in the mucosa/submucosa of CAL tissue compared to CAH.

Results regarding the second aim of the project showed an enrichment of the adaptive immune responses in the anastomosis of the DCF-treated mice. Confirming the detrimental effects of adaptive immune responses, we observed a significant reduction in ACS and enrichment of extracellular matrix-associated pathways in DCF-treated *Rag1*$^{-/-}$ mice. We identified PGE2 as the most abundant prostaglandin in the anastomotic tissues. While dmPGE2 supplementation did not prevent anastomotic healing deficiencies in the DCF-induced CAL model, 10 mg/kg SW033291 treatment significantly reduced ACS in insufficient suture CAL mouse model.

Conclusions

Mucosa/submucosa and muscularis externa are mostly in synchronization during the inflammation, proliferation, and extracellular remodelling stages during CAH. Transcriptional profiles within the anastomotic mucosa/submucosa differ between CAH and CAL in genes related to extracellular modeling and wound healing, indicating that genes of these pathways may contribute to CAL.

Exaggerated adaptive immune response is one of the causative factors for DCF-induced CAL. As the main type of prostaglandin in the anastomotic tissue, PGE2 promotes CAH, however, the lack of PGE2 signalling may not be the sole reason behind DCF-induced CAL. Future studies would be needed to further descipher the effect of PGE2 signalling on NSAID-(un)related CAL.

6 List of Figures

7 List of Tables

8 References

Adas, Gokhan; Percem, Askın; Adas, Mine; Kemik, Ozgur; Arikan, Soykan; Ustek, Duran et al. (2011): VEGF-A and FGF gene therapy accelerate healing of ischemic colonic anastomoses (experimental study). In International journal of surgery (London, England) 9 (6), pp. 467–471. DOI: 10.1016/j .ijsu.2011.05.002.

Aiken, Jayne; Buscaglia, Georgia; Bates, Emily A.; Moore, Jeffrey K. (2017): The α-Tubulin gene TUBA1A in Brain Development: A Key Ingredient in the Neuronal Isotype Blend. In Journal of developmental biology 5 (3). DOI: 10.3390/jdb5030008 .

Alverdy, John C.; Schardey, Hans Martin (2021): Anastomotic Leak: Toward an Understanding of Its Root Causes. In Journal of gastrointestinal surgery : official journal of the Society for Surgery of the Alimentary Tract. DOI: 10.1007/s11605-021-05048-4 .

Alzoghaibi, Mohammed A.; Zubaidi, Ahmed M. (2014): Upregulation of the proinflammatory cytokine-induced neutrophil chemoattractant-1 and monocyte chemoattractant protein-1 in rats' intestinal anastomotic wound healing–does it matter? In Asian journal of surgery 37 (2), pp. 86–92. DOI: 10.1016/j .asjsur.2013.07.016 .

Arron, Melissa N.N.; Lier, Elisabeth J.; Wilt, Johannes H.W. de; Stommel, Martijn W.J.; van Goor, Harry; Broek, Richard P.G. ten (2020): Postoperative administration of non-steroidal anti-inflammatory drugs in colorectal cancer surgery does not increase anastomotic leak rate; A systematic review and meta-analysis. In European Journal of Surgical Oncology 46 (12), pp. 2167–2173. DOI: 10.1016/j.ejso.2020.07.017 .

Bachmann, Radu; van Hul, Matthias; Baldin, Pamela; Léonard, Daniel; Delzenne, Nathalie M.; Belzer, Clara et al. (2022): Akkermansia muciniphila Reduces Peritonitis and Improves Intestinal Tissue Wound Healing after a Colonic Transmural Defect by a MyD88-Dependent Mechanism. In Cells 11 (17). DOI: 10.3390/cells11172666 .

Berg, Daniel J.; Zhang, Juan; Weinstock, Joel V.; Ismail, Hanan F.; Earle, Keith A.; Alila, Hector et al. (2002): Rapid development of colitis in NSAID-treated IL-10-deficient mice. In Gastroenterology 123 (5), pp. 1527–1542. DOI: 10.1053/gast.2002.1231527 .

Biel, Carin; Faber, Klaas Nico; Bank, Ruud A.; Olinga, Peter (2024): Matrix metalloproteinases in intestinal fibrosis. In Journal of Crohn's & colitis 18 (3), pp. 462–478. DOI: 10.1093/ecco-jcc/jjad178.

Binnebösel, Marcel; Schuler, Tim; Klink, Christian D.; Busch, Daniel; Schöb, Dominik S.; Trotha, Klaus T. von et al. (2014): Influence of CD68+ macrophages and neutrophils on anastomotic healing following laparoscopic sigmoid resection due to diverticulitis. In International journal of colorectal disease 29 (6), pp. 681–688. DOI: 10.1007/s00384-014-1855-5 .

Bjarnason, I.; Hayllar, J.; MacPherson, A. J.; Russell, A. S. (1993): Side effects of nonsteroidal anti-inflammatory drugs on the small and large intestine in humans. In Gastroenterology 104 (6), pp. 1832–1847. DOI: 10.1016/0016-5085(93)90667-2 .

Blair, P. J.; Bayguinov, Y.; Sanders, K. M.; Ward, S. M. (2012): Relationship between enteric neurons and interstitial cells in the primate gastrointestinal tract. In Neurogastroenterology and motility 24 (9), e437-49. DOI:10.1111/j.1365-2982.2012.01975.x .

Boniface, Katia; Bak-Jensen, Kristian S.; Li, Ying; Blumenschein, Wendy M.; McGeachy, Mandy J.; McClanahan, Terrill K. et al. (2009): Prostaglandin E2 regulates Th17 cell differentiation and function through cyclic AMP and EP2/EP4 receptor signaling. In The Journal of experimental medicine 206 (3), pp. 535–548. DOI: 10.1084/jem.20082293 .

Bosmans, J. W. A. M.; Jongen, A. C. H. M.; Birchenough, G. M. H.; Nyström, E. E. L.; Gijbels, M. J. J.; Derikx, J. P. M. et al. (2017): Functional mucous layer and healing of proximal colonic anastomoses in an experimental model. In The British journal of surgery 104 (5), pp. 619–630. DOI: 10.1002/bjs.10456 .

Bosmans, Joanna W. A. M.; Jongen, Audrey C. H. M.; Bouvy, Nicole D.; Derikx, Joep P. M. (2015): Colorectal anastomotic healing: why the biological processes that lead to

anastomotic leakage should be revealed prior to conducting intervention studies. In BMC gastroenterology 15, p. 180. DOI: 10.1186/s12876-015-0410-3 .

Cahill, R. A.; Sheehan, K. M.; Scanlon, R. W.; Murray, F. E.; Kay, E. W.; Redmond, H. P. (2004): Effects of a selective cyclo-oxygenase 2 inhibitor on colonic anastomotic and skin wound integrity. In The British journal of surgery 91 (12), pp. 1613–1618. DOI: 10.1002/bjs.4722 .

Chadi, Sami A.; Fingerhut, Abe; Berho, Mariana; DeMeester, Steven R.; Fleshman, James W.; Hyman, Neil H. et al. (2016): Emerging Trends in the Etiology, Prevention, and Treatment of Gastrointestinal Anastomotic Leakage. In Journal of gastrointestinal surgery : official journal of the Society for Surgery of the Alimentary Tract 20 (12), pp. 2035–2051. DOI: 10.1007/s11605-016-3255-3 .

Chen, Ke; You, Jingyi; Yang, Shimin; Meng, Xinyao; Chen, Xuyong; Wu, Luyao et al. (2023): Abnormally elevated expression of ACTA2 of circular smooth muscle leads to hyperactive contraction in aganglionic segments of HSCR. In Pediatric surgery international 39 (1), p. 214. DOI: 10.1007/s00383-023-05479-x .

Chen, Wen; Liu, Jing; Yang, Yongqiang; Ai, Yanhong; Yang, Yueting (2022): Ketorolac Administration After Colorectal Surgery Increases Anastomotic Leak Rate: A Meta-Analysis and Systematic Review. In Frontiers in surgery 9, p. 652806. DOI: 10.3389/fsurg.2022.652806 .

Chen, Wen Li Kelly; Suter, Emily; Miyazaki, Hikaru; Velazquez, Jason; Lauffenburger, Douglas A.; Griffith, Linda G.; Carrier, Rebecca L. (2021): Synergistic Action of Diclofenac with Endotoxin-Mediated Inflammation Exacerbates Intestinal Injury in Vitro. In ACS infectious diseases 7 (4), pp. 838–848. DOI: 10.1021/acsinfecdis.0c00762 .

Cheng, Hui; Huang, Haoyan; Guo, Zhikun; Chang, Ying; Li, Zongjin (2021): Role of prostaglandin E2 in tissue repair and regeneration. In Theranostics 11 (18), pp. 8836–8854. DOI: 10.7150/thno.63396 .

Chiarello, Maria Michela; Fransvea, Pietro; Cariati, Maria; Adams, Neill James; Bianchi,

Valentina; Brisinda, Giuseppe (2022): Anastomotic leakage in colorectal cancer surgery. In Surgical oncology 40, p. 101708. DOI: 10.1016/j .suronc.2022.101708.

Coleman, R. A.; Smith, W. L.; Narumiya, S. (1994): International Union of Pharmacology classification of prostanoid receptors: properties, distribution, and structure of the receptors and their subtypes. In Pharmacological reviews 46 (2), pp. 205–229.

Conte, Caroline; Riant, Elodie; Toutain, Céline; Pujol, Françoise; Arnal, Jean-François; Lenfant, Françoise; Prats, Anne-Catherine (2008): FGF2 translationally induced by hypoxia is involved in negative and positive feedback loops with HIF-1alpha. In PloS one 3 (8), e3078. DOI: 10.1371/journal.pone.0003078 .

Coquenlorge, Sabrina; van Landeghem, Laurianne; Jaulin, Julie; Cenac, Nicolas; Vergnolle, Nathalie; Duchalais, Emilie et al. (2016): The arachidonic acid metabolite 11β-ProstaglandinF2α controls intestinal epithelial healing: deficiency in patients with Crohn's disease. In Scientific reports 6, p. 25203. DOI: 10.1038/srep25203 .

Crittenden, Siobhan; Goepp, Marie; Pollock, Jolinda; Robb, Calum T.; Smyth, Danielle J.; Zhou, You et al. (2021): Prostaglandin E2 promotes intestinal inflammation via inhibiting microbiota-dependent regulatory T cells. In Science advances 7 (7). DOI: 10.1126/sciadv.abd7954.

Daams, F.; Monkhorst, K.; van den Broek, J.; Slieker, J. C.; Jeekel, J.; Lange, J. F. (2013): Local ischaemia does not influence anastomotic healing: an experimental study. In European surgical research. Europaische chirurgische Forschung. Recherches chirurgicales europeennes 50 (1), pp. 24–31. DOI: 10.1159/000348411 .

Dorris, Stacy L.; Peebles, R. Stokes (2012): PGI2 as a regulator of inflammatory diseases. In Mediators of inflammation 2012, p. 926968. DOI: 10.1155/2012/926968 .

Duffin, Rodger; O'Connor, Richard A.; Crittenden, Siobhan; Forster, Thorsten; Yu, Cunjing; Zheng, Xiaozhong et al. (2016): Prostaglandin E2 constrains systemic inflammation through an innate lymphoid cell-IL-22 axis. In Science (New York, N.Y.) 351 (6279), pp. 1333–1338. DOI: 10.1126/science .aad9903.

Duncan, Kyle D.; Bergman, Hilde-Marléne; Lanekoff, Ingela (2017): A pneumatically assisted nanospray desorption electrospray ionization source for increased solvent versatility and enhanced metabolite detection from tissue. In The Analyst 142 (18), pp. 3424–3431. DOI: 10.1039/c7an00901a .

Duncan, Kyle D.; Fang, Ru; Yuan, Jia; Chu, Rosalie K.; Dey, Sudhansu K.; Burnum-Johnson, Kristin E.; Lanekoff, Ingela (2018): Quantitative Mass Spectrometry Imaging of Prostaglandins as Silver Ion Adducts with Nanospray Desorption Electrospray Ionization. In Analytical chemistry 90 (12), pp. 7246–7252. DOI:10.1021/acs.analchem.8b00350 .

EuroSurg Collaborative (2020): Safety and efficacy of non-steroidal anti-inflammatory drugs to reduce ileus after colorectal surgery. In The British journal of surgery 107 (2), e161-e169. DOI: 10.1002/bjs.11326 .

Flor-Lorente, Blas; Noguera-Aguilar, José Francisco; Delgado-Rivilla, Salvadora; García-González, José María; Rodriguez-Martín, Marcos; Salinas-Ortega, Laura et al. (2023): The economic impact of anastomotic leak after colorectal cancer surgery. In Health economics review 13 (1), p. 12. DOI:10.1186/s13561-023-00425-y .

Funk, C. D. (2001): Prostaglandins and leukotrienes: advances in eicosanoid biology. In Science (New York, N.Y.) 294 (5548), pp. 1871–1875. DOI: 10.1126/science.294.5548.1871 .

Gao, Liang; Yu, Qian; Zhang, Huasheng; Wang, Zhengting; Zhang, Tianyu; Xiang, Jinnan et al. (2021): A resident stromal cell population actively restrains innate immune response in the propagation phase of colitis pathogenesis in mice. In Science translational medicine 13 (603). DOI:10.1126/scitranslmed.abb5071 .

Gelman, David; Gelmanas, Arūnas; Urbanaitė, Dalia; Tamošiūnas, Ramūnas; Sadauskas, Saulius; Bilskienė, Diana et al. (2018): Role of Multimodal Analgesia in the Evolving Enhanced Recovery after Surgery Pathways. In Medicina (Kaunas, Lithuania) 54 (2). DOI: 10.3390/medicina54020020 .

Gilman, Kristy E.; Limesand, Kirsten H. (2021): The complex role of prostaglandin E2-EP receptor signaling in wound healing. In American journal of physiology. Regulatory, integrative and comparative physiology 320 (3), R287-R296. DOI: 10.1152/ajpregu.00185.2020 .

Guo, S.; DiPietro, L. A. (2010): Factors affecting wound healing. In Journal of Dental Research 89 (3), pp. 219–229. DOI: 10.1177/0022034509359125 .

Haghi, Sarvin Es; Khanzadeh, Monireh; Sarejloo, Shirin; Mirakhori, Fariba; Hernandez, Jairo; Dioso, Emma et al. (2024): Systematic review of the significance of neutrophil to lymphocyte ratio in anastomotic leak after gastrointestinal surgeries. In BMC surgery 24 (1), p. 15. DOI: 10.1186/s12893-023-02292-0 .

Hajjar, Roy; Gonzalez, Emmanuel; Fragoso, Gabriela; Oliero, Manon; Alaoui, Ahmed Amine; Calvé, Annie et al. (2023): Gut microbiota influence anastomotic healing in colorectal cancer surgery through modulation of mucosal proinflammatory cytokines. In Gut 72 (6), pp. 1143–1154. DOI: 10.1136/gutjnl-2022-328389 .

Hakkarainen, Timo W.; Steele, Scott R.; Bastaworous, Amir; Dellinger, E. Patchen; Farrokhi, Ellen; Farjah, Farhood et al. (2015): Nonsteroidal anti-inflammatory drugs and the risk for anastomotic failure: a report from Washington State's Surgical Care and Outcomes Assessment Program (SCOAP). In JAMA surgery 150 (3), pp. 223–228. DOI: 10.1001/jamasurg.2014.2239 .

Hammond, Jeffrey; Lim, Sangtaeck; Wan, Yin; Gao, Xin; Patkar, Anuprita (2014): The burden of gastrointestinal anastomotic leaks: an evaluation of clinical and economic outcomes. In Journal of gastrointestinal surgery : official journal of the Society for Surgery of the Alimentary Tract 18 (6), pp. 1176–1185. DOI: 10.1007/s11605-014-2506-4 .

Han, Gao-Hua; Lu, Kai-Jin; Huang, Jun-Xing; Zhang, Li-Xin; Dai, Sheng-Bin; Dai, Chun-Lei (2018): Association of serum annexin A1 with treatment response and prognosis in patients with esophageal squamous cell carcinoma. In Journal of cancer research and therapeutics 14 (Supplement), S667-S674. DOI: 10.4103/0973-1482.187297 .

Hayashi, Akane; Sakamoto, Naoaki; Kobayashi, Koji; Murata, Takahisa (2023): Enhancement of prostaglandin D2-D prostanoid 1 signaling reduces intestinal permeability by stimulating mucus secretion. In Frontiers in immunology 14, p. 1276852. DOI: 10.3389/fimmu.2023.1276852 .

Hochrein, H.; Shortman, K.; Vremec, D.; Scott, B.; Hertzog, P.; O'Keeffe, M. (2001): Differential production of IL-12, IFN-alpha, and IFN-gamma by mouse dendritic cell subsets. In Journal of immunology (Baltimore, Md. : 1950) 166 (9), pp. 5448–5455. DOI: 10.4049/jimmunol.166.9.5448 .

Hove, Anne S. ten; Mallesh, Shilpashree; Zafeiropoulou, Konstantina; Kleer, Janna W. M. de; van Hamersveld, Patricia H. P.; Welting, Olaf et al. (2023): Sympathetic activity regulates epithelial proliferation and wound healing via adrenergic receptor α2A. In Scientific reports 13 (1), p. 17990. DOI:10.1038/s41598-023-45160-w .

Hsu, Hsi-Hsien; Lin, Yueh-Min; Shen, Chia-Yao; Shibu, Marthandam Asokan; Li, Shin-Yi; Chang, Sheng-Huang et al. (2017): Prostaglandin E2-Induced COX-2 Expressions via EP2 and EP4 Signaling Pathways in Human LoVo Colon Cancer Cells. In International journal of molecular sciences 18 (6). DOI:10.3390/ijms18061132 .

Huang, Yeqian; Tang, Stephen R.; Young, Christopher J. (2018): Nonsteroidal anti-inflammatory drugs and anastomotic dehiscence after colorectal surgery: a meta-analysis. In ANZ journal of surgery 88 (10), pp. 959–965. DOI:10.1111/ans.14322 .

Hyman, Neil; Manchester, Thomas L.; Osler, Turner; Burns, Betsy; Cataldo, Peter A. (2007): Anastomotic leaks after intestinal anastomosis: it's later than you think. In Annals of Surgery 245 (2), pp. 254–258. DOI:10.1097/01 .sla.0000225083.27182.85.

Inan, Aydin; Koca, Cemile; Sen, Meral (2006): Effects of diclofenac sodium on bursting pressures of anastomoses and hydroxyproline contents of perianastomotic tissues in a laboratory study. In International journal of surgery (London, England) 4 (4), pp. 222–227. DOI: 10.1016/j .ijsu.2006.01.002.

Ito, R.; Shin-Ya, M.; Kishida, T.; Urano, A.; Takada, R.; Sakagami, J. et al. (2006): Interferon-gamma is causatively involved in experimental inflammatory bowel disease in mice. In Clinical and experimental immunology 146 (2), pp. 330–338. DOI: 10.1111/j.1365-2249.2006.03214.x .

Jain, Umang; Lai, Chin-Wen; Xiong, Shanshan; Goodwin, Victoria M.; Lu, Qiuhe; Muegge, Brian D. et al. (2018): Temporal Regulation of the Bacterial Metabolite Deoxycholate during Colonic Repair Is Critical for Crypt Regeneration. In Cell host & microbe 24 (3), 353-363.e5. DOI: 10.1016/j .chom.2018.07.019.

Jamjittrong, Supaschin; Matsuda, Akihisa; Matsumoto, Satoshi; Kamonvarapitak, Tunyaporn; Sakurazawa, Nobuyuki; Kawano, Youichi et al. (2020): Postoperative non-steroidal anti-inflammatory drugs and anastomotic leakage after gastrointestinal anastomoses: Systematic review and meta-analysis. In Annals of gastroenterological surgery 4 (1), pp. 64–75. DOI: 10.1002/ags3.12300 .

Jensen, Christina; Nielsen, Signe H.; Mortensen, Joachim H.; Kjeldsen, Jens; Klinge, Lone G.; Krag, Aleksander et al. (2018): Serum type XVI collagen is associated with colorectal cancer and ulcerative colitis indicating a pathological role in gastrointestinal disorders. In Cancer medicine 7 (9), pp. 4619–4626. DOI: 10.1002/cam4.1692 .

Jørgensen, Anders Bech; Jonsson, Isabella; Friis-Hansen, Lennart; Brandstrup, Birgitte (2023): Collagenase-producing bacteria are common in anastomotic leakage after colorectal surgery: a systematic review. In International journal of colorectal disease 38 (1), p. 275. DOI: 10.1007/s00384-023-04562-y .

Kabashima, Kenji; Saji, Tomomi; Murata, Takahiko; Nagamachi, Miyako; Matsuoka, Toshiyuki; Segi, Eri et al. (2002): The prostaglandin receptor EP4 suppresses colitis, mucosal damage and CD4 cell activation in the gut. In The Journal of clinical investigation 109 (7), pp. 883–893. DOI: 10.1172/JCI14459 .

Komen, N.; Bruin, R. W. F. de; Kleinrensink, G. J.; Jeekel, J.; Lange, J. F. (2008): Anastomotic leakage, the search for a reliable biomarker. A review of the literature. In Colorectal

disease : the official journal of the Association of Coloproctology of Great Britain and Ireland 10 (2), 109-15; discussion 115-7. DOI: 10.1111/j.1463-1318.2007.01430.x .

Kozlowska, Mariana; Rodziewicz, Pawel; Kaczmarek-Kedziera, Anna (2017): Structural stability of diclofenac vs. inhibition activity from ab initio molecular dynamics simulations. Comparative study with ibuprofen and ketoprofen. In Struct Chem 28 (4), pp. 999–1008. DOI: 10.1007/s11224-016-0893-8 .

Kunikata, T.; Araki, H.; Takeeda, M.; Kato, S.; Takeuchi, K. (2001): Prostaglandin E prevents indomethacin-induced gastric and intestinal damage through different EP receptor subtypes. In Journal of physiology, Paris 95 (1-6), pp. 157–163. DOI: 10.1016/s0928-4257(01)00021-3 .

Kunikata, Tomonori; Tanaka, Akiko; Miyazawa, Tohru; Kato, Shinichi; Takeuchi, Koji (2002): 16,16-Dimethyl prostaglandin E2 inhibits indomethacin-induced small intestinal lesions through EP3 and EP4 receptors. In Digestive diseases and sciences 47 (4), pp. 894–904. DOI: 10.1023/a:1014725024519 .

Lam, Adam; Fleischer, Brian; Alverdy, John (2020): The Biology of Anastomotic Healing-the Unknown Overwhelms the Known. In Journal of gastrointestinal surgery : official journal of the Society for Surgery of the Alimentary Tract 24 (9), pp. 2160–2166. DOI: 10.1007/s11605-020-04680-w .

Langer, Victoria; Vivi, Eugenia; Regensburger, Daniela; Winkler, Thomas H.; Waldner, Maximilian J.; Rath, Timo et al. (2019): IFN-γ drives inflammatory bowel disease pathogenesis through VE-cadherin-directed vascular barrier disruption. In The Journal of clinical investigation 129 (11), pp. 4691–4707. DOI: 10.1172/JCI124884 .

Laronha, Helena; Caldeira, Jorge (2020): Structure and Function of Human Matrix Metalloproteinases. In Cells 9 (5). DOI: 10.3390/cells9051076 .

Lee, Chansu; An, Minae; Joung, Je-Gun; Park, Woong-Yang; Chang, Dong Kyung; Kim, Young-Ho; Hong, Sung Noh (2022): TNFα Induces LGR5+ Stem Cell Dysfunction In Patients With Crohn's Disease. In Cellular and molecular gastroenterology and hepatology

13 (3), pp. 789–808. DOI: 10.1016/j .jcmgh.2021.10.010.

Lee, Jou A.; Chico, Timothy J. A.; Renshaw, Stephen A. (2018): The triune of intestinal microbiome, genetics and inflammatory status and its impact on the healing of lower gastrointestinal anastomoses. In The FEBS journal 285 (7), pp. 1212–1225. DOI: 10.1111/febs.14346 .

Lengeling, Randall W.; Mitros, Frank A.; Brennan, John A.; Schulze, Konrad S. (2003): Ulcerative ileitis encountered at ileo-colonoscopy: likely role of nonsteroidal agents. In Clinical gastroenterology and hepatology : the official clinical practice journal of the American Gastroenterological Association 1 (3), pp. 160–169. DOI: 10.1053/cgh.2003.50024.

Lenselink, Ellie A. (2015): Role of fibronectin in normal wound healing. In International wound journal 12 (3), pp. 313–316. DOI: 10.1111/iwj.12109 .

Lewis, James A.; Khan, Shabuddin; Tilney, Henry S.; Wilson, Jonathan M.; Vitone, Louis J.; Souvatzi, Maria et al. (2021): An Observational Analysis of a Novel Digital Rectoscope. In Diseases of the colon and rectum 64 (12), e728-e734. DOI: 10.1097/DCR.0000000000002248 .

Li, Ting; Ding, Ning; Guo, Hanqing; Hua, Rui; Lin, Zehao; Tian, Huohuan et al. (2024): A gut microbiota-bile acid axis promotes intestinal homeostasis upon aspirin-mediated damage. In Cell host & microbe 32 (2), 191-208.e9. DOI: 10.1016/j .chom.2023.12.015 .

Li, Yuan; Soendergaard, Christoffer; Bergenheim, Fredrik Holmberg; Aronoff, David M.; Milne, Ginger; Riis, Lene Buhl et al. (2018): COX-2-PGE2 Signaling Impairs Intestinal Epithelial Regeneration and Associates with TNF Inhibitor Responsiveness in Ulcerative Colitis. In EBioMedicine 36, pp. 497–507. DOI: 10.1016/j .ebiom.2018.08.040 .

Lillja, Johan; Duncan, Kyle D.; Lanekoff, Ingela (2023): Ion-to-Image, i2i, a Mass Spectrometry Imaging Data Analysis Platform for Continuous Ionization Techniques. In Analytical chemistry 95 (31), pp. 11589–11595. DOI: 10.1021/acs.analchem.3c01615 .

Lin, Jinpiao; Li, Ningli; Chen, Huijuan; Liu, Can; Yang, Bin; Ou, Qishui (2015): Serum

Cyr61 is associated with clinical disease activity and inflammation in patients with systemic lupus erythematosus. In Medicine 94 (19), e834. DOI: 10.1097/MD.0000000000000834 .

Lin, Qiuxia; Zhang, Binbin; Dai, Manyun; Cheng, Yan; Li, Fei (2024): Aspirin Caused Intestinal Damage through FXR and ET-1 Signaling Pathways. In International journal of molecular sciences 25 (6). DOI: 10.3390/ijms25063424.

Linden, S. K.; Sutton, P.; Karlsson, N. G.; Korolik, V.; McGuckin, M. A. (2008): Mucins in the mucosal barrier to infection. In Mucosal immunology 1 (3), pp. 183–197. DOI: 10.1038/mi.2008.5 .

Lundy, Jonathan (2014): A Primer on Wound Healing in Colorectal Surgery in the Age of Bioprosthetic Materials. In Clinics in Colon and Rectal Surgery 27 (04), pp. 125–133. DOI: 10.1055/s-0034-1394086 .

Maiden, Laurence; Thjodleifsson, Bjarni; Seigal, Anna; Bjarnason, Ingvar Iain; Scott, David; Birgisson, Sigurbjorn; Bjarnason, Ingvar (2007): Long-term effects of nonsteroidal anti-inflammatory drugs and cyclooxygenase-2 selective agents on the small bowel: a cross-sectional capsule enteroscopy study. In Clinical gastroenterology and hepatology : the official clinical practice journal of the American Gastroenterological Association 5 (9), pp. 1040–1045. DOI: 10.1016/j .cgh.2007.04.031 .

Markovič, Tijana; Jakopin, Žiga; Dolenc, Marija Sollner; Mlinarič-Raščan, Irena (2017): Structural features of subtype-selective EP receptor modulators. In Drug discovery today 22 (1), pp. 57–71. DOI: 10.1016/j .drudis.2016.08.003.

Marônek, Martin; Marafini, Irene; Gardlík, Roman; Link, René; Troncone, Edoardo; Monteleone, Giovanni (2021): Metalloproteinases in Inflammatory Bowel Diseases. In Journal of inflammation research 14, pp. 1029–1041. DOI: 10.2147/JIR.S288280 .

Martinez, Fernando O.; Gordon, Siamon (2014): The M1 and M2 paradigm of macrophage activation: time for reassessment. In F1000prime reports 6, p. 13. DOI: 10.12703/P6-13 .

Maseda, Damian; Zackular, Joseph P.; Trindade, Bruno; Kirk, Leslie; Roxas, Jennifer

Lising; Rogers, Lisa M. et al. (2019): Nonsteroidal Anti-inflammatory Drugs Alter the Microbiota and Exacerbate Clostridium difficile Colitis while Dysregulating the Inflammatory Response. In mBio 10 (1). DOI:10.1128/mBio.02282-18 .

Matsuda, Takeru; Yamashita, Kimihiro; Hasegawa, Hiroshi; Oshikiri, Taro; Hosono, Masayoshi; Higashino, Nobuhide et al. (2018): Recent updates in the surgical treatment of colorectal cancer. In Annals of Gastroent Surgery 2 (2), pp. 129–136. DOI: 10.1002/ags3.12061 .

Mavroudakis, Leonidas; Lanekoff, Ingela (2023): Identification and Imaging of Prostaglandin Isomers Utilizing MS3 Product Ions and Silver Cationization. In Journal of the American Society for Mass Spectrometry 34 (10), pp. 2341–2349. DOI: 10.1021/jasms.3c00233 .

McDermott, F. D.; Heeney, A.; Kelly, M. E.; Steele, R. J.; Carlson, G. L.; Winter, D. C. (2015): Systematic review of preoperative, intraoperative and postoperative risk factors for colorectal anastomotic leaks. In The British journal of surgery 102 (5), pp. 462–479. DOI: 10.1002/bjs.9697 .

Mehta, Hema; Tasin, Irene; Hackstein, Carl Philipp; Willberg, Christian; Klenerman, Paul (2023): Prostaglandins differentially modulate mucosal-associated invariant T-cell activation and function according to stimulus. In Immunology and cell biology 101 (3), pp. 262–272. DOI: 10.1111/imcb.12617.

Miltschitzky, J. R. E.; Clees, Z.; Weber, M-C; Vieregge, V.; Walter, R. L.; Friess, H. et al. (2021): Intestinal anastomotic healing models during experimental colitis. In International journal of colorectal disease 36 (10), pp. 2247–2259. DOI: 10.1007/s00384-021-04014-5 .

Miyoshi, Hiroyuki; VanDussen, Kelli L.; Malvin, Nicole P.; Ryu, Stacy H.; Wang, Yi; Sonnek, Naomi M. et al. (2017): Prostaglandin E2 promotes intestinal repair through an adaptive cellular response of the epithelium. In The EMBO journal 36 (1), pp. 5–24. DOI: 10.15252/embj.201694660 .

Modasi, Aryan; Pace, David; Godwin, Marshall; Smith, Chris; Curtis, Bryan (2019): NSAID administration post colorectal surgery increases anastomotic leak rate: systematic review/meta-analysis. In Surgical endoscopy 33 (3), pp. 879–885. DOI: 10.1007/s00464-018-6355-1 .

Mogor, Fruzsina; Kovács, Tamás; Lohinai, Zoltan; Dora, David (2021): The Enteric Nervous System and the Microenvironment of the Gut: The Translational Aspects of the Microbiome-Gut-Brain Axis. In Applied Sciences 11 (24), p. 12000. DOI: 10.3390/app112412000 .

Morgan, Ryan B.; Shogan, Benjamin D. (2022): The Science of Anastomotic Healing. In Seminars in colon and rectal surgery 33 (2). DOI: 10.1016/j .scrs.2022.100879.

Na, Yi Rang; Jung, Daun; Stakenborg, Michelle; Jang, Hyeri; Gu, Gyo Jeong; Jeong, Mi Reu et al. (2021): Prostaglandin E2 receptor PTGER4-expressing macrophages promote intestinal epithelial barrier regeneration upon inflammation. In Gut 70 (12), pp. 2249–2260. DOI: 10.1136/gutjnl-2020-322146 .

Nagy, Nandor; Barad, Csilla; Hotta, Ryo; Bhave, Sukhada; Arciero, Emily; Dora, David; Goldstein, Allan M. (2018): Collagen 18 and agrin are secreted by neural crest cells to remodel their microenvironment and regulate their migration during enteric nervous system development. In Development (Cambridge, England) 145 (9). DOI: 10.1242/dev.160317 .

Nandakumar, Govind; Stein, Sharon L.; Michelassi, Fabrizio (2009): Anastomoses of the lower gastrointestinal tract. In Nature reviews. Gastroenterology and hepatology 6 (12), pp. 709–716. DOI: 10.1038/nrgastro.2009.185.

Neumann, Philipp-Alexander; Twardy, Vanessa; Becker, Felix; Geyer, Christiane; Schwegmann, Katrin; Mohr, Annika et al. (2018): Assessment of MMP-2/-9 expression by fluorescence endoscopy for evaluation of anastomotic healing in a murine model of anastomotic leakage. In PloS one 13 (3), e0194249. DOI: 10.1371/journal.pone.0194249 .

Neuschäfer-Rube, Frank; Schön, Theresa; Kahnt, Ines; Püschel, Gerhard Paul (2023):

LDL-Dependent Regulation of TNFα/PGE2 Induced COX-2/mPGES-1 Expression in Human Macrophage Cell Lines. In Inflammation 46 (3), pp. 893–911. DOI: 10.1007/s10753-022-01778-y .

Obermajer, Natasa; Muthuswamy, Ravikumar; Lesnock, Jamie; Edwards, Robert P.; Kalinski, Pawel (2011): Positive feedback between PGE2 and COX2 redirects the differentiation of human dendritic cells toward stable myeloid-derived suppressor cells. In Blood 118 (20), pp. 5498–5505. DOI: 10.1182/blood-2011-07-365825 .

Olsen Hult, Lene Th; Kleiveland, Charlotte R.; Fosnes, Kjetil; Jacobsen, Morten; Lea, Tor (2011): EP receptor expression in human intestinal epithelium and localization relative to the stem cell zone of the crypts. In PloS one 6 (10), e26816. DOI: 10.1371/journal.pone.0026816 .

Pasternak, B.; Matthiessen, P.; Jansson, K.; Andersson, M.; Aspenberg, P. (2010): Elevated intraperitoneal matrix metalloproteinases-8 and -9 in patients who develop anastomotic leakage after rectal cancer surgery: a pilot study. In Colorectal disease : the official journal of the Association of Coloproctology of Great Britain and Ireland 12 (7 Online), e93-8. DOI: 10.1111/j.1463-1318.2009.01908.x .

Patankar, Jay V.; Müller, Tanja M.; Kantham, Srinivas; Acera, Miguel Gonzalez; Mascia, Fabrizio; Scheibe, Kristina et al. (2021): E-type prostanoid receptor 4 drives resolution of intestinal inflammation by blocking epithelial necroptosis. In Nature cell biology 23 (7), pp. 796–807. DOI: 10.1038/s41556-021-00708-8 .

Pinchuk, Irina V.; Beswick, Ellen J.; Saada, Jamal I.; Boya, Gushyalatha; Schmitt, David; Raju, Gottumukkala S. et al. (2011): Human colonic myofibroblasts promote expansion of CD4+ CD25high Foxp3+ regulatory T cells. In Gastroenterology 140 (7), pp. 2019–2030. DOI: 10.1053/j .gastro.2011.02.059.

Pochard, Camille; Gonzales, Jacques; Bessard, Anne; Mahe, Maxime M.; Bourreille, Arnaud; Cenac, Nicolas et al. (2021): PGI2 Inhibits Intestinal Epithelial Permeability and Apoptosis to Alleviate Colitis. In Cellular and molecular gastroenterology and hepatology

12 (3), pp. 1037–1060. DOI: 10.1016/j .jcmgh.2021.05.001 .

Qi, Xin-Yu; Tan, Fei; Liu, Mao-Xing; Xu, Kai; Gao, Pin; Yao, Zhen-Dan et al. (2023): Serum and peritoneal biomarkers for the early prediction of symptomatic anastomotic leakage in patients following laparoscopic low anterior resection: A single-center prospective cohort study. In Cancer reports (Hoboken, N.J.) 6 (4), e1781. DOI: 10.1002/cnr2.1781 .

Ramphal, Winesh; Boeding, Jeske R. E.; Gobardhan, Paul D.; Rutten, Harm J. T.; Winter, Leandra J. M. Boonman de; Crolla, Rogier M. P. H.; Schreinemakers, Jennifer M. J. (2018): Oncologic outcome and recurrence rate following anastomotic leakage after curative resection for colorectal cancer. In Surgical oncology 27 (4), pp. 730–736. DOI: 10.1016/j .suronc.2018.10.003 .

Rao, Jaladanki N.; Wang, Jian-Ying (2010): Regulation of Gastrointestinal Mucosal Growth. DOI: 10.4199/C00028ED1V01Y201103ISP015 .

Reisinger, Kostan W.; Schellekens, Dirk H. S. M.; Bosmans, Joanna W. A. M.; Boonen, Bas; Hulsewé, Karel W. E.; Sastrowijoto, Prapto et al. (2017): Cyclooxygenase-2 Is Essential for Colorectal Anastomotic Healing. In Annals of Surgery 265 (3), pp. 547–554. DOI: 10.1097/SLA.0000000000001744 .

Rijcken, Emile; Sachs, Larissa; Fuchs, Thomas; Spiegel, Hans-Ullrich; Neumann, Philipp-Alexander (2014): Growth factors and gastrointestinal anastomotic healing. In The Journal of surgical research 187 (1), pp. 202–210. DOI: 10.1016/j .jss.2013.10.013 .

Rosendorf, J.; Klicova, M.; Herrmann, I.; Anthis, A.; Cervenkova, L.; Palek, R. et al. (2022): Intestinal Anastomotic Healing: What do We Know About Processes Behind Anastomotic Complications. In Frontiers in surgery 9, p. 904810. DOI: 10.3389/fsurg.2022.904810 .

Sawayama, Hiroshi; Miyamoto, Yuji; Yoshida, Naoya; Baba, Hideo (2022): Essential updates 2020/2021: Colorectal diseases (benign)—Current topics in the surgical and medical treatment of benign colorectal diseases. In Annals of Gastroent Surgery 6 (3), pp. 321–335. DOI:10.1002/ags3.12548 .

Schepper, Sebastiaan de; Stakenborg, Nathalie; Matteoli, Gianluca; Verheijden, Simon; Boeckxstaens, Guy E. (2018): Muscularis macrophages: Key players in intestinal homeostasis and disease. In Cellular immunology 330, pp. 142–150. DOI:10.1016/j .cellimm.2017.12.009.

Schneider, Reiner; Leven, Patrick; Glowka, Tim; Kuzmanov, Ivan; Lysson, Mariola; Schneiker, Bianca et al. (2021): A novel P2X2-dependent purinergic mechanism of enteric gliosis in intestinal inflammation. In EMBO molecular medicine 13 (1), e12724. DOI: 10.15252/emmm.202012724 .

Schneider, Reiner; Leven, Patrick; Mallesh, Shilpashree; Breßer, Mona; Schneider, Linda; Mazzotta, Elvio et al. (2022): IL-1-dependent enteric gliosis guides intestinal inflammation and dysmotility and modulates macrophage function. In Communications biology 5 (1), p. 811. DOI: 10.1038/s42003-022-03772-4 .

Sengul, Hilal; Bantavi, Vasiliki; Yim, Andrew Y.F. Li; Efferz, Patrik; Schneiker, Bianca; Jonge, Wouter J. de; Wehner, Sven (2024): Layer-specific Transcriptional Signatures of Colon Anastomotic Healing and Leakage in Mice.

Shi, Jinyao; Wu, Zhouqiao; Li, Ziyu; Ji, Jiafu (2018): Roles of Macrophage Subtypes in Bowel Anastomotic Healing and Anastomotic Leakage. In Journal of immunology research 2018, p. 6827237. DOI: 10.1155/2018/6827237 .

Shi, Shang; Liu, Yang; Wang, Zhiyue; Jin, Xiangren; Yan, Wei; Guo, Xiao et al. (2022): Fusobacterium nucleatum induces colon anastomosis leak by activating epithelial cells to express MMP9. In Frontiers in microbiology 13, p. 1031882. DOI: 10.3389/fmicb.2022.1031882.

Shogan, Benjamin D.; Belogortseva, Natalia; Luong, Preston M.; Zaborin, Alexander; Lax, Simon; Bethel, Cindy et al. (2015): Collagen degradation and MMP9 activation by Enterococcus faecalis contribute to intestinal anastomotic leak. In Science translational medicine 7 (286), 286ra68. DOI:10.1126/scitranslmed.3010658.

Signorelli, Mirko; Ayoglu, Burcu; Johansson, Camilla; Lochmüller, Hanns; Straub, Volker;

Muntoni, Francesco et al. (2020): Longitudinal serum biomarker screening identifies malate dehydrogenase 2 as candidate prognostic biomarker for Duchenne muscular dystrophy. In Journal of cachexia, sarcopenia and muscle 11 (2), pp. 505–517. DOI: 10.1002/jcsm.12517.

Singh, Drishtant; Rai, Vikrant; Agrawal, Devendra K. (2023): Regulation of Collagen I and Collagen III in Tissue Injury and Regeneration. In Cardiology and cardiovascular medicine 7 (1), pp. 5–16. DOI: 10.26502/fccm.92920302.

Smith, Stephen A.; Roberts, Derek J.; Lipson, Mark E.; Buie, W. Donald; MacLean, Anthony R. (2016): Postoperative Nonsteroidal Anti-inflammatory Drug Use and Intestinal Anastomotic Dehiscence: A Systematic Review and Meta-Analysis. In Diseases of the colon and rectum 59 (11), pp. 1087–1097. DOI: 10.1097/DCR.0000000000000666 .

Snijders, H. S.; Wouters, M. W. J. M.; van Leersum, N. J.; Kolfschoten, N. E.; Henneman, D.; Vries, A. C. de et al. (2012): Meta-analysis of the risk for anastomotic leakage, the postoperative mortality caused by leakage in relation to the overall postoperative mortality. In European journal of surgical oncology : the journal of the European Society of Surgical Oncology and the British Association of Surgical Oncology 38 (11), pp. 1013–1019. DOI:10.1016/j .ejso.2012.07.111.

Steffenrud, S. (1980): Metabolism of 16, 16-dimethyl-prostaglandin E2 in the human female. In Biochemical medicine 24 (3), pp. 274–292.DOI: 10.1016/0006-2944(80)90022-8 .

Stitham, Jeremiah; Midgett, Charles; Martin, Kathleen A.; Hwa, John (2011): Prostacyclin: an inflammatory paradox. In Frontiers in pharmacology 2, p. 24. DOI: 10.3389/fphar.2011.00024 .

Stoffels, Burkhard; Hupa, Kristof Johannes; Snoek, Susanne A.; van Bree, Sjoerd; Stein, Kathy; Schwandt, Timo et al. (2014): Postoperative ileus involves interleukin-1 receptor signaling in enteric glia. In Gastroenterology 146 (1), 176-87.e1. DOI: 10.1053/j .gastro.2013.09.030 .

Stumpf, Michael; Cao, Wei; Klinge, Uwe; Klosterhalfen, Bernd; Kasperk, Reinhard; Schumpelick, Volker (2002): Collagen distribution and expression of matrix metalloproteinases 1 and 13 in patients with anastomotic leakage after large-bowel surgery. In Langenbeck's archives of surgery 386 (7), pp. 502–506. DOI: 10.1007/s00423-001-0255-9 .

Stumpf, Michael; Klinge, Uwe; Wilms, Arnulf; Zabrocki, Robert; Rosch, Rafael; Junge, Karsten et al. (2005): Changes of the extracellular matrix as a risk factor for anastomotic leakage after large bowel surgery. In Surgery 137 (2), pp. 229–234. DOI: 10.1016/j .surg.2004.07.011.

Sturm, Eva M.; Radnai, Balazs; Jandl, Katharina; Stančić, Angela; Parzmair, Gerald P.; Högenauer, Christoph et al. (2014): Opposing roles of prostaglandin D2 receptors in ulcerative colitis. In Journal of immunology (Baltimore, Md.: 1950) 193 (2), pp. 827–839. DOI: 10.4049/jimmunol.1303484 .

Su'a, B. U.; Mikaere, H. L.; Rahiri, J. L.; Bissett, I. B.; Hill, A. G. (2017): Systematic review of the role of biomarkers in diagnosing anastomotic leakage following colorectal surgery. In The British journal of surgery 104 (5), pp. 503–512. DOI: 10.1002/bjs.10487 .

Sun, L.; Feng, Y. (2020): Comment on: Safety and efficacy of non-steroidal anti-inflammatory drugs to reduce ileus after colorectal surgery. In The British journal of surgery 107 (3), pp. 316–317. DOI: 10.1002/bjs.11484 .

Sun, Xiaoting; Li, Qi (2018): Prostaglandin EP2 receptor: Novel therapeutic target for human cancers (Review). In International journal of molecular medicine 42 (3), pp. 1203–1214. DOI: 10.3892/ijmm.2018.3744.

Tanaka, Akiko; Hase, Shoko; Miyazawa, Tohru; Takeuchi, Koji (2002): Up-regulation of cyclooxygenase-2 by inhibition of cyclooxygenase-1: a key to nonsteroidal anti-inflammatory drug-induced intestinal damage. In The Journal of pharmacology and experimental therapeutics 300 (3), pp. 754–761. DOI: 10.1124/jpet.300.3.754.

Thompson, Sarah K.; Chang, Eugene Y.; Jobe, Blair A. (2006): Clinical review: Heal-

ing in gastrointestinal anastomoses, part I. In Microsurgery 26 (3), pp. 131–136. DOI: 10.1002/micr.20197.

Thumkeo, Dean; Punyawatthananukool, Siwakorn; Prasongtanakij, Somsak; Matsuura, Ryuma; Arima, Kentaro; Nie, Huan et al. (2022): PGE2-EP2/EP4 signaling elicits immunosuppression by driving the mregDC-Treg axis in inflammatory tumor microenvironment. In Cell reports 39 (10), p. 110914. DOI: 10.1016/j .celrep.2022.110914.

Tilley, S. L.; Coffman, T. M.; Koller, B. H. (2001): Mixed messages: modulation of inflammation and immune responses by prostaglandins and thromboxanes. In The Journal of clinical investigation 108 (1), pp. 15–23. DOI: 10.1172/JCI13416 .

Törkvist L, Månsson P, Raud J, Larsson J, Thorlacius H. Role of CD18-dependent neutrophil recruitment in skin and intestinal wound healing. Eur Surg Res. 2001 Jul-Aug;33(4):249-54. doi: 10.1159/000049714 . PMID: 11684830 .

Tsalikidis, Christos; Mitsala, Athanasia; Mentonis, Vasileios I.; Romanidis, Konstantinos; Pappas-Gogos, George; Tsaroucha, Alexandra K.; Pitiakoudis, Michail (2023): Predictive Factors for Anastomotic Leakage Following Colorectal Cancer Surgery: Where Are We and Where Are We Going? In Current oncology (Toronto, Ont.) 30 (3), pp. 3111–3137. DOI:10.3390/curroncol30030236 .

van Helsdingen, Claire P. M.; Wildeboer, Aurelia C. L.; Zafeiropoulou, Konstantina; Jongen, Audrey C. H. M.; Bosmans, Joanna W. A. M.; Gallé, Camille et al. (2023): Histology and transcriptome insights into the early processes of intestinal anastomotic healing: a rat model. In BJS open 7 (5). DOI: 10.1093/bjsopen/zrad099 .

Vane, J. R.; Botting, R. M. (1998): Mechanism of action of nonsteroidal anti-inflammatory drugs. In The American journal of medicine 104 (3A), 2S-8S; discussion 21S-22S. DOI: 10.1016/s0002-9343(97)00203-9 .

Vardhan, Sauvik; Deshpande, Swati G.; Singh, Abhinesh; Aravind Kumar, Chava; Bisen, Yuganshu T.; Dighe, Onkar R. (2023): Techniques for Diagnosing Anastomotic Leaks Intraoperatively in Colorectal Surgeries: A Review. In Cureus 15 (1), e34168. DOI:

10.7759/cureus.34168

Wang, Gang; Yang, Feifei; Zhou, Weiying; Xiao, Nanyang; Luo, Mao; Tang, Zonghao (2023): The initiation of oxidative stress and therapeutic strategies in wound healing. In Biomedicine and pharmacotherapy, 157, p. 114004.DOI: 10.1016/j.biopha.2022.114004 .

Weber, Marie-Christin; Berlet, Maximilian; Stoess, Christian; Reischl, Stefan; Wilhelm, Dirk; Friess, Helmut; Neumann, Philipp-Alexander (2023): A nationwide population-based study on the clinical and economic burden of anastomotic leakage in colorectal surgery. In Langenbeck's archives of surgery 408 (1), p. 55. DOI: 10.1007/s00423-023-02809-4 .

Wickham, Hadley; Averick, Mara; Bryan, Jennifer; Chang, Winston; McGowan, Lucy; François, Romain et al. (2019): Welcome to the Tidyverse. In JOSS 4 (43), p. 1686. DOI: 10.21105/joss.01686 .

Wilson, C. E.; Dickie, A. P.; Schreiter, K.; Wehr, R.; Wilson, E. M.; Bial, J. et al. (2018): The pharmacokinetics and metabolism of diclofenac in chimeric humanized and murinized FRG mice. In Archives of toxicology 92 (6), pp. 1953–1967. DOI: 10.1007/s00204-018-2212-1.

Winter, Maximiliane; Heitplatz, Barbara; Koppers, Nils; Mohr, Annika; Bungert, Alexander D.; Juratli, Mazen A. et al. (2023): The Impact of Phase-Specific Macrophage Depletion on Intestinal Anastomotic Healing. In Cells 12 (7). DOI: 10.3390/cells12071039 .

Wright, Emma C.; Connolly, Patricia; Vella, Mark; Moug, Susan (2017): Peritoneal fluid biomarkers in the detection of colorectal anastomotic leaks: a systematic review. In International journal of colorectal disease 32 (7), pp. 935–945. DOI: 10.1007/s00384-017-2799-3 .

Wu, Guoyao; Fang, Yun-Zhong; Yang, Sheng; Lupton, Joanne R.; Turner, Nancy D. (2004): Glutathione metabolism and its implications for health. In The Journal of nutrition 134 (3), pp. 489–492. DOI: 10.1093/jn/134.3.489 .

Wu, Tianzhi; Hu, Erqiang; Xu, Shuangbin; Chen, Meijun; Guo, Pingfan; Dai, Zehan et al. (2021): clusterProfiler 4.0: A universal enrichment tool for interpreting omics data. In

Innovation (Cambridge (Mass.)) 2 (3), p. 100141. DOI: 10.1016/j .xinn.2021.100141.

Yao, Chengcan; Sakata, Daiji; Esaki, Yoshiyasu; Li, Youxian; Matsuoka, Toshiyuki; Kuroiwa, Kenji et al. (2009): Prostaglandin E2-EP4 signaling promotes immune inflammation through Th1 cell differentiation and Th17 cell expansion. In Nature medicine 15 (6), pp. 633–640. DOI: 10.1038/nm.1968 .

Yauw, S. T. K.; Lomme, R. M. L. M.; van den Broek, P.; Greupink, R.; Russel, F. G. M.; van Goor, H. (2018a): Experimental study of diclofenac and its biliary metabolites on anastomotic healing. In BJS open 2 (4), pp. 220–228. DOI: 10.1002/bjs5.63 .

Yauw, Simon T. K.; Arron, Melissa; Lomme, Roger M. L. M.; van den Broek, Petra; Greupink, Rick; Bhatt, Aadra P. et al. (2018b): Microbial Glucuronidase Inhibition Reduces Severity of Diclofenac-Induced Anastomotic Leak in Rats. In Surgical infections 19 (4), pp. 417–423. DOI: 10.1089/sur.2017.245 .

Yauw, Simon T. K.; Lomme, Roger M. L. M.; van der Vijver, Rozemarijn J.; Hendriks, Thijs; van Laarhoven, Kees J. H. M.; van Goor, Harry (2015): Diclofenac causes anastomotic leakage in the proximal colon but not in the distal colon of the rat. In American journal of surgery 210 (2), pp. 382–388. DOI: 10.1016/j .amjsurg.2014.10.028 .

Yu, Guangchuang; Wang, Li-Gen; Han, Yanyan; He, Qing-Yu (2012): clusterProfiler: an R package for comparing biological themes among gene clusters. In Omics : a journal of integrative biology 16 (5), pp. 284–287. DOI: 10.1089/omi.2011.0118 .

Yu, Guangchuang; Wang, Li-Gen; Yan, Guang-Rong; He, Qing-Yu (2015): DOSE: an R/Bioconductor package for disease ontology semantic and enrichment analysis. In Bioinformatics (Oxford, England) 31 (4), pp. 608–609. DOI: 10.1093/bioinformatics/btu684 .

Zarnescu, Eugenia Claudia; Zarnescu, Narcis Octavian; Costea, Radu (2021): Updates of Risk Factors for Anastomotic Leakage after Colorectal Surgery. In Diagnostics (Basel, Switzerland) 11 (12). DOI: 10.3390/diagnostics11122382 .

Zhang, Feng; Qiao, Song; Li, Chunqiao; Wu, Bo; Reischl, Stefan; Neumann, Philipp-

Alexander (2020): The immunologic changes during different phases of intestinal anastomotic healing. In Journal of clinical laboratory analysis, 34 (11), e23493.DOI: 10.1002/jcla.23493 .

Zhang, Yongyou; Desai, Amar; Yang, Sung Yeun; Bae, Ki Beom; Antczak, Monika I.; Fink, Stephen P. et al. (2015): TISSUE REGENERATION. Inhibition of the prostaglandin-degrading enzyme 15-PGDH potentiates tissue regeneration. In Science (New York, N.Y.) 348 (6240), aaa2340. DOI: 10.1126/science .aaa2340.

Zheng, Ziwen; Wieder, Thomas; Mauerer, Bernhard; Schäfer, Luisa; Kesselring, Rebecca; Braumüller, Heidi (2023): T Cells in Colorectal Cancer: Unravelling the Function of Different T Cell Subsets in the Tumor Microenvironment. In International journal of molecular sciences 24 (14). DOI: 10.3390/ijms241411673

Zhu, Xiaoliang; Zhu, Jinfang (2020): CD4 T Helper Cell Subsets and Related Human Immunological Disorders. In International journal of molecular sciences 21 (21). DOI: 10.3390/ijms21218011 .

9 Acknowledgements

Obtaining a doctorate has been a long-held dream come true. I am forever grateful to the people who helped and supported me throughout my PhD, as well as to everyone who provided the foundation for me to pursue this dream.

First of all, I would like to thank my supervisor **Prof Sven Wehner** for giving me this opportunity and supporting me throughout the project both in Bonn and Amsterdam. I highly appreciate the freedom you gave me to explore different topics and acquire new skills. Every interaction we had taught me valuable lessons, which I will carry in the rest of my career. It was delightful to work with you.

I also would like to thank **Prof Wouter J de Jonge** for hosting me in at the Tytgat Institute for two years. Your support and insights have made valuable contributions to the projects. During my stay in your research group, I not only grew as a scientist but also developed friendships. Therefore, thank you for creating a great working environment as well.

I would like to thank my team anastomosis as I owe huge portion of this work to their efforts. **Patrik**, thank you very much for teaching me how to operate confidently and for your assistance throughout surgeries. Our conversations during the long hours of surgeries made those days enjoyable. **Olaf**, it was a mission impossible to successfully finish all the experiments, but somehow we managed to pull it off. Thank you very much for fighting for me to get IvD protocols approved and assisting me throughout what felt like never-ending surgeries. You were incredibly reliable and flexible, for which I will be forever grateful. I very much enjoyed our conversations, and I could not ask for a better teammate. I will certainly miss your humor and hearing your laugh across the hallway. **Patricia**, millions of thanks for being there for injections, assisting with surgeries, and being a flexible teammate. Your friendliness calmed me down even during stressful experiments. I will miss working with you.

This work would not have been possible without the golden hands of our technicians. **Bianca and Mariola**, thank you for being there whenever I needed help; you made adapt-

ing to a new lab environment much easier. **Iris**, thank you very much for your support during the most demanding experiments of my PhD. We worked together when I was under immense time pressure, and I cannot thank you enough for caring and lifting the weight with me so that I could reach the finish line successfully.

This work would not have been possible without the magic of bioinformatics either. Hence, thank you very much, **Andrew**, for supervising me as I learned how to code and analyze data. As a wet lab scientist, it was not easy to acquire coding skills, but your support allowed me to implement what I learned very quickly.

I would also like to thank **René**. You are one of the scientists I have always looked up to. Your sincere curiosity about science has been an inspiration for me, and your questions have consistently made me reconsider subjects I thought I knew well. Thank you very much for being generous with your time and kind words in supporting me. I will always appreciate this. **Bruno**, thank you for caring about my problems and listening to me when I needed it. You have not only provided valuable insights into my work but have also been there to celebrate successes and offer support when things didn't go as planned. Your excitement about research and optimism have been an inspiration throughout my PhD.

I also would like to thank my colleagues at the University Hospital Bonn **Shilpashree, Mona, Linda, Patrick, and Balbina** for welcoming me to the team in Bonn and supporting me during my time in Germany. I am happy to have met and worked with you.

I would like to thank room S2-164 at the Tytgat Institute. **Caroline**, many thanks for answering my questions with patience, even when the answers were probably written in one of the SOPs. In my defense, you have a talent for solving problems within seconds, and I consider myself very lucky to have worked with you. **Mohammed**, thank you so very much for listening to me whenever I needed to rant about life, career, weather, or really anything. Your positive and calm mindset helped me through difficult times. Even though I still have a long way to go, I strive to acquire a similar mindset and will always remember you as an inspiration. **Femke**, I am very happy to have met you, not only because you were a great colleague but, more importantly, a wonderful friend. Thank you for being there for emo-

tional and mental support. Also, many thanks for offering help endlessly whenever you saw me overwhelmed. I hope we will continue to be friends and keep sharing wonderful recipes.

I also would like to thank my dear friends at the Tygat Institute. **Lilly**, we had a crazy ride together and I am proud of what we achieved. I am also proud that through tough times we flourished a beautiful friendship that I wish to keep. Many thanks for your friendship and all your contributions to my projects. It was a pleasure to work, think, and laugh with you. **Konstantina**, thank you from the bottom of my heart for sharing the joys, laughs, and challenges of this long journey. You are not only a brilliant scientist but also a wonderful friend. I feel incredibly lucky to have met and worked with you, and I hope we will continue to be friends throughout our lives. **Irini**, you have quickly become one of my friends at Tytgat, making my stay much more enjoyable. I have always thoroughly enjoyed the time we spent together, whether it was working in the lab, having project meetings, or having long chats about life over delicious meals. Thank you for your friendship, which I hope to maintain. **Gemma**, you have always impressed me with your exceptional work ethic. Thank you for being an inspiring colleague and an awesome friend who was there for me during the happiest and also the darkest times. You are a part of almost all of my good memories in Amsterdam, and I wish you many more wonderful memories in the future. **Florine**, you are one of my dear friends who I believe is on the same wavelength as me. Thank you for the great conversations, for being there during celebrations, and for taking a genuine interest in my struggles while offering help in the best way you could. Also, a huge thank you for starting Books and Cooks, which has become one of my all-time favorite friendship clubs. **Naomi**, I have always learned a lot from your intelligent and creative questions. Not only that, but ever since we were paired up at the beginning of the consortium, you have become one of my friends with whom I could talk and think deeply. Thank you for being a great colleague and friend. **Paula**, you have always amazed me with your extensive knowledge of social issues and the history of cultures and countries. Thank you very much for the enjoyable conversations and for your support throughout my stay at the institute. **Annemijn**, I always felt your sincerity when you asked how I was doing, and I am truly grateful for that. You are full of positive energy, and I will miss being

around you. **Ivan**, even if our research paths crossed only for a short period of time, it was very enjoyable working with you. Thank you for teaching me new skills and delightful conversations. **Yannick**, thank you for being available whenever I needed help. It was a great pleasure to work and brainstorm with you.

Esin, Bu uzun maceranın her anında yanımda olduğun için çok teşekkür ederim. Tanıştığımız günden beri hayatımın her aşamasını uzun uzun anlatabildiğim tek arkadaşımsın. Bunca yıldır beni bıkmadan dinlediğin ve arkadaşlığımıza değer verdiğin için binlerce teşekkürler.

I would like to thank my precious PhD penpal **Charles Bokor**. Darling, expressing my gratitude for you in words feels inadequate, as they can not fully capture how truly thankful I am. I have driven so much strength from our relationship without which it would not have been possible to complete my PhD. You have made me not only a better person but also a much better scientist. Thank you very much for supporting me and believing in me when I doubted myself. I will always be grateful for everything you have done for me.

Lastly, I would like to thank **my sister Elif Şengül, mother İlknur Şengül and father Ramazan Şengül.** Without them, none of my achievements would have been possible or meaningful.

Elif, dünyanın neresinde olursam olayım, ihtiyacım olduğu an uçağa atlayıp yanıma geldiğin için, sevinçlerimi ve üzüntülerimi gönülden paylaştığın için ve düşünmeden birçok maceraya benimle atıldığın için binlerce kez teşekkür ederim. Eminim ki bu hayattaki en büyük şanslarımdan birisi senin gibi muhteşem bir kardeşe sahip olmak. Her şey için gönülden teşekkürler.

Sevgili **anneciğim ve babacığım**, bana destekleriniz için sonsuz teşekkür ederim. Siz arkamda durmasaydınız bu kadar uzun bir yol kat edemezdim. Sizden öğrendiğim değerler ve aldığım güçle kendi ayaklarımın üzerinde durup gurur duyduğum bir hayat inşa edebildim. Umarım ki bu zaman zarfında sizi de gururlandırmışımdır ve gururlandırmaya devam edebilirim. Başardığım her şey sizin sayenizde ve siz yanımda olduğunuz için daha anlamlı. Yürekten teşekkürler.